Microbial degradation of plastic : comparison of synthetic and natural communities

Auteur : Carlier, Louise
Promoteur(s) : Delvigne, Frank
Faculté : Gembloux Agro-Bio Tech (GxABT)
Diplôme : Master en bioingénieur : chimie et bioindustries, à finalité spécialisée
Année académique : 2017-2018
URI/URL : http://hdl.handle.net/2268.2/5117

LIÈGE université
Gembloux
Agro-Bio Tech

MICROBIAL DEGRADATION OF PLASTIC : COMPARISON OF SYNTHETIC AND NATURAL COMMUNITIES

LOUISE CARLIER

TRAVAIL DE FIN D'ETUDES PRESENTE EN VUE DE L'OBTENTION DU DIPLOME DE MASTER BIOINGENIEUR EN CHIMIE ET BIOINDUSTRIES

ANNÉE ACADÉMIQUE 2017-2018

PROMOTEUR: PR. FRANK DELVIGNE

LIÈGE université
Gembloux
Agro-Bio Tech

MICROBIAL DEGRADATION OF PLASTIC : COMPARISON OF SYNTHETIC AND NATURAL COMMUNITIES

LOUISE CARLIER

TRAVAIL DE FIN D'ETUDES PRESENTE EN VUE DE L'OBTENTION DU DIPLOME DE MASTER BIOINGENIEUR EN CHIMIE ET BIOINDUSTRIES

ANNÉE ACADÉMIQUE 2017-2018

PROMOTEUR: PR. FRANK DELVIGNE

Tout d'abord, je tiens à adresser mes remerciements au professeur Frank Delvigne, promoteur de ce présent mémoire, pour le suivi et les conseils donnés lors de la réalisation de ce travail. Je tiens également à remercier l'ensemble des membres du MiPI pour leur bonne humeur, leurs conseils et encouragements. Un chaleureux remerciement est tout particulièrement adressé à Sébastien Steels pour son soutien et surtout pour l'aide apportée tout au long des manipulations et les nombreuses discussions et réflexions portant sur la biologie moléculaire.

Ensuite, je voudrais remercier monsieur le Doyen et l'unité d'entomologie de laquelle j'ai pu obtenir du matériel pour parvenir à bien mes manipulations. Merci également à Samuel Latour, étudiant Tfiste, pour les échanges portant sur nos travaux respectifs mais néanmoins complémentaires.

Je remercie également le professeur Christophe Blecker et les membres de son laboratoire pour m'avoir fait découvrir le vaste domaine de la physico-chimie appliqué à la microbiologie.

Je tiens à remercier également Alice Delacuvellerie, doctorante à l'université de Mons, pour l'accueil et le temps consacré aux analyses SEM réalisées dans son laboratoire.

Merci à Barbara Fifani ainsi qu'à Ariane Theatre pour leur contribution dans la mise en place de ce travail, tant au laboratoire que lors de la rédaction.

Enfin, j'adresse un énorme merci à ma famille et mes proches pour leurs encouragements, leur soutien et leurs aides qui ont su faire la différence durant ces cinq années et tout particulièrement ces derniers mois, merci pour tout!

Abstract

The processes of plastic biodegradation take into account a wide field of study involving several multidisciplinary approaches. The aim of this present work is to investigate plastic degradation from two ways. The first one is the study of the impact of diets on the intestinal microbiota of *Galleria mellonella* caterpillar, known to assimilate polyethylene. To this end, a denaturing gradient gel electrophoresis (DGGE) was performed, highlighting specie diversity variation but a constant specie richness. Moreover, identification of cultivable bacteria from the gut of *G. mellonella* larvae displays interesting species able to degrade polymer. The second approach is the study of the adhesion of biofilms on polyethylene surface, which is the first step of plastic biodegradation. For this purpose, XDLVO theory was explored through Zeta potential (ZP) measurement and contact angle measurement on microbial co-culture composed of *Bacillus amyloliquefaciens* and *Trichoderma harzianum*. The obtained ZP variation exhibits the complexity and heterogeneity of biofilms through time and space. These physicochemical analyses were performed on plastic surface supporting biofilms. Small variations were exhibited compared to the controls. This observation can be the consequence of a chemical modification of plastic surface caused by the microbial degradation and leading to a better adhesion of biofilm.

Keywords: Plastic degradation. *Galleria mellonella*. DGGE. Co-culture. Biofilm adhesion. XDLVO theory.

Résumé

Le processus de biodégradation des plastiques prend en compte un large champs d'étude impliquant diverses approches multidisciplinaires. Le but de ce présent travail est d'étudier la dégradation du plastique à partir de deux voies. La première consiste en l'étude de l'impact des régimes sur le microbiote intestinal de la chenille de *Galleria mellonella*, connue pour assimiler le polyéthylène. À cette fin, une électrophorèse sur gel en gradient dénaturant (DGGE) a été réalisée, mettant en évidence une variation de la diversité spécifique mais une richesse specifique constante. De plus, l'identification des bacteries cultivables issues de l'intestin de *G. mellonella* montre d'intéressantes espèces capables de dégrader des polymères. La seconde approche est l'étude de l'adhésion des biofilms sur la surface du polyéthylène, ce qui constitue la première étape de la biodegradation du plastique. Dans ce but, la théorie XDVLO a été investiguée à travers la mesure du potentiel Zéta (ZP) et celle de l'angle de contact sur une co-culture microbienne composée de *Bacillus amyloliquefaciens* et *Trichoderma harzianum*. Les variations des valeurs du ZP obtenues montrent la complexité et l'hétérogénéité spatiale et temporelle des biofilms. Ces analyses physico-chimiques ont été réalisées sur la surface de plastique supportant les biofilms. De légères variations sont apparues comparativement aux contrôles. Cette observation peut être la conséquence d'une modification chimique de la surface de plastique, causée par la dégradation microbienne pour permettre une meilleure adhésion du biofilm.

Mots clés: Dégradation du plastique. *Galleria mellonella*. DGGE. Co-culture. Adhésion du biofilm. Theorie XDLVO.

Abbreviations

AB Short-range Lewis acid-base.

AFM Atomic force microscopy.

AMP Antimicrobial peptide.

APS Ammonium persulfate.

BFI Bacterial-fungal interaction.

CAM Contact angle measurement.

CLP Cyclic lipopeptides.

DGGE Denaturing gradient gel electrophoresis.

DLVO Derjaguin, Landau, Verwey, and Overbeek.

DSC Differential scanning calorimetry.

EPS Extracellular polymeric substances.

FTIR Fourier transform infrared spectroscopy.

GPC Gel permeation chromatography.

HDPE High density polyethylene.

HDXLPE High density cross-linked polyethylene.

HMWPE High molecular weight polyethylene.

LDPE Low density polyethylene.

LLDPE Linear low density polyethylene.

LW Lifshitz-van der Waals.

MDPE Medium density polyethylene.

microATR Microattenuated total reflectance.

OD Optical density.

PCR Polymerase chain reaction.

PE Polyethylene.

PET Polyethylene therephtalate.

PGPR Plant growth-promoting rhizo-bacteria.

PHB Polyhydroxybutyrate.

POP Persistent organic pollutant.

PP Polypropylene.

PS Polystyrene.

PUR Polyurethane.

PVC Polyvinyl chloride.

SD Standard deviation.

SEM Scanning electron microscopy.

TEMED Tetramethylethylenediamine.

TGA Thermo gravimetric analysis.

UHMWPE Ultrahigh molecular weight polyethylene.

ULMWPE Ultralow molecular weight polyethylene.

VLDPE Very low density polyethylene.

XDLVO Extended DLVO.

XLPE Cross-linked polyethylene.

XPS X-ray photoelectron spectroscopy.

ZP Zeta potential.

Contents

List of Figures

List of Tables

1 Goal of this study

It is not a secret anymore; the increasing worldwide use of synthetic polymer, such as plastics, leads to a dramatic rise of plastic debris through ecosystems, which is not without consequences on wildlife. At the same time, the natural degradation of this waste is more and more investigated, including several scientific disciplines working on biological, physical and chemical aspects of this natural biodegradation.

In that context, a natural community from the gut of *Galleria mellonella* larvae, a caterpillar known to assimilate plastic bags, has been studied as a microbial ecosystem. On the other hand, a synthetic community has been cultivated on polyethylene films and explored through its physicochemical interactions. To that end, this present work has been achieved due to laboratory experimentations based on these multidisciplinary approaches which have been led on abiotic and biotic systems, namely polyethylene and microbial communities.

The specie richness and the specie diversity have been investigated on the intestinal microbiota from the *Galleria mellonella* larvae due to several denaturing gradient gel electrophoreses (DGGE). Moreover, in order to identify cultivable bacteria isolated from this microbiota, a 16S rDNA sequencing has been carried out.

Inspired by the natural relationship of microorganisms in soil, a synthetic community was set up to study its adhesion on polyethylene and its abilities to degrade this synthetic polymer. This co-culture, constituted by a bactarial strain, *Bacillus amyloliquefaciens*, and a fungal one, *Trichoderma harzianum*, both growing on a polyethylene surface, was investigated. Through Zeta potential and contact angle measurement, the physicochemical behavior was explored according to the XDLVO theory.

2 State of the art

2.1 Plastics in our current world

Since the invention of Bakelite by the Belgian chemist Leo Baekeland in the early 20th century, the expansion of plastic manufacturing and its applications have been a revolution in our daily life [1].

Obviously, the consequences of this revolution are more and more important, but not always visible. Indeed, plastics are synthetic materials widely used across the world and therefore concerns about their contributions to pollution of terrestrial and aquatic biomes, but also their impacts on human health, are more and more investigated. This leads to the creation of new laws such as the bannishment of micro-plastic in cosmetics, plastic bags in supermarkets, plastic cutlery, cotton swabs and so on. Discoveries about biodegradation of plastic are always presented as victory but public awareness about plastic issues remains too weak, even if we are overrun with pictures and videos showing plastic pollution through ecosystems.

2.1.1 Plastic, a synthetic polymer

Plastic materials are polymers derived from the fossil fuel cracking or bio-based products. Eitherway, plastic is always synthetic (as human made). As polymers, all plastics are characterized by a long-chain molecular structure. The repeat unit along the chain, the monomers, varies from a plastic to another one (Table 1), classified as "resins" [2]. Commonly, plastics are classified into 2 main categories: thermoplastics and thermosets, characterized by their ability to be reshaped by heating or not [3]. This property is due to the individual polymer chain characteristics for thermoplastics, while thermosetting polymers are chemically crosslinked.

TABLE 1: Thermoplastics and thermosets: chemical structure of monomers

Thermoplastic	**Monomer**
Polypropylene (PP)	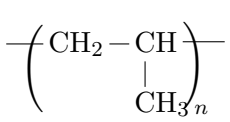
Polyethylene (PE)	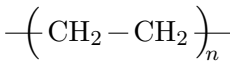
Polyvinyl chloride (PVC)	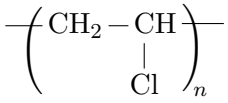
Polyethylene therephtalate (PET)	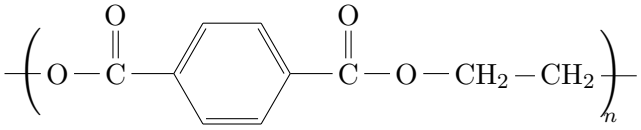
Polystyrene (PS)	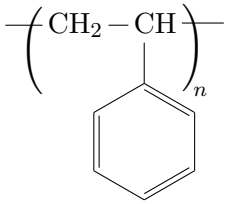
Thermoset	**Monomer**
Polyurethane (PUR)	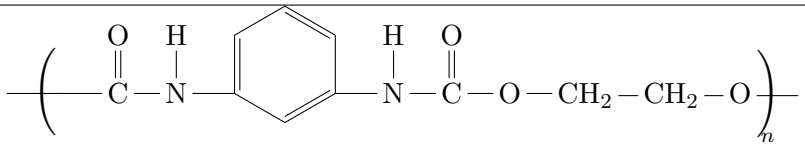

Content source: [4]

Polyethylene is commonly used in packaging sector. Globally, LDPE and LLDPE are found in agricultural film, food packaging film and bags. Whereas HDPE and MDPE are mostly used to make current items such as toys, milk bottles, shampoo bottles, pipes, houseware, etc (Table 2). Because PE is mainly manufactured for short-term and single-use items, this type of synthetic polymer is continuously demanded on a large proportion compared to the other kind of plastics [3].

Table 2: Thermoplastics and thermosets: European plastic demand and common usages

Thermoplastic	**Demand**	**Usage**
Polypropylene (PP)	19.3 %	Food packaging, sweet and snack wrappers, hinged caps, microwave proof containers, pipes, automotive parts, etc.
Polyethylene (LDPE/LLDPE)	17.5%	Reusable bags, trays and containers, agricultural film, food packaging, film, etc.
Polyethylene (HDPE/MDPE)	12.3%	Toys, milk bottles, shampoo bottles, pipes, houseware, etc.
Polyvinyl chloride (PVC)	10%	Building (windows frames, profils, floor, wall covering, etc.)
Polyethylene therephtalate (PET)	7.4%	Bottles for drinks and cleaners
Polystyrene (PS)	6.7%	Eyeglasses frames, plastics cups, egg trays packaging, building insulation, etc.
Thermoset	**Demand**	**Usage**
Polyurethane (PUR)	7.5%	Building insulation, pillows and mattresses, insulating foams, etc.

Content source: [3]

Among all these synthetic polymers, polyethylene (PE), or polythene, is the largest tonnage plastics material manufactured and the simplest plastic in terms of structure and composition, having the chemical formula $(C_2H_4)_nH_2$ [5]. Indeed, PE is a polyolefin characterized by the polymerization of ethylene. However, several methods had been developed to produce polyethylene, impacting its structure and thus its properties such as mechanical, thermal, chemical and electrical properties [6]. So, polyethylene is classified by the chain branching and thus by its density. These grades of PE include among others: very low density polyethylene (VLDPE), low density polyethylene (LDPE), linear low density polyethylene (LLDPE), medium density polyethylene (MDPE), cross-linked polyethylene (XLPE), high-density polyethylene (HDPE), high-density cross-linked polyethylene (HDXLPE), high molecular weight polyethylene (HMWPE), ultrahigh molecular weight polyethylene (UHMWPE) and ultralow molecular weight polyethylene (ULMWPE) [7].

Packaging is the main demanding sectors of plastics reaching 39.5 % for Europe in 2014 (Figure 1). This percentage remains constant, reaching 39.9% in 2016. Polyethylene, and especially low-density polyethylene, is the major polymer used for packaging (Figure 1) which exposes the demand of the main sectors for the main resin types. These amounts remain stable between 2014 and 2016, according to the facts of 2017 [3].

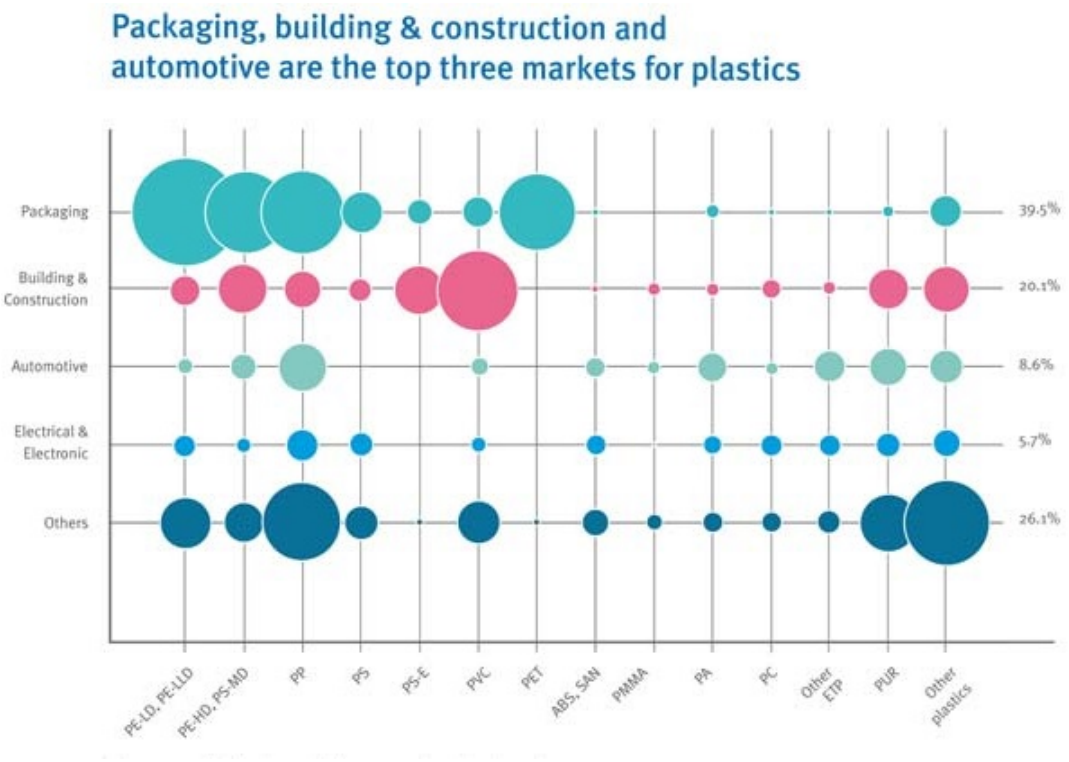

FIGURE 1: European plastics demand by polymer types in 2014

Source: [8]

Hence, it is not surprising that these single-use items constitute the greater plastic pollutant [9]. Furthermore, they are easily transported in nature by wind and water due to the low mass of LDPE.

2.1.2 Plastic management

Global production of plastics reached 335 million tons in 2016, with almost 18% of it being produced in Europe. Plastic demand increases with population growth, resulting in a higher demand which would lead to a depletion of this material if the only production source was fossil fuel, a non-renewable source. In this context, it is time to rethink plastic consumption and management, including valorization of plastic waste. 27.1 million tons

of plastic waste were collected trough Europe in 2016. 31% of these collected plastics are recycled (63% were treated inside Europe), 41.6% are turned into energy, while 27.3% are destined for landfilling [3].

2.1.2.1 Recycling

Nowadays, the recycling turns plastic waste into a resource, leading to a circular economy and developing an international market of recycled plastic. It also helps avoid the processing of petrochemical feedstocks and its linked pollution [9, 10]. However, the number of cycles of the recycling process is limited by the decrease of the quality of this synthetic polymer. Moreover, recycling could be hazardous due to the mixing of additives included in manufactured plastic materials [5]. Indeed, raw polymers do not meet the expected properties of plastic material. Additives are used to perform essential functions such as the thermal stability and the durability of the material in order to obtain useful items. For example, nucleating agents, antioxidants, dyes or pigments, reinforcing fibers, fillers and flame retardants may be added to adjust the previous properties. Furthermore, other agents may also improve the quality of plastic materials like surface modifiers, wetting agents, coupling agents, biocides, plasticizers, mold release agents, etc [11]. Another limiting factor for recycling is the required energy and water to wash items. The first key challenge to improve plastic recycling is the efficiency of the separation of the different plastic materials. Another main challenge is the improvement of quality of waste plastic containing undesirable additives and contaminants in order to deliver a better quality of recycled plastic materials [9].

2.1.2.2 Landfilling

Landfilling does not solve the problem of plastic waste management and remains an unsustainable solution. This accumulation of plastics postpones the problem to the next generations. Moreover, lands dedicated to the landfilling are not available for more valuable activities such as agriculture. As a further matter, a non-well-operated landfill can lead to an uncontrolled pollution. Indeed, besides the physical pollution of plastics, landfill leachates contain hazardous additives which could, if not treated, induce a pollution of the aquatic environment [12, 13].

Landfilling also remains an inappropriate management of plastics because of its persistence in the environment. Indeed, the degradation of plastics can take between hundreds and thousands years, according to estimations. However, inappropriate human behavior and improper waste management are the major causes of plastics released in the environment [12].

2.1.2.3 Pollution

The problem of plastic pollution is associated with both the physical plastic items and chemical components included in this synthetic material (both additives and adsorbed pollutants). Besides the persistence of plastics in nature, the low degradation rate implies mechanical fragmentation of plastics and thus the spreading of micro- and nano-plastics in the environment. The dissemination of those particles leads to their presence everywhere and the disruption of the environment. For example, the ingestion of macro-plastics by both marine and terrestrial organisms leads to a blockage of the digestive tract due to its undigestibility in the gut. Moreover, the ubiquity of plastic also impacts all the trophic chain trough bio-accumulation and bio-magnification [13, 14].

Furthermore, plastics can act as a sorbant of hydrophobic contaminants. Among these contaminants, persistent organic pollutants (POBs), known as carcinogenic and endocrine disruptors, are concentrated onto plastic materials. Actually, micro- and nano-plastics present a higher surface area to volume ratio compared to larger plastics, resulting in an higher concentration of adsorbed contaminants by volume unit. Moreover, the smaller the plastic item is, the higher the number of particles that can be ingested by an organism is [12]. Next to the ingestion, chemical additives and adsorbed contaminants associated with the plastic can be released in the organisms and accumulated in adipose tissues [13]. By this way, POPs could be bio-accumulated in food chain, impacting more significantly the predators such as humans [15].

Nowadays, no ecosystem is free of plastics. The well-known "7th continent of plastics", called the Plastic Trash Vortex, is unfortunately a perfect example of marine pollution by plastics. Many beaches are covered of plastics items whereas agroecosystems are not more saved. Mulching film are directly involved in soil pollution while water easily transports plastics, supporting aquatic pollution. Moreover, it has been demonstrated that microplastics pass trought waste water treatment, highlighting the total uncontrolled plastic spreading [14].

2.2 Biodegradation of plastics

Biotic degradation refers to be "a chemical degradation of materials provoked by the action of microorganisms such as bacteria, fungi and algae" [16].

As a synthetic polymer, the first function of polyethylene is not to be biodegradable. Moreover, polyolefins, including PE, are strong linear chains or branching of carbon without any functional groups. They thus have a high hydrophobicity, preventing an easy fragmentation by microorganisms [17]. However, environmental conditions can lead to a physical, chemical and biological degradation of polymers including a depolymerization step and a mineralization one. This environmental degradation includes a range of factors such as oxygen, heat, sunlight, moisture, water, wind, dust, living organisms, etc. Indeed, it has been observed that degradation appears due to a natural pre-ageing, caused by the exposure of UV light and heating for example. These photodegradation and thermo-oxidative degradation result in the formation of free radicals and trigger the oxidation of the polymer (Figure 2), with as consequence the insertion of carbonyl groups in the carbon chain. These additional functional groups allow the propagation of Norrish type I and II reactions, leading to the fragmentation of the PE and its oxidation, and decreasing the hydrophobicity of the polymer [16, 18–20]. So, the pre-oxidation step allows the formation of low molecular weight fragments of polymers, the adhesion of biofilm on these fragments, the biodegradation and the bioassimilation by microorganisms [16, 18, 19]. By this way, the carboxylic acids of the plastics can react with coenzyme A to form acetyl-CoA and enter into the citric acid cycle. Thus, the final biodegradation products are carbon dioxide and water in aerobic conditions, but also methane in anaerobic environment [17].

The biodegradative ability can be charged through additives. Some conventional plastics contain anti-oxidants preventing this natural oxidation and thus the degradability of this polymeric material. On the contrary, some biodegradable plastics contain pro-oxidants in order to speed up the degradation [21]. Yet, pure PE, i.e. without any additional compounds improving the quality of plastic, is non-absorbing in UV-light due to its saturated bonds (C-C and C-H). UV-light could have an impact due to the presence of chromophores such as additives, impurities and chemical modifications during the processing [22]. However, it has also been shown that micro-organisms could degrade pure PE without any pretreatment such as photo and thermal pretreatment [23], and that additives, stabilizers and colorings could be toxic for micro-organisms involve in the biodegradation process [16].

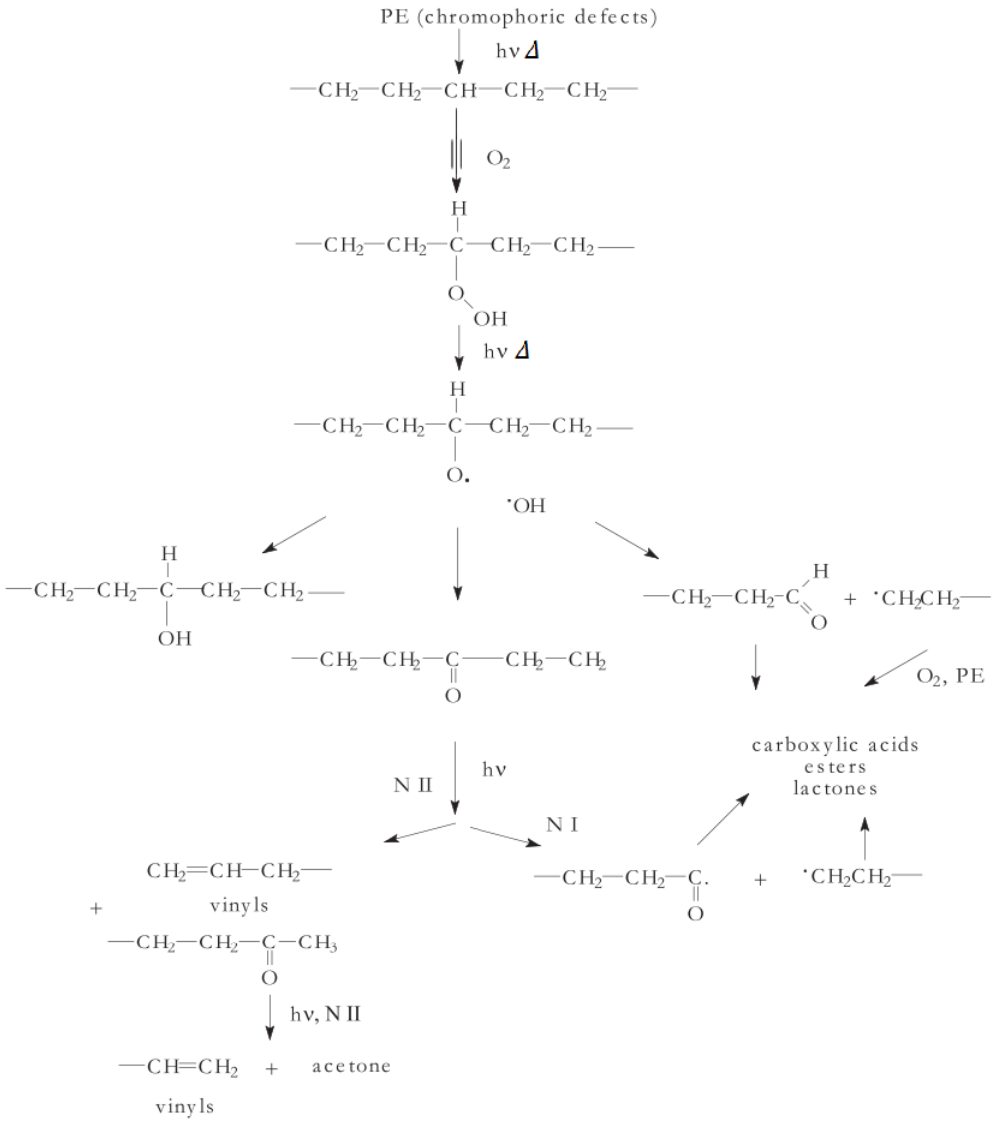

FIGURE 2: Mechanism of photodegradation and thermo-oxidative degradation of polyethylene

Source: Modified from [20]

2.2.1 Focus on *Galleria mellonella*

The recent work of Bombelli *et al.* (2017) highlights the biodegradation of polyethylene by caterpillars of *Galleria mellonella*, the greater wax moth. Nevertheless, the digestive mechanism of this plastic by this butterfly remains unknown. The enzymatic activities of both the symbiotic bacteria from the gut and caterpillars itself are still not investigated, asking the question of which species effectively entail plastic degradation [24].

Wax moth name refers to the specie known as a pest of honeybee colonies. Indeed, *Galleria mellonella* is found through the world, where beekeeping is practiced. Its ability to consume beewax, including hydrocarbon chains (polymers), may help to understand the ability to assimilate plastic, a synthetic polymer. The greater wax moth is a Lepidepteran insect of the Pyralidae family. As a holometabolous insect, *G. mellonella* has a life cycle with four stages : egg, larvae, pupa and adult. Stage period depends on environmental conditions [24, 25].

Galleria mellonella is commonly used as *in vivo* model for infection processes of many human microbial pathogens but also used as model to value the efficiency of an antimicrobial drug. Indeed, immune response in insects shows analogies with innate immune response of vertebrate. Hemocytes, phagocytic cells, are involved in the immune system of *Galleria mellonella*, which are similar to mammals. Moreover, the greater wax moth expresses some proteins presenting similarities with mammalian proteins and involved in humoral immune response as pattern recognition molecules. Finally, *Galleria mellonella* produces antibacterial peptides (AMPs) against bacteria and fungi [26].

Furthermore, polyethylene degradation by intestinal bacterial strains in waxworms gut (*Plodia interpunctella*, a Pyralidae) had been studied by Yang *et al.* (2014). It had been observed that this waxworm was able to consume PE bags resulting in observable deterioration of this PE film. Microbiota from gut of these insects, which had previously chewed PE, were recovered and cultivated first in flasks containing PE films. After two months of growth, plastic film were removed and analyzed whereas culture medium was spread across several plates with varied compositions of medium. Colonies were isolated and then purified in order to screen it. A total of eight bacterial strains was isolated including two visible and cultivable colonies; *Bacillus* spp. and *Enterobacter asburidae*. These two strains were selected to study PE degradation in a carbon-free medium. Their abilities to degrade PE had been highlighted thanks to several analyses such as the topography analysis with scanning electron microscopy (SEM) and atomic force microscopy (AFM) showing surface deterioration of PE film. Microattenuated total reflectance (microATR), Fourier transform infrared spectroscopy (FTIR) imaging and X-ray photoelectron spectroscopy (XPS) exposed concordant results resulting in additional carbonyl group to the polyethylene [23]. Indeed, the addition of carbonyl group to the polyethylene is known to be a mark of polyethylene degradation. Moreover, this observed oxidation of PE appeared without pre-treatment of the plastic.

Nevertheless, this kind of research remain limited by the observation of impacts on biodegradation of cultivable microorganisms. Furthermore, the enzymatic impact involved in PE degradation remains an unexplored field of study.

2.2.2 Focus on *Bacillus* spp

Among the microorganisms able to degrade plastics, it has been reported that *Bacillus amyloliquefaciens* (strains BSM-1 and BSM-2) can form a biofilm on low density polyethylene (LDPE) films [27]. Moreover, biomineralization of LDPE was observed due to the excretion of CO_2 and H_2O with LDPE as the sole carbon source in these culture conditions. The metabolic activity of *Bacillus amyloliquefaciens* was assessed by the pH change, supporting the degradation of LDPE. Changes of polymer surface have been proved by a scanning electron microscopy (SEM). Furthermore, a Fourier transform infrared spectroscopy (FTIR) determined the addition of functional groups on the LDPE 60 days after the inoculation of *Bacillus*, and thus supporting degradation of LDPE [27].

The choice of *Bacillus* spp. as a degrading bacteria is based on a previous study carried out by Das MP. and Kumar S. (2013) [28]. Indeed, LDPE films coming from waste were recovered in order to isolate attached microorganisms. The identification of the bacterial isolates were carried out thanks to 16S rDNA method and compared with GenBank database. Only two strains of the same specie (*Bacillus amyloliquefaciens* BSM-1 and BSM-2) were demonstrated to be degrading bacteria of LDPE films and thus used to evaluate cell surface hydrophobicity impacting the biofilm formation. However, this study presents some failures. Indeed, the authors assume that *Bacillus* spp. is the only bacteria of LDPE waste able to degrade LDPE film, without highlighting bacterial diversity of LDPE film waste and the link between this diversity and PE degradation abilities. So with *Bacillus* spp. as the sole bacteria tested for the biofilm formation among the supposed large bacterial diversity, the results could be incorrect. Furthermore, biodegradation of LDPE was not highlighted. Indeed, firstly they claimed a PE degradation without evidences. The hydrophobicity was measured thanks to a ratio based on the optical density (OD), according to the well-known Rosenberg's method currently named 'MATH' (microbial adhesion to hydrocarbon) [29].

The work of Roy *et al.* (2008) demonstrated the ability of a consortium of species of *Bacillus* (*Bacillus pumilus, Bacillus halodenitrificans* and *Bacillus cereus*) to degrade polyethylene [30]. Furthermore, this work highlights the abiotic impact to the biodegradation of LDPE film. Indeed, cobalt stearate were introduce to the LDPE films who were

irradiated with UV light, allowing a bacterial growth and hence a biodegradation of the plastic. So, cobalt stearate led to a photodegradable plastic film.

According to these previous studies, *Bacillus* genus seems to be a potential candidate to experiment polyethylene biodegradation and biofilm adhesion. Indeed, Nowak *et al.* (2011) exposed the LDPE film colonization abilities of *Bacillus* spp. in regards to the other isolated bacteria coming from the same soil sample [31].

Bacilli are a bacterial class representing a large group of species present in many environments like air, water, soil and even in food. *Bacillus amyloliquefaciens* is a widely studied specie in the agriculture field, inspiring new biotechnological approaches [32]. Indeed, the ability of *Bacillus* to produce cyclic lipopeptides (CLPs) enhances its development on surface due to the surface-active properties of CLPs [33]. Moreover, the capacity to sporulate is an interesting characteristic for commercial aims [34]. These traits are desired by biotechnology and pharmaceutical applications. Among this specie, *B. amyloliquefaciens* GA1 strain synthetizes amphiphilic molecules such as iturin A, fengycin A and B, and surfactin. Together, these tree lipopeptides act as biocontrol agents in the rhizosphere [33], classifying *Bacillus* spp. as plant growth-promoting rhizo-bacteria (PGPR) [35]. Furthermore, lipopeptides improve the cell spreading and the biofilm formation [33]. Indeed, this multicellular structure is partially due to the social motility named swarming [36].

2.2.3 Characteristics of a biofilm

2.2.3.1 Ecology

Biofilm is defined as "aggregates of microorganisms in which cells are frequently embedded in a self-produced matrix of extracellular polymeric substances (EPS) that are adherent to each other and or a surface" [37]. Biofilm is a natural mode of life widely spread through the world. Biofilm communities can be found in soil, marine environment, in plant and higher organisms, and even in extreme environment. It plays a key role in degradation of organic and inorganic matter, however their presence in some industrial processes or in the medical field is not always wanted [38].

This aggregate of microorganisms is a complex system composed of either a community or a population. From an ecological point of view, a population is characterized by organisms of the same specie whereas a community is defined as a group of several species [38]. Biodiversity and development of microorganisms of the biofilm depend on local conditions,

creating social and physical interactions inside the system itself but also with its external environment. Inter-cellular communication in biofilms is possible thanks to chemical and electric signals [38, 39].

The biofilm development is characterized by 5 main steps (Figure 3) [40]. The first step of the biofilm development itself (Figure 3 B) allows the initial attachment of planktonic cells to the surface. Besides intrinsic mobility of bacteria, cellular motility is due to diffusion, Brownian motion, gravitation and convection. Then, EPS production by attached bacteria induces a stronger adhesion of cells. This second step (Figure 3 C) is characterized by the irreversible bondings conducting to a micro-colony formation due to co-adhesion of cells (Figure 3 D). In these conditions, maturation of the biofilm can start (Figure 3 E). The last stage is the dispersion of free cells from the biofilm (Figure 3 F) [40–42].

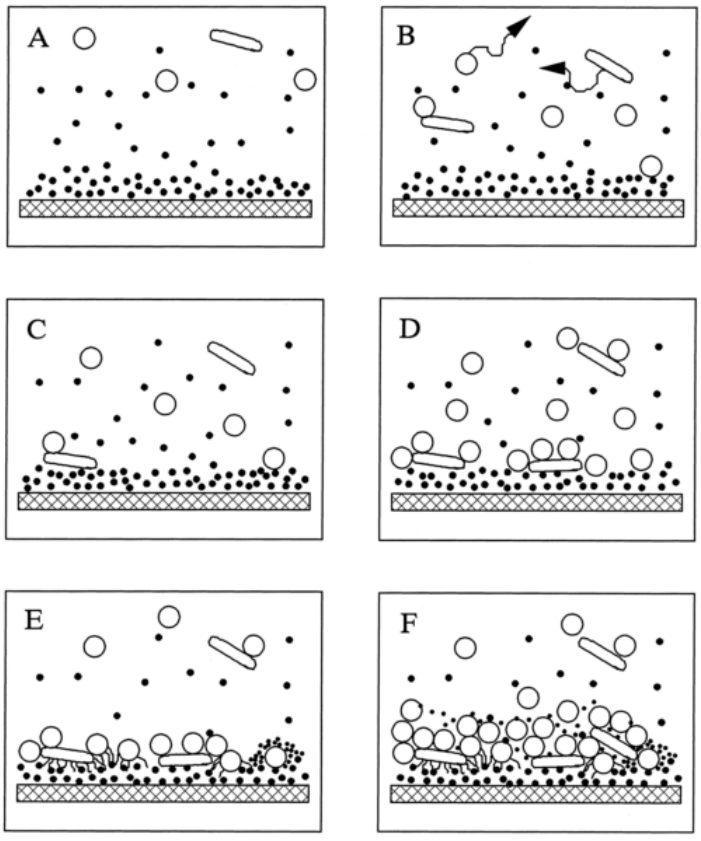

FIGURE 3: Biofilm formation : sequential development

A: two strains in an aqueous environment containing organic matter which coverts the substratum surface ; **B**: initial attachment of planktonic cells; **C**: EPS production and irreversible attachment ; **D**: micro-colony formation; **E**: maturation of the biofilm; **F**: dispersion of the single cell from the biofilm. Source: [40]

2.2.3.2 Physicochemical properties

Surface attachment is the first step of biofilm formation. Besides surface roughness and extracellular organelles interacting with the substrate surface, physicochemical properties of both surfaces, cells and substratum, are crucial to well understand biofilm formation, and particularly the bacterial adhesion process. Critical factors are: hydrophobicity (steric interactions) [43], DLVO theory (Derjaguin-Landau-Verwey-Overbeek) and its thermodynamic approach (surface free energy) [44]. Indeed, the work of Marshall *et al.* (1971) [45] seems to be the first one highlighting the process implied in the microbial adhesion (*Pseudomonas* spp.) to the substratum, taking into account the DLVO theory.

The classical DLVO theory (Equation (1)) of colloid stability results from the Lifshitz-van der Waals interactions (V^{LW}), generally attractive, and from the electrostatic charge of the cell (V^{EL}), attractive or repulsive (depending on the surface charge), to a net interaction (V^{DLVO}) [46].

$$V^{DLVO} = V^{LW} + V^{EL} \tag{1}$$

The Lifshitz-van der Waals interaction includes three types of forces : orientation forces of Keesom (dipole-dipole), induction forces of Debye (dipole-induced-dipole) and dispersive forces of London (induced-dipole-induced dipole interaction) [47].

The electrostatic interaction is developed by the electric double layer of the surface (Figure 4). This electric double layer is composed of a strong layer, the Stern layer, that balances the surface charge thanks to counter ions to reach electro-neutrality. Nevertheless, outside this layer, the diffuse electric double layer is defined by a mix of positive and negative charges reaching the electro-neutrality of the system. However the ions of this region are less attached to the surface than the Stern layer, and due to this, the electrical forces during an electrophoresis cause de detachment of the diffuse layer [48].

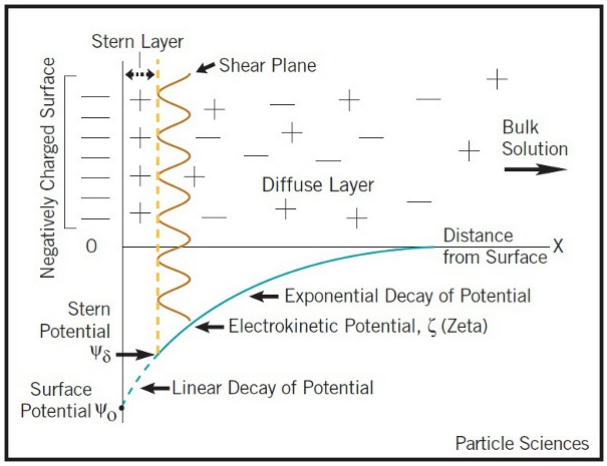

FIGURE 4: Model of the electric double-layer at a charged interface in aqueous solution

Source: [49]

Thanks to this kinetic phenomenon, the electrophoretic mobility may be measured and then converted into the Zeta potential (ζ) by the Helmoltz Von Smoluchowski relation (Equation (2)) [48]:

$$\mu = \frac{\epsilon_r \epsilon_0 \ \zeta}{\eta} \tag{2}$$

Moreover, surface potential (ψ, illustrated on Figure 4) is proportional to Zeta potential. The electrostatic interaction is thus defined as (Equation (3)) [48]:

$$V^{EL} \approx \psi^2 e^{-\kappa d} \tag{3}$$

Where ψ is the surface potential, d is the distance between the cell and the substratum and κ is the Debye lenght, the inverse of the thickness of diffuse double layer. This κ parameter depends on the dielectric constant of the solution, and hence V^{EL} depends on the ionic strength of the solution [44].

The surface free energy derives from the thermodynamic approach of the DLVO theory (Equation (4)) [46]. The adhesion energy, or net interaction energy (G_{slb}^{DLVO}), is function of the distance (d) between the bacterial cell (b) and the substratum (s), both included in a liquid medium (l). From a thermodynamic point of view, a negative total surface free energy (G^{DLVO}) leads to adhesion between two surfaces whereas a repulsion occurs for a positive G^{DLVO} value.

$$G_{slb}^{DLVO} = G_{slb}^{LW} + G_{slb}^{EL} \tag{4}$$

However, this classical DLVO theory assumes the inert surface property. This theory seems invalid for the bacterial surface and substratum surface immersed in a polar solvent, due to hydrogen and chemical bonds of bacterial surface [48]. A new term, referring to the extension of the DLVO theory (XDLVO), was introduced by van Oss *et al.* (1985) [47] to explain the contribution of energy of the hydrogen bond: the short range Lewis acid-base (AB) interactions [50]. The total adhesion energy (Equation (5)) is thus related to Lifshitz-van der Waals forces, electrostatic forces and Lewis acid-base and is defined as:

$$G_{slb}^{XDLVO} = G_{slb}^{LW} + G_{slb}^{EL} + G_{slb}^{AB} \tag{5}$$

The Dupré equation (Equation (6)) exposes the following thermodynamic approach including interfacial tension between two surfaces (γ_{ij}):

$$G_{slb}^{adh} = \gamma_{sb} - \gamma_{sl} - \gamma_{bl} \tag{6}$$

In order to obtain an adhesion (i.e. $G_{slb}^{adh} < 0$) between the cell and the substratum, γ_{sb} value has to be lower than the sum of γ_{sl} and γ_{bl} values.

The surface tension of one substrate (γ_i) takes into account both apolar aspect (Lifshitz-van der Waals) and polar aspect (Lewis acid-base) (Equation (7)) where the polar component (γ_i^{AB}) is defined by electron donor (γ^-) and electron acceptor (γ^+) surface tension subcomponents (Equation (8)) [51].

$$\gamma_i = \gamma_i^{LW} + \gamma_i^{AB} \tag{7}$$

$$\gamma_i^{AB} = 2\sqrt{\gamma_i^+ \gamma_i^-} \tag{8}$$

Whereas apolar and polar interfacial tensions between two substrates (γ_{ij}) are expressed respectively by the Equation (9) and the Equation (10).

$$\gamma_{ij}^{LW} = (\sqrt{\gamma_i^{LW}} - \sqrt{\gamma_j^{LW}})^2 \tag{9}$$

$$\gamma_{ij}^{AB} = 2(\sqrt{\gamma_i^+ \gamma_i^-} + \sqrt{\gamma_j^+ \gamma_j^-} - \sqrt{\gamma_i^+ \gamma_j^-} - \sqrt{\gamma_j^+ \gamma_i^-}) \tag{10}$$

According to Equations (6), (7) (9) and (10), the total interaction G^{adh}, also called the free energy, between different substrates (i.e. cell bacteria (b) and substratum (s)) immersed in a liquid (l) is thus described by Equation (11), neglecting the electrostatic interaction [51]:

$$G_{slb}^{adh} = (\sqrt{\gamma_s^{LW}} - \sqrt{\gamma_b^{LW}})^2 - (\sqrt{\gamma_s^{LW}} - \sqrt{\gamma_l^{LW}})^2 - (\sqrt{\gamma_b^{LW}} - \sqrt{\gamma_l^{LW}})^2 + 2[\sqrt{\gamma_l^+}(\sqrt{\gamma_s^-} + \sqrt{\gamma_b^-} - \sqrt{\gamma_l^-}) + \sqrt{\gamma_l^-}(\sqrt{\gamma_s^+} + \sqrt{\gamma_b^+} - \sqrt{\gamma_l^+}) - \sqrt{\gamma_s^+\gamma_b^-} - \sqrt{\gamma_s^-\gamma_b^+}] \quad (11)$$

However, the polar and apolar surface tension of substrates ($\gamma_s^{LW}, \gamma_s^+, \gamma_s^-, \gamma_b^{LW}, \gamma_b^+$ and γ_b^-) remains unknown. Thanks to Young's relation (Equation (12) and Equation (13) for substrate s and b respectively) [52], these values of surface tension can be found by contact angle measurement (CAM) with 3 kind of liquids (including a polar, an apolar one and a third one that can be either one of them) giving the contact angle value (θ) for each liquid on the considered substrate (s or b) (Equation (14) or Equation (15) respectively). Surface tensions of liquids ($\gamma_l^{LW}, \gamma_l^+$ and γ_l^-) are supposed to be known.

$$\gamma_l . \cos\theta = \gamma_s - \gamma_{sl} \quad (12)$$

$$\gamma_l . \cos\theta = \gamma_b - \gamma_{bl} \quad (13)$$

$$(1 + \cos\theta).\gamma_l = 2(\sqrt{\gamma_s^{LW}\gamma_l^{LW}} + \sqrt{\gamma_s^+\gamma_l^-} + \sqrt{\gamma_s^-\gamma_l^+}) \quad (14)$$

$$(1 + \cos\theta).\gamma_l = 2(\sqrt{\gamma_b^{LW}\gamma_l^{LW}} + \sqrt{\gamma_b^+\gamma_l^-} + \sqrt{\gamma_b^-\gamma_l^+}) \quad (15)$$

However, Equation (11) neglects the surface free energy induced by the electrostatic interaction (Equation (16)). If taken into account, G_{slb}^{EL} is expressed as Equation (17) assuming the ion-penetrable of the spheric cell and a constant fixed charge density [53]. This ion-penetrable layer is associated with peptidoglycan layer in the cell wall of gram-positive bacteria, such as *Bacillus amyloliquefaciens* [53,54]. Indeed, ion-penetrable bacterial surfaces do not possess a Stern layer. The measured electrical potential (ψ) is thus induced by the ion-penetrable layer (Figure 5) [54].

$$G_{slb}^{adh} = G_{slb}^{LW} + G_{slb}^{AB} \quad (16)$$

$$G_{slb}^{EL} = 4\pi\epsilon a[\psi_b\psi_s e^{-\kappa h} - \frac{1}{4}\psi_b^2 \frac{a}{a+h} e^{-2\kappa h}] \quad (17)$$

Where ϵ is the dielectric permittivity in the solution, a represents the radius of the cell, κ is the diffuse double layer thickness including the ion-penetrable thickness layer and h is the surface to surface separation distance between the cell and the substratum. Bacterial surface potential (ψ_x) is related to the charge density resulting from the charged groups of the surface constituting the ion-penetrable layer (Figure 5b).

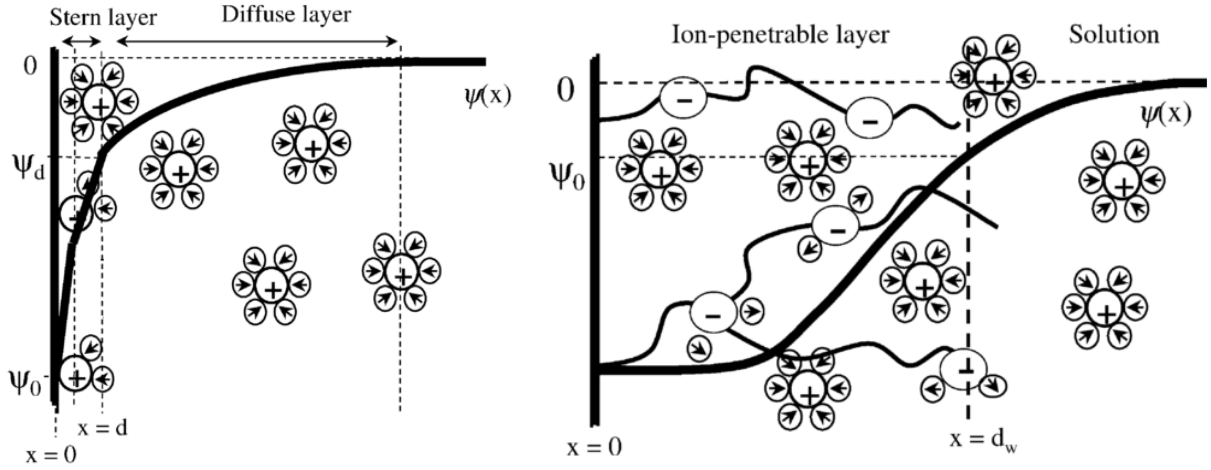

(A) Charged ion-impenetrable layer (Stern model) (B) Ion-penetrable bacterium

FIGURE 5: Electric potential profile (ψ)

Source: [53]

The properties of substrate surface and microorganisms surface influence the interactions between each other. However, these properties are models and adapted models of abiotic materials. The dynamic nature of cell surface of bacteria conducts to the modification of the chemical composition of cell wall, resulting in physicochemical variations. Moreover, ionic strength and pH of suspending medium, as well as EPS influence the surface charge. Indeed, associated or dissociated charged groups on cell surface change with pH and ionic strength. Furthermore, approaching a cell to the surface, either another bacterium or an inert surface, also influences surface properties. More specifically, the electric double layer is influence by the cell wall, in itself composed of charged groups [53, 54]. The heterogeneity of the cell wall has to be highlighted too, resulting in the heterogeneity of surface properties. Due to this complex structure and chemical composition, the short-range steric interactions are part of the bacterial adhesion to a substrate and have to be considered. Presence of steric interactions is assumed to impact energy and thus is predicted in DLVO theory [55, 56].

Another interpretation of the interaction energy is the Derjaguin approximation taking into account distance separation between surfaces. Concerning electrostatic interactions, this approximation is assumed to be applied in case of: $\kappa a \gg 1$ [57]. The total adhesion energy (G_{slb}^{XDLVO}) is then the sum of the three followed equations (Equation (18), (19) and (20)) [58]:

$$G_{slb}^{LW}(d) = -\frac{Aa}{6d} \tag{18}$$

$$G_{slb}^{AB}(d) = 2\pi a\lambda G_{slb}^{AB} e^{\frac{d_0-d}{\lambda}} \tag{19}$$

$$G_{slb}^{EL}(d) = \pi\epsilon\epsilon_0 a[2\psi_b\psi_s ln\frac{1+e^{-\kappa d}}{1-e^{-\kappa d}} + (\psi_b^2+\psi_s^2)ln(1-e^{-2\kappa d})] \tag{20}$$

Where A is the Hamaker constant in water, a is the radius of the cell, d is the minimum surface-to-surface separation, λ is the decay length for acid-base interaction, d_0 is the minimum separation distance due to Born repulsion, ϵ_0 is the dielectric permittivity of vacuum and ϵ is the dielectric constant of water.

Besides interactions between two different surfaces, free energy of cohesion is the interaction of two identical surfaces and is expressed by the Equation (21) and could be taken into account in biofilm formation [59].

$$\Delta G_{blb}^{coh} = -2\gamma_{lb} \tag{21}$$

2.3 Co-culture approach

Inspired by nature, a co-culture involves two or more populations of cells, growing with a certain degree of contact, to reach a stable, efficient and robust consortium [5, 60]. For example, industrial applications require co-culture systems to increase productivity of target molecules by the improvement of cell behavior thanks to the other cell population [61]. Indeed, the phenotypic expression is induced by both genotype and environmental factors which include other cell population, itself influenced by environmental conditions.

Spatial structure is an environmental factor affecting interactions inside the co-culture system and thus *in fine* impacting community dynamics. Indeed, interfaces solid-liquid, gas-liquid and gas-solid are involved in mass transfer and molecules spreading and it could lead to gradients of concentrations in given conditions and ultimately to conduct to localized effects, creating ecological niches. Due to the niches complementary, this heterogeneous environment could maintain a more performed microbial consortium compared to a homogeneous environment or a mono-culture suystem [62]. Degree of contact of populations included in the co-culture system are variable and are provided by several technologies. Among others,

microfluidics set up micro-scale environment in order to manage environmental conditions, whereas the use of membrane in co-culture system allows to study the impacts of molecules diffusion and share, without cell contact [63].

Definitively, coordination of cell populations perform specific metabolic networks [64] and can act as catalyst [65]. These metabolic interactions are thought to reach a stable culture of individually uncultivable microorganisms [66]. In addition, microbial consortia are more robust to environmental variations than a single population culture [67]. Natural examples such as lichens (biological structure including algae, fungal and bacterial symbionts) and biofilms illustrate this resilience through environmental variations and extreme conditions [63]. Furthermore, co-culture takes in consideration ecological interactions such as symbiosis like mutualism, commensalism or parasitism and non-symbiotic relations like predation and competition. In co-culture systems, the population ratio is a key factor to reach a stable and optimized system for given conditions [61]. Indeed, faster growing population could bestride the system and create competition for resource availabilities. Adjusting the population ratio may solve these problems [60, 63].

One the other hand, synthetic microbial ecology reaches two purposes. The first one is to understand the community properties derive from different microbial genotypes and their interactions. And the second one is to optimize production of synthetic microbial applications. Controlled experimental conditions allow to well define environmental properties for the study of microbial interactions and thus the monitoring of these microbial interactions [62]. Indeed, genetic engineering can lead relations to a specific and desired behavior of the established consortium [68], in a given environment [61].

The mathematical modeling is one of benefits of co-culture communities compared to natural communities, to predict long-term and over time behavior, but also to optimize growth or production parameters [61, 62]. Obviously, model design has to be validated by experiments [61].

However, community studies are much more complex than individual species. Indeed, even mono-cultures develop heterogeneous behaviors and phenotypes [61]. Moreover, co-culture does not represent the sum of individual activities but takes into account interactions such as energy, information and material exchanges between the different populations [68].

2.3.1 *Bacillus* spp. in co-culture with *Trichoderma* spp.

Among the infinite combinations of co-culture involving two populations, the use of fungal matrix for colonization by bacteria in rhizosphere was set up *in vitro* thanks to *Trichoderma* spp. and a PGPR like *Bacillus* spp [69]. Indeed, Triveli *et al.* (2013) highlighted the efficiency of both the biofilm formation and the co-culture system to reach an effective production of desired molecules and the target antifungal activity [69]. According to Deveau *et al.* (2018), bacterial-fungal interaction (BFI) are more and more investigated in varied fields such as biotechnology, environment, medicine, food processing and agriculture. This co-culture system integrates multidisciplinary studies such as chemical and microbial ecology, -omics approaches, molecular biology, biophysics and ecological modelling [70]. Moreover, these neighboring fungi manage bacterial spreading due to mycelial networks formed by multicellular filamentous fungi whereas biological and physical interactions are not totally understood [71].

As mentioned above, the common point between bacteria *Bacillus* spp. and fungi *Trichoderma* spp. is their abilities to have a symbiotic behavior with plant roots. Both species have a huge value for agriculture: its plant disease control and plant nutrients uptake can therefore help plant development, plant growth and resistance to pathogens [72]. In addition, several studies highlight the interaction between *Bacillus* spp. and *Trichoderma* spp. enhancing biocontrol properties [73–75]. *Trichoderma* spp. is a filamentous fungus and ubiquitous inhabitant of soil and rhizosphere. This is a green-spored ascomycete resisting to chemical pesticide [76]. According to Sowmya *et al.* (2014), *T. harzianum* is able to degrade UV-treated polyethylene by laccase and manganese peroxidase. Biodegradation was monitored by classical method such as SEM imaging, NMR, weight loss and FTIR. Moreover, in that case, the UV pre-treatment seems to be essential to improve this fungal degradation, causing the oxidation of the plastic surface. Crude laccase abilities to degrade PE was also investigated and results in FTIR spectrum modifications and weight loss, indicating a degradation of polyethylene [77].

3 Material and method

3.1 Extraction of microbial community from the gut of *Galleria mellonella* larvae

Insects breeding and digestive tract extraction of *Galleria mellonella* were realized by Samuel Latour during his Master's thesis [78], including beneficial results to this present work.

3.1.1 *Galleria mellonella* breeding

Insects breeding took place at 26 ± 3°C in boxes containing four caterpillars per box. On one hand, 0.1 g of PE film and 4 g of wax were added to the container. On the other hand, a standard diet was set up without plastic, thus only 4 g of wax. All larvae recovered for the analysis were 7 days old. Studied larvae were chosen on the basis on their stoutness and before the first stage of nymph metamorphosis.

3.1.2 Microbiota extraction

3.1.2.1 Digestive tract extraction

3 larvae of each diet were chosen for microbiota extraction. Intestinal bacteria coming from *Galleria mellonella* were extracted in sterile conditions. Firstly, the larva was immersed in ethanol in order to kill it and to disinfect the cuticle. The caterpillars was then rinsed in pure water. Seccondly, the extraction of midgut and hindgut was realized in sterile PBS 1X thanks to classical dissection material and a microscope, under a laminar-flow hood for sterile conditions. Finally, the foregut was removed in order to avoid environmental contaminations and for practical reasons linked to the method of dissection.

3.1.2.2 Microbiota recovery

The 3 digestive tracts were pooled together into 2 mL of PBS. A light vortex was applied, followed by a stronger vortex with glass beads in order to suspend microbiota in the PBS solution. 200 µL were recovered for the cultivation step (see below). A light centrifugation was applied on the rest of the mixture in order to decant insect residues and hence to recover the rest of the solution containing microbiota. This supernatant was then centrifugated during five minutes at 13.000 rpm. Three phases appeared; the upper one (phase C) seemed to be fat material (adipose tissues), the middle (phase B) one was the PBS solution containing biological soluble molecules and finally the cells were in the third phase (phase A),

thus at the bottom. Each phase was isolated separately and conserved at -20°C for further analyses.

3.1.3 Microbiota cultivation

The microbiota coming from larvae which grew with standard diet was cultivated. The recovered 200 µL were diluted until 10^6 (step of dilution: 10). 100 µL of each dilution were spread on Petri dishes containing LB medium (10% tryptone, 5% yeast extract, 10% NaCl, 20% agar).

Colonies were isolated and cultivated on Petri dishes (LB medium). The isolation was realized on the basis of the phenotypic appearance of each cultivable microorganism and identified thanks to numbers.

3.1.4 DNA screening

The main aim of the natural community investigation is the composition of intestinal microbiota of *Galleria mellonella* larvae. In order to obtain it, a Denaturing Gradient Gel Electrophoresis (DGGE) is a method used because it allows the visualization of the species richness and diversity. However, anterior steps had to be firstly optimized.

3.1.4.1 DNA extraction

Two methods of DNA extraction were done in order to compare the yield in term of species diversity from the recovered DNA and to compare cellular lysis efficiency to reach a better DGGE quality.

- **A** : DNA extraction was set up thanks to QIAamp® DNA Micro Kit according to the protocol for isolation of genomic DNA from urine. This protocol was applied on intestinal bacteria from standard diet, the related isolated colonies (numbered sample) and on intestinal bacteria from PE diet.

- **B** : A second method of DNA extraction was performed due to the unclear DGGE results obtained from the first one (Appendices page 75, Figure 21). This method was tested on intestinal bacteria from PE diet. Cells were resuspended into a 200 µL of a lysis buffer (2% Triton X-100, 1% SDS, NaCl 0.1 M, TRIS-HCl pH 8 0.01 M and EDTA 0.001 M) with 0.3 g of glass beads (acid washed, Sigma-Aldrich) and 200 µL of a phenol/chloroform/isoamyl alcohol solution (25/24/1) was added. Sample was then put into the dismembrator during 1 minute at 2000 rpm (Sartorius Mikro-Dismembrator

U). 200 µL of TE buffer (TRIS 10 mM and EDTA 1 mM) were added and sample was shaken during 30 seconds. A centrifugation (13000 rpm, 5 minutes, 4°C) was applied and the aqueous phase was transfered. 1 mL of iced ethanol 100% was added and the solution was slightly agitated. A new centrifugation was applied during 10 minutes. Supernatant was withdrawn and the pellet was resuspended in 400µl of TE buffer. 3 µL of RNase A Roche (10 mg/mL) was added followed by an incubation at 37°C during 5 minutes. 10 µL of ammonium acetate 4 M and iced ethanol 100% were added. The sample was slightly shaken. A third centrifugation was applied and the pellet was dried after removing the supernatant. Salts were removed thanks a wash of ethanol 70%. DNA was finally resuspended into 100 µL of sterile water.

3.1.4.2 DNA amplification

In order to carry out the DGGE, a polymerase chain reaction (PCR) had to be applied. Indeed, the PCR is a method amplifying nucleotide sequences. The PCR amplification was performed with PCR Using Q5® High-Fidelity DNA Polymerase (M0491). The used primers were Eu GC-F341-357 5' - CGCCCGCCGCGCGCGGCGGGCGGGGCGGGGGCA CGGGGGGCCTACGGGAGGCAGCAG - 3'and Eu R518-534 5' - ATTACCGCGGCTGCTG G - 3', amplifying the 16S rDNA region corresponding to the hyper-variable region V3 (position 341 to position 534). In this study case, an adjustment of thermocycling conditions had been set up thanks to the analysis beforhead of several species and strains of *Bacillus* spp. (MJ Research PTC-200 Peltier Thermal Cycler). Moreover, according to Muyzer *et al.* (1993), an addition of 40-bp GC rich clamp in 5' primer (5X Q5 High GC Enhancer) is useful for an optimal resolution of the fragments in the acrylamide gel [79]. All PCR reactions were checked thanks to the electroporesis gel results (2% agarose and 0.00005% midori in TAE buffer 0.5X, migration at 100 V). Two PCR thermocycling conditions were tested in order to enhance DGGE fingerprints.

- **A**: Thermocycling conditions were composed of an initial denaturation at 98°C during 30 seconds, an hybridization at 65°C and an elongation at 72°C. 35 cycles of hybridization and elongation were applied (30 seconds per cycle and 2 minutes for the last one). Hybridization temperature was optimized thanks to *Bacillus* spp. samples. A range from 55 to 70 °C with steps of 5°C was tested. Due to the addition of an enhancer, a hybridization temperature of 65°C was selected on the basis of the electrophoresis gel results (0.8% agarose and 0.00005% midori in TAE buffer 0.5X, migration at 100 V) and the T_m obtain from the online NEB Tm Calculator (Appendices page 74, Figure

20).

- **B**: Due to the apparition of double bands on the DGGE with method A, some enhancements had to be established. So, this PCR took into account two improvements of the PCR cycle. Firstly, the *touch down* method was set up. Then, a longer final cycle of elongation was carried out. The *touch down* method means that the applied temperature of hybridization is higher than the upper limit of annealing temperature [80]. By this way, the primer binding is much more specific. In order to favor amplification of desired sequences, the temperature is then gradually decreased to reach optimal temperature of primers [79]. The Hot Start *Taq* DNA polymerase (NEB) was used in this case. The second step of PCR cycle enhancement is an extension of the final cycle of elongation including 3 phases. Indeed, according to Janse *et al.* (2004), this step allows to withdraw additional strains appearing on DGGE [81]. For the first step, the thermocycling conditions were thus an initial denaturation at 95°C during 3 minutes. After that, for the second step, a second denaturation followed by an hybridization and then an elongation were applied at 95°C, 65°C and 68°C and during 30 seconds, 1 minutes and 1 minutes respectively. 20 cycles were realized in these conditions, with a reduction of 0.5°C at each hybridization cycle. Finally, the last phase was 20 cycles of a denaturation at 95°C, an hybridization at 55°C and an elongation at 68°C during the same times as the steps of the previous phase. However, the last elongation step lasted 15 minutes.

3.1.4.3 DNA purification

Purification step was processed thanks to the Monarch® Nucleic Acid Purification Kit (NEB). This test was carried out after the PCR in order to avoid potential artefacts coming from primers or sequence residues and appearing on the DGGE. Moreover the purification step allows to concentrate the DNA.

3.1.4.4 DGGE

In order to assess bacterial richness and diversity in the gut of *Galleria mellonella* larvae, a denaturing gradient gel electrophoresis was applied. This technique is based on the separation of the DNA molecules by their nucleotide sequences. The DNA fragments are exposed to a gradient of chemical denaturants, such as formamide and urea (increasing concentration from the top to the bottom), within an acrylamide gel. The melting properties of DNA fragments is the key factor for this electrophoretic separation. The denaturation of

DNA involves the unzipping of the double-stranded molecule and thus the decrease of the mobility in the gel. The higher the G-C pairing content is, the quicker the DNA fragment progress is. Thus a higher concentration of denaturant is required to melt DNA and to stop its migration through the gel matrix. That is the reason why a GC clamp is added to the primer. The migration also depends on GC positioning on the DNA sequence, allowing the differentiation of DNA comporting the same amount of GC pairing. A DNA binding fluorescent dye permits to observe stains in the gel under a UV light. Due to the specificity of DNA and the separation capacity, one band represents one specie of the sample and thus the species richness. However, closed species could be not distinguished. The relative abundance of each specie in one sample is evaluated by the intensity of their corresponding band to the other ones, illustrating the species diversity.

In order to set up a linear denaturating gradient inside the acrylamide gel, two solutions were prepared (Table 3); one with the lower concentration of denaturants (S1) and the other one with the higher concentration (S2). The choice of both concentrations depends on the DNA diversity. Solutions were mixed with ammonium persulfate solution (APS) 10 % and tetramethylethylenediamine (TEMED) in order to polymerize the solutions and thus to form the gel. A simple system based on atmospheric pressure was used to realize the linear gradient (from S1 to S2) during the gel formation. Polymerization took several hours. After that, the migration was realized in a TAE buffer 1X tank at 60°C (C.B.S Scientific compagny, DGGE-2001 model). Migration time depends on voltage applied. Finally, the acrylamide gel was immersed in a midori solution (0.015% in TAE buffer 0.5X) during one hour before being visualized under a UV-light.

TABLE 3: Composition of denaturant solutions used for the acrylamide gel formation

		Denaturant solutions			
Components	**Units**	**20%**	**40%**	**60%**	**80%**
40% acrylamide/bis	mL	18.8	18.8	18.8	18.8
TAE buffer 50x	mL	2	2	2	2
Glycerol	mL	2	2	2	2
H_2O	mL	69.2	61.2	53.2	45.2
Formamide	mL	8	16	24	32
Urea	g	8.4	16.8	25.2	33.6

DGGE was carried out with microbiota recoveries and cultivated microbiota from free polyethylene diet or with polyethylene diet (Table 4).

- **Test 1** included microbiota recovery from the standard diet (phases A and B) and the associated cultivated microbiota (samples number 1 to 10). The gradient used was 20% to 80%, including 80 µl of APS and 10 µl of TEMED. Migration lasted 14 hours at 60 V.

- **Test 2** concerned microbiota recovery from standard diet (MSDq) and associated cultivated microbiota (numbered samples). The microbiota recovery from PE diet were divided into two samples. For DNA extraction, one (MPEDq) was treated with the kit (Extraction A) whereas the second (MPEDp) was treated with phenol/chloroform (Extraction B). The gradient used was 40% to 60%, including 100 µl of APS and 10 µl of TEMED. Migration last 18 hours at 40 V.

- **Test 3** took into account two improvements of PCR cycles (DNA amplification test B). First, the *touch down* method was set up. Then, a longer final cycle of elongation was carried out. These improvements were performed on cultivated microbiota from standard diet (numbered samples) and on a mix of 3 *Bacillus* stains.

Table 4: Summary of achieved DGGE

	DNA treatment			**DGGE conditions**		
	Extraction	Amplification	Purification	Gradient	Current	Time
Test 1	A	A	No	20 - 80 %	60 V	14 hours
Test 2	A+B	A	Yes	40 - 60 %	40 V	18 hours
Test 3	A+B	B	No	40 - 60 %	50 V	17 hours

3.1.4.5 Amplicon sequencing

The PCR for the 16S rDNA sequencing was performed with the Q5® High-Fidelity DNA Polymerase (M0491) and the primers used were 8F and 1492R (T_m=64°C, cycle of 1 minute). The amplified fragments were sequenced by Eurofins GATC Biotech (Germany) and the sequences were red by the software SnapGene Viewer. The obtained sequences were then compared to the GenBank thanks to the basic local alignment tool (BLAST NCBI), avoiding bordered nucleotides (presence of background noise). The first four species exhibiting 100% (or 99%) of identity, the lower E-value and the 100% of query cover were taken into account.

3.2 Design of synthetic community for degradation of LDPE

3.2.1 Strains used

3.2.1.1 *Trichoderma harzianum*

The strain used was *Trichoderma harzianum* coming from the laboratory of Microbial Processes and Interaction (MiPI) in Gembloux Agro-Bio Tech, ULiège (Belgium). Spores were recovered after the mycelium development on Petri dishes containing a minimal medium (0.59 % $NaNO_3$, 0.052 % KCl, 0.15% KH_2PO_4, 1% glucose, 0.2 mM $MgSO_4$, trace elements 1X(500x: 38 mM $ZnSO_4$, 89 mM H_3BO_3, 12.5 mM $MnCl_2$, 9 mM $FeSO_4$, 3.55 mM $CoCl_2$, 3.2 mM $CuSO_4$, 3.1 mM Na_2MnO_4 and 87 mM EDTA) and 1.6 % agar). The average number of cells was estimated thanks to cytometry analyses (BD Biosciences, NJ USA).The concentration inoculated in the experimental culture was equal to $10^6 cells/mL$.

3.2.1.2 *Bacillus amyloliquefaciens*

The strain used was *Bacillus amyloliquefaciens* GA1 coming from the laboratory of Microbial Processes and Interaction (MiPI) in Gembloux Agro-Bio Tech, ULiège (Belgium). Bacteria were inoculated on Petri dishes with LB medium (1% of tryptone, 0.5% of yeast extract and 1% of NaCl). After 24 hours growth at 30°C, 1 colonies was recovered and suspended in a liquid culture as pre-culture (LB medium, 120 rpm, 30°C). It was used after 17h to inoculate the experimental culture with an OD_{600} of 0.1 (Thermo scientific Genesys 10 Bio).

3.2.2 Plastic and culture settlement

PE used for the experimentations was low density polyethylene (GoodFellow; LDPE Film - thickness : 0.23 mm). Squares of 8 x 5 cm of LDPE film were immersed in ethanol 70% overnight and finally dried in a laminar-flow hood. In order to study biofilm adhesion on plastic, one square was vertically placed in a 100 mL flask and fixed thanks to the wadding. This assembly was put in the oven at 105°C overnight.

Flasks were filled with 40 mL of TY medium (1% tryptone, 0.5% yeast extract, 0.5 % NaCl and 0.000094 % $MnCl_2$) and then inoculated first with *Trichoderma* spp. (10^6 cells/mL) and then, after 48h of fungal growth on the plastic, with *Bacillus* spp. (OD_{600} =0.1). Mono-cultures (*Bacillus amyloliquefaciens* and *Trichoderma harzianum* individually) were also carried out on plastic. Plastic controls were set up in a microbe-free medium.

Analyses were achieved over time. Indeed, measurement were performed on the first, the fourth and seventh days after the inoculation of *B. amyloliquefaciens*.

Each plastic square contained in a flask was cut into two parts (Figure 6). The first one was used to measure Zeta potential (ZP) of biofilm in its natural state (see Section 3.2.3.1). After that, sonication was applied on these samples in ice bath to remove biofilm formation and avoiding to heat the sample (Bandelin Sonolus HD 2070 and Bandelin electronic UW 2070). Repetitions of 9 pulses were applied on biofilm during 12 seconds (power 30%). The plastic was then immersed overnight in a KOH solution (1M) in order to lysis the cells, and then rinsed in pure water and dried. The plastic samples were then ready to measure the Zeta potential (see Section 3.2.3.1) and the contact angle (see Section 3.2.3.2). The second part of the plastic square was sonicated into PBS and ice, in order to remove the biofilm. The plastic substrate was then immersed in KOH 1M and was prepared for SEM analyses (see Section 3.2.5).

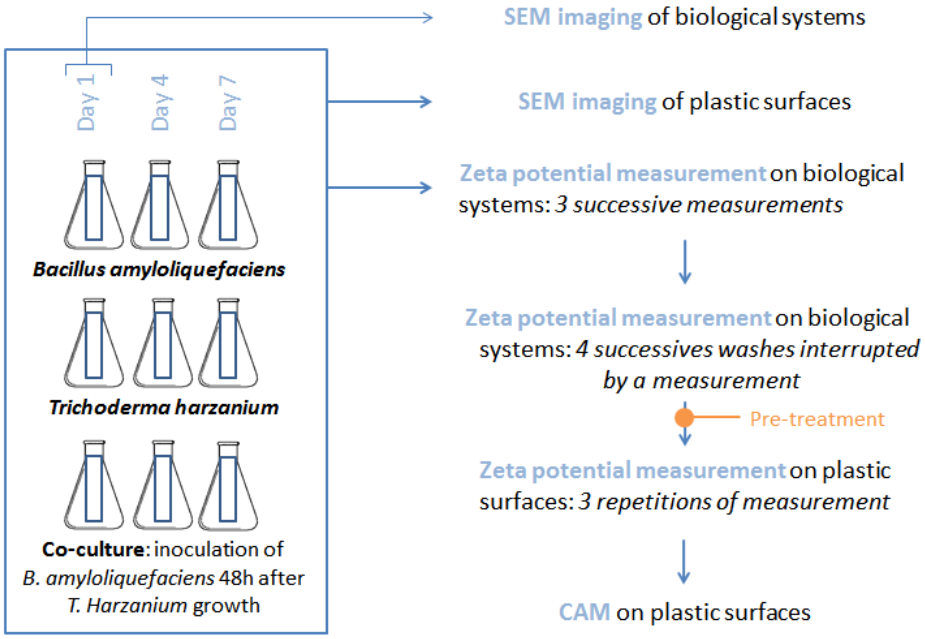

FIGURE 6: Experimental design applied on the synthetic communities

A total of 9 flasks containing a plastic square were analyzed. Two factors were tested: a biological one (mono-culture of *B. amyloliquefaciens*, mono-culture of *T. harzianum* and a co-culture of *B. amyloliquefaciens* and *T. harzianum*) and a temporal one: 24 hours (Day 1), 96 hours (Day 4) and 168 hours (Day 7) after inoculation of *B. amyloliquefaciens*.

3.2.3 Surface properties

3.2.3.1 Zeta potential measurement

In order to understand interactions between microbial surface and polyethylene, zeta potential (ζ) is a parameter leading to electrostatic interactions establishment. Based on the light scattering, the particle analyzer $Delsa^{TM}Nano$ C (Beckman Coulter Inc.) converts frequencies shift of light scattering into zeta potentials. Indeed, as previously exposed, an electric field (E) applied to charged particles makes it move toward an electrode opposite to the particle charge. The incident laser is scattered due to the particle moving and the frequency shift (V_D) of the light scattering is proportional to velocity of the particle (V) (Equation (22)), itself proportional to the electrophoretic mobility (µ) (Equation (23)) [82]. n is the refractive index of the solution, λ is the wavelength of the incident light and θ is the scattering angle.

$$V_D = \frac{\mu\ n}{\lambda} \sin\theta \tag{22}$$

$$\mu = \frac{V}{E} \tag{23}$$

Related to the Helmholtz von Smoluchowski relation, the zeta potential could be calculated (Equation (24)) taking into account the relative permittivity (ϵ_r), the vacuum permittivity (ϵ_0) and the viscosity of the solution (η):

$$\mu = \frac{\epsilon_r \epsilon_0\ \zeta}{\eta} \tag{24}$$

In order to carry out the Zeta potential measurement, a *Flat surface cell* was used. It is used for Zeta potential measurement of solid surfaces. The viscosity and the conductivity were monitored for each analysis. Cell center was adjusted if the intensity monitor showed that the sample concentration was too low, and/or the pinhole was established at 50 or 100 µm, still depending on the intensity monitor. The *Flat surface cell* was filled with milliQ water (Rephile, direct pure water system) previously immersed in ultrasonic water bath in order to withdraw gas (Branson 3200). .

Three successive measurements of biofilm samples were carried out one after the other, without removing the *Flat surface cell* from the instrument. After that, the water included in the *Flat surface cell* was replaced with 3 mL of milliQ. This change was done by just adding the water in the cell, pushing the old one outside. A measurement was then

achieved. This procedure of washing was repeated 4 times on each biofilm sample, followed by a measurement. Moreover, the Zeta potential of the plastic where the biofilm was attached was measured. Three repetitions of this measurement were carried out on each plastic sample.

3.2.3.2 Contact angle measurement

Surface tension is calculated thanks to Young's relation including the contact angle measurement. The surface tension is defined by the polar aspect named Lifshitz van der Waals component (γ^{LW}) and the apolar aspect named Lewis acid-base (γ^{AB}), itself defined by the basic part, electron donor (γ^{-}), and the acidic part, electron acceptor (γ^{+}). Thus, the Young relation exposes 3 unknown values (Equation (25)). Three contact angles have to be measured thanks to three solvents including at least an apolar and a polar one.

$$(1 + \cos\theta).\gamma_l = 2(\sqrt{\gamma_s^{LW}\gamma_l^{LW}} + \sqrt{\gamma_s^{+}\gamma_l^{-}} + \sqrt{\gamma_s^{-}\gamma_l^{+}}) \tag{25}$$

In order to carry out this measurement, TRACKER P.N./Tensiomètre/99 (I.T. Concept) was used. An automated drop of 2 µL was dropped off the surface of plastics used as solid substrate of the biofilm formation. The drop was deposited manually. Three solvents were used: milliQ water (Rephile, direct pure water system), ethanol (absolute for analysis EMSURE® ACS,ISO,Reag. Ph Eur, Sigma-Aldrich) and hexane (absolute for analysis EMSURE® ACS, Reag. Ph Eur, MERCK) (Table 5). The software connected to a camera carried out the measurement of the contact angle.

TABLE 5: Solvents used for CAM and its surface tension values (mJ/m^2)

Solvent	γ^{LW}	γ^{+}	γ^{-}	γ^{Tot}
Water	21.8	25.5	25.5	72.8
Ethanol	18.8	0.02	68	24.1
Hexane	18.43	0	0	18.43

3.2.4 Statistical analyses

The SAS software was used for the statistical analyses. Results from Zeta potential measurement of plastic surface were analyzed thanks to a two-way ANOVA; a crossed factors and mix model (n=3) was carried out with the day as a random factor (day 1, day 4 and day 7) and the biofilm was the fix one (*Bacilus amyloliquefaciens*, *Trichoderma harzianum* and the co-culture of both). Controls were taken into account.

3.2.5 SEM imaging

In order to observe plastic biodegradation, a scanning electron microscope imagery (SEM) was set up on each plastic sample and on two controls. Moreover, biofilm formation after the first day was observed thanks to this method.

First of all, several baths of ethanol were applied on the samples in order to fix bacteria and fungi on the substrate. This procedure was also applied on biofilm-free plastic samples and controls. The first bath consisted of EtOH 70 % during 30 minutes. The second one was EtOH 70% overnight followed by a third during 30 minutes (EtOH 70%). Two baths of EtOH 90% were applied during 30 minutes each. The last bath was composed of EtOH 100% and the samples were kept into this condition until the drying.

Indeed, super critical carbon dioxide allows to dry biological samples without any impacts on the shape of cells. The Polaron Critical Point Drier was used at 38°C and 80 bars. After 20 minutes, ethanol was withdrawn, and the process was repeated two more times.

The samples were then fixed on cylinders SEM (Ø 12.2x10 mm) with conductive doubled sided adhesive carbon tabs. The plastic samples where the biofilm was removed were cut into two parts in order to observe both surfaces of plastics.

SEM process is based on the surface-electron interaction. Indeed, photons are used in classical microscopy. But in the present case, an electron beam is focused on the surface of the sample producing various signals illustrating topography of the surface. These signals are the consequence of energy exchange between the electron beam and the surface. This interaction is possible due to an electronically conductive coating applied on the surface. Jeol JFC-11000E ion sputter was used to coat samples with gold in vacuum conditions during 2 minutes. Samples were observed thanks to a SEM Jeol 7200F 2000V (University of Mons).

4 Results and discussion

4.1 Extraction of microbial community from the gut of *Galleria mellonella* larvae

The first part of this work focuses on the identification of the microbiota present in the gut of caterpillar of *Galleria mellonella*, which is known to assimilate polyethylene [24]. This identification was carried out thanks to 16S rDNA sequencing applied on isolated cultivable colonies from the gut of the larvae fed with the standard diet (wax in this case). The results were then compared to a database to identify species (at least up to genus). Moreover, species richness and diversity of microbiotas were evaluated thanks to the DGGE method. Two diets were compared, the standard one and the polyethylene diet containing LDPE and wax. Finally, these investigations were compared to those obtained during a Master thesis performed on the study of the microbiota of digestive tract of *Galleria mellonella* based on omic approaches [78].

4.1.1 Community profiling by DGGE

Based on DNA migration, the DGGE is a method highlighting the species richness and diversity of a microbial community. The species richness is the number of species present in the studied ecological environment. The species diversity is the abundance of these species in the considered environment. The species richness is thus represented by the number of bands occurring on the gel, while the species diversity is illustrated by the intensity of these bands, giving a relative abundance (see Section 3.1.4.4, page 25).

Several tests of DGGE including different PCR conditions and DNA extractions were performed. Indeed, based on the first DGGE results, improvements needed to be made due to occurring double bands of certain individual cultivated bacteria and due to the poor species richness from the intestinal microbiota of *G. mellonella* larvae (Appendices page 75, Figure 21).

Firstly, the denaturating gradient was reduced (40-60%, instead of 20-80%). This adjustment allowed to obtain a better separation of the DNA fragments and thus a better resolution. Indeed, close species (from the same genus for example) are difficult to separate on a larger denaturing gradient. A low species richness is illustrated by only two stains on the DGGE, meaning that few genus are present in the microbiota of the gut of *Galleria mellonella* (Appendices page 75, Figure 21). However, the band intensity depends on the

specific abundance of DNA of the given specie. It means that other genus which are not noticeable on a DGGE gel because of its low DNA abundance in the mix could exist. In other words, two genus are mainly present in the gut of caterpillars of *Galleria mellonella* according to the first gel. This hypothesis of non-displayed species is supported by the comparison between microbiota and individual cultivable species (numbered samples on the DGGE banding pattern). Indeed, these second ones do not occur systematically in the intestinal microbiota band although individual cultivable species came from this same mix. The double band does not occur for each individual specie, meaning that the hypothesis of an inappropriate gradient gel is non valid.

For this technique, it is impossible to get information about the genus present in the mix without any positive control, and thus to know the bacterial flora of the gut in this case. A sequencing of the DGGE fingerprints could be an alternative to this lack of information. However, a positive control does not ensure a perfect match, close species may not be separable.

Secondly, intestinal bacteria from standard diet (MSD) was compared to intestinal bacteria from PE diet (MPED). Concerning this last one, two methods of DNA extraction were evaluated (see Section 3.1.4.1, page 23). The first one was the DNA kit extraction (samples MSDq and MPEDq) and the second one was phenol/chloroform DNA extraction (sample MPEDp) (Figure 7a). As mentioned above, the intensity of stains depends on DNA abundance. The purpose of testing another type of DNA extraction is to increase the amount of recovered DNA. In this way, underrepresented species may appear on the DGGE through supplementary bands for both microbiotas (from standard diet and PE diet). Moreover, a supplementary step was performed on the extracted DNA. Indeed, a DNA purification was carried out in order to isolate high-molecular-weight DNA by removing primers, including the enhancer. Indeed, double bands could be a consequence of the manifestation of inappropriate nucleotide sequences or shorter amplicons (Figure 7a). The expected improvements have not been achieved. Indeed, the stains appear weaker and scatter and no new stain occurs. Definitively, DNA extraction with phenol/chloroform is less efficient. Concerning the purification step, it has no impact because the double bands persist.

Finally, a combination of two PCR improvements was performed. The DNA extracted from the kit (without a purification step) went trough a PCR *touch down* and a longer final elongation time. The PCR *touch down* combined with the Hot Start polymerase is used to

increase the specificity. Moreover, this enzyme is known to be more accurate. The gradual decrease of annealing temperature increases yield of the amplification while higher annealing temperatures at first are used to be highly specific. Indeed, a misplaced nucleotide or a wrong one is enough to carry out a different migration than one from the correct DNA fragment. Concerning the longer final elongation time, it is believed to upset undesirable structure blocking the polymerase action [81]. However, no improvements are observed (Figure 7b). Indeed, the double bands and the smears persist. Thus, all these adjustments do not allow to withdraw double bands which arey a bias for species richness and diversity investigations.

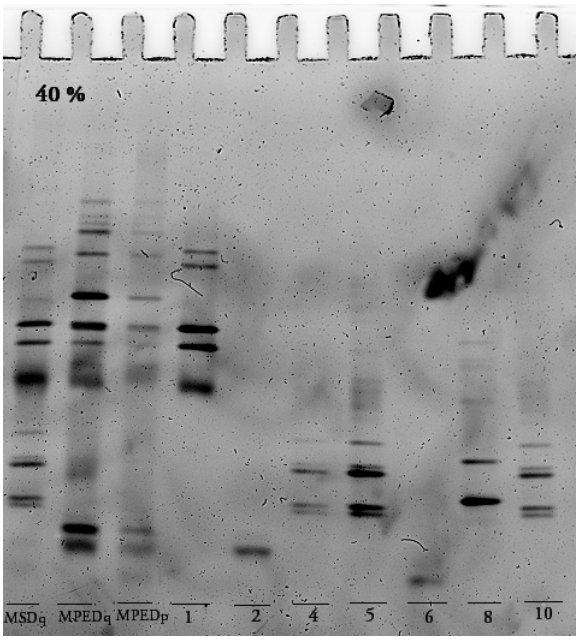

(A) Comparison of DNA extraction methods

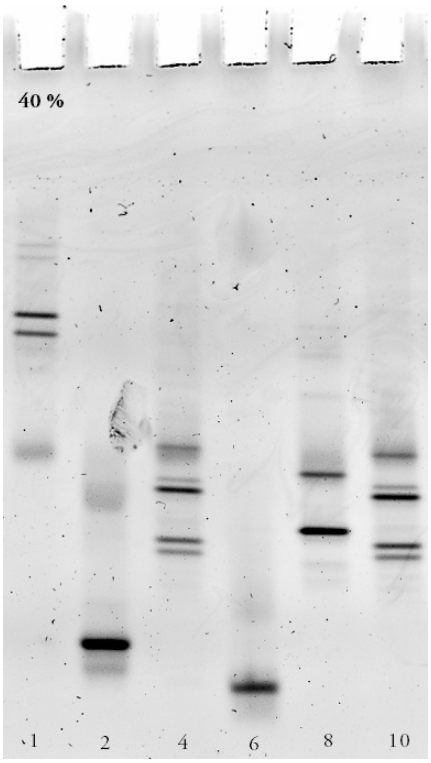

(B) DGGE results from the PCR "touch down" combined with a longer final elongation time

FIGURE 7: DGGE results from the pre-treated DNA adaptation

MSDq: Intestinal bacteria from standard diet (DNA kit extraction); **MPEDq**: Intestinal bacteria from PE diet (DNA kit extraction); **MPEDp**: Intestinal bacteria from PE diet (phenol chloroform DNA extraction) ; **Numbered samples**: Isolated colonies from standard diet; *Enterococcus spp.* (1); *Bacillus spp.* (2); *Paenibacillus spp.* or *Brevibacillus spp.* (4); Unidentified (5); *Micrococcus spp.* (6); *Bacillus spp.* (8); *Paenibacillus spp.* or *Brevibacillus spp.* (10)

Numbered samples related to isolated colonies from standard diet microbiota were identified (see next section), proving to purity of samples and stating the fact that double bands don't come from a contamination. For a better understanding, DGGE fingerprints were gathered and named with letters (Figure 8).

Next to these issues, Figure 8, showing a gel, gives interesting information about microbiota richness and diversity and its evolution between the standard diet and the PE diet. Indeed, the bands B and E of PE diet (sample MPEDq) don't occur in the case of standard diet (MSDq). The reverse is also true; bands A and D of standard diet are not present in the mix of PE diet. Moreover, identical bands C appear for both diets but thickness of these bands varies between the diets. It means that the ratio of bacterial diversity from a diet to the other differs. On the other hand, species richness (number and kind of species) of each diet could be equal, only the species diversity (its abundance) could be different between both diets. Indeed, low abundant species can be underestimated and may not be displayed on DGGE fingerprint.

Some isolated cultivable microorganisms are present in the standard diet microbiota where they came from; samples 4, 5 and 10 are included in the sample MSDq (square D, Figure 8). Sample 1 occurs both in the standard diet microbiota and in PE diet microbiota meaning that it is not impacted by the diet, even if its proportions could vary. Surprisingly, the bands called "A" do not occur in the PE mix whereas sample 1 is proved to be pure. In other words, squares A et C should represent together one specie whereas the A part is not present in the PE mix. At the reverse, the samples 2, 6 and 8 are not represented in any of two mixes. These species are thus underrepresented in both initial microbiotas. Based on this simple comparison between mixes and isolated colonies, species richness investigation has no sense in this case. Indeed, multiple bands occur but represent only one specie. Species richness and diversity are thus distorted. Furthermore, according to the DGGE results, standard diet mix contained only two major species (or genus) represented by the letters A and D (the letters C and A represent the same specie, according to sample 1), corresponding to samples 1 (A), 4, 5 and 10 (D). This hypothesis confirms that posited for the first unclear test. Concerning the species richness of PE diet microbiota, it is not more diversified. This mix displays the stains B, C and E on DGGE. However, B and E were not cultivated while stains A, C and D are sequenced strains and thus cultivable. A sequencing of excised bands B and E should be a way to overcome this lack of information.

Concerning isolated colonies, samples 4, 5 and 10 show the same profile meaning that these three samples may be the same species. Thus, number of isolated species is reduce to 5 (samples 1, 2, 4, 6 and 8). However, samples 5 and 10 display light supplementary bands above the square D. Sample 8 also shows 2 main bands and some lighter ones above them (Figure 8).

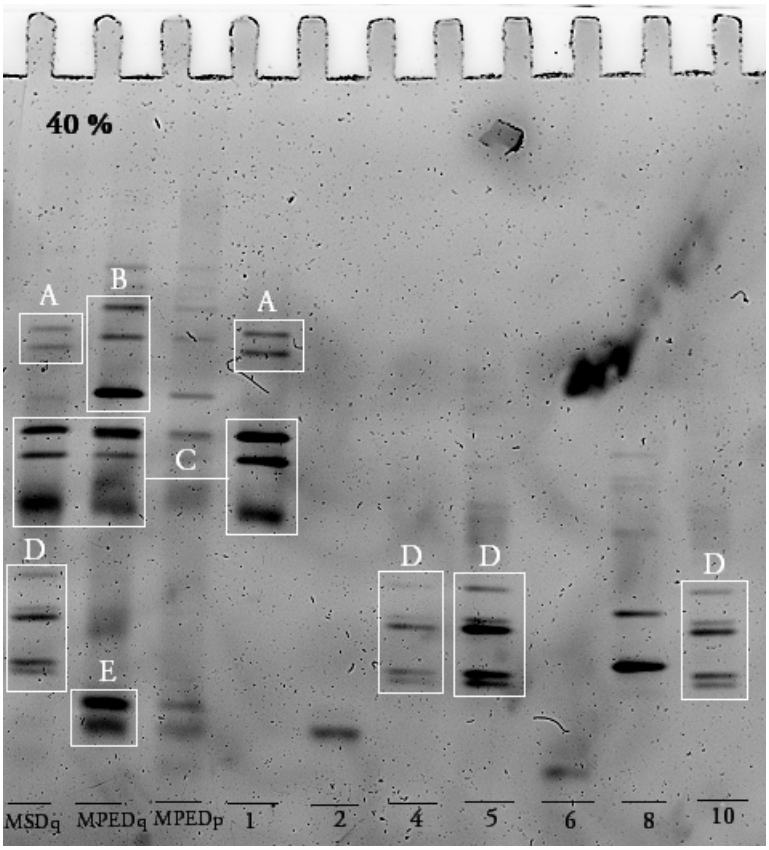

FIGURE 8: DGGE results of bacterial diversity and richness from the gut of *G. mellonella* and the associated cultivable strains

MSDq: Intestinal bacteria from standard diet (DNA kit extraction); **MPEDq**: Intestinal bacteria from PE diet (DNA kit extraction); **MPEDp**: Intestinal bacteria from PE diet (phenol chloroform DNA extraction) ; **Numbered samples**: Isolated colonies from standard diet; *Enterococcus spp.* (1); *Bacillus spp.* (2); *Paenibacillus spp.* or *Brevibacillus spp.* (4); Unidentified (5); *Micrococcus spp.* (6); *Bacillus spp.* (8); *Paenibacillus spp.* or *Brevibacillus spp.* (10)

In the case of this work, DGGE is not fit for species richness and diversity investigation. To overcome this issue, more reliable methods of diversity analyses are possible such as metagenomic approach. The low species richness could be due to a wrong bacteria recovery from the gut of larvae or, as suggested previously, it could be due to outstanding classes (Bacili and Actinobacteria). Indeed, the preliminary step of bacteria extraction from the gut was

not necessary for a DNA extraction of microbiota. Universal and specific primers were used for 16S rDNA amplification, excluding the hypothesis of a wrong amplifications regarding the set up of PCR optimization, although unsuitable primers for the entire diversified genome present in microbiota is not excluded [83].

However, diversity analyses by DGGE are currently carried out on caterpillar guts. Among other, the work of Shi *et al.* (2011) exhibited a low species richness of intestinal microbiota of silkworms. The DGGE results showed 13 stains including clearly double-band occurrence which were not examined by the authors [84] .

4.1.2 Amplicon sequencing for species identification

Microbiota of larvae fed with the standard diet (i.e. wax) was recovered and cultivated on Petri dishes. Obtained colonies were then isolated to get pure one. Its 16S rDNA sequencings were achieved and compared to GenBank database. Table 6 displays microbial ecology related to cultivable bacteria isolated from the gut of caterpillar of greater wax moth. Based on literature investigation, a sum up of its biology is then reported. Finally, these cultivated species are correlated to the global genomic and phylogenetic analyses of microbiotas (from standard diet and PE diet) of the gut of *Galleria mellonella* from [78].

First of all, all identified species change from a sample to another one, except for samples 4 and 10 showing the same results (Table 6), supporting the previous established hypothesis concerning the same isolated colonies according to the DGGE outline. However, sample 5, presenting the same stains profile than samples 4 and 10, is a mix of different species, as previously suggested. But concerning samples 8 and 10, lighter upper bands are definitively artefacts and are not a consequence of a hypothetical contamination because sequencing exhibits pure samples. As a reminder, the first four species (with high Query cover, 100% of identity and low E value) matching with the database were selected as potential present species in the gut (Appendices page 75, Tables 7 and 8). This comparison between DGGE results and sequencing allows to state that sampling based on the appearance of colonies on Petri Dishes is a limiting method. Indeed, it proves that the phenotype as a selection criteria for sampling is not satisfactory. Ideally, a maximum of isolated colonies should be considered to avoid any lack of genotype. Moreover, DNA sequencing proves the purity of samples. Thus, double bands occurring on the DGGE results are not a consequence of the presence of a mix of species in the numbered samples.

TABLE 6: Identification of cultivated bacteria from standard diet based on 16S rDNA sequencing results

	Specie	Forward	Reverse
Sample 1	*Enterococcus casseliflavus*	Yes	Yes
	Enteroccocus avium	No	Yes
	Enterococcus gallinarium	No	Yes
Sample 2	*Bacillus amyloliquefaciens*	Yes	Yes
	Bacillus velezensis	Yes	Yes
	Bacillus subtilis	No	Yes
Sample 4	*Peanibacillus larvae*	Yes (99%)	No
	Brevibacillus laterosporus	Yes (99%)	Yes
	Brevibacillus halotolerans	No	Yes
Sample 6	*Micrococcus yunnanensis*	Yes	Yes
	Micrococcus aloaevera	Yes	Yes
	Micrococcus luteus	Yes	Yes
Sample 8	*Bacillus cereus*	Yes	Yes
	Bacillus thuringiensis	Yes	Yes
	Bacillus subtilis	No	Yes
	Bacillus wiedmannii	No	Yes
Sample 10	*Paenibacillus larvae*	Yes	No
	Brevibacillus laterosporus	Yes	Yes
	Brevibacillus halotolerans	No	Yes

Enterococcus casseliflavus is a lactic acid bacterium belonging to the bacilli class, used in probiotic manufacturing and yogurt processing [85]. Tang *et al.* (2016) showed the ability of this bacterium to degrade decabromodiphenyl ether, a flame retardant considered as a persistent organic pollutant (POP) [86]. This molecule is uptaken into the microbial cell by transmembrane transport and used as carbon source through enzymatic activity. Absorption of POP is possible due to the hydrophobic characteristic of this substance and the cell membrane. This kind of flame retardant is used during plastic manufacturing. Its biodegradation is thus a complement to polyethylene degradation. Such as *Enterococcus casseliflavus*, *E. avium* produces a bacteriocin against *Listeria monocytogenes*, isolated from a honeybee beebread [87]. Moreover, *E. gallinarium* and *E. casseliflavus* were both classified

as lignocellulose degrading bacteria, a complex polymer [88].

The being of *Bacillus* spp., and more specifically *Bacillus amyloliquefaciens* is not odd. Indeed, as previously mentioned, *B. amyloliquefaciens* is an ubiquitous bacterium. On the other hand, surprisingly, *B. thuringiensis* is used as bioinsecticide due to the production of crystal proteins upsetting the peritrophic matrix of the insect gut [89]. The consequence is an easier access of virion to intestinal epithelial cells of lepidopterans [90]. Genes coding for that viral enhancin protein are also found in *Bacillus cereus* genome [91,92]. *B. cereus* group includes *B. thuringiensis* and the novel specie *B. wiedmannii*. This last one is found in dairy product and is able to hydrolyse starch and casein [93]. Concerning *Bacillus subtilis*, Vimala P. and Mathew L. (2016) demonstrated the ability of this Gram positive bacteria to degrade PE. They concluded that a UV light pretreament of plastic improves the degradation, as well as an addition of biosurfactant synthesized by *B. subtilis*. After 30 days of incubation, weight loss percentage of 9.26% were achieved for LDPE 18 µm of thickness [94]. *Bacillus velezensis* acts as biocontrol agent such as *B. amyloliquefaciens* and *B. subtilis*, by CLPs production [95]. Furthermore, among other *Bacillus* spp. [96], *B. velezensis* is able to degrade azo dye thanks to an azoreductase [97]. The degradation of this synthetic pigment was tested in a batch biofilm reactor with polyethylene used as packing media and thanks to microorganisms from wastewater treatment plant [98]. This process seems to be an efficient method of bioremediation against azo dye. The LDPE used to feed *Galleria mellonella* larvae was supposed to be pure, thus without any pigments. However, current plastic items are plenty of additives including dyes. This approach is thus complementary to PE degradation.

Another isolated bacilli is *Paenibacillus larvae*, a pathogen responsible of American Foulbrood of honey bees. According to Ebeling *et al.* (2016), this parasite is present in only one host: the gut of honey bee larvae [99]. However, its presence in the caterpillar gut of *G. mellonella* is not meaningless because of the characteristic of this lepidopteran parasiting this hymenoptera. *P. larvae* secretes a chitin-degrading protein hydrolyzing the polymer composing the peritrophic matrix coating the gut epithelium of most insects [100]. *Brevibacillus laterosporus* exhibits a chitinase activity, just as *P. larvae* [101]. Furthemore, *P. larvae* is able degrade dye as well as *Bacillus velezensis* [102]. *Brevibacillus halotolerans* is a novel aerobic bacteria found in saline soil (China). Its 16S rDNA is close to that of *B. laterosporus* [103].

Another phylum takes part of the microbiota present in the gut of *G. mellonella* caterpillar: Actinobacteria represented by *Micrococcus* spp. Among them, *Micrococcus luteus*

is able to degrade azo dye, according to Singh *et al.* (2015) [104]. This biodegradation is carried out by laccase [105], an oxidoreductase enzyme also synthesized by fungus and proved to be able to degrade PVC [106] and gamma-irradiated LDPE in fungal cultures [107]. Indeed, as previously mentioned, laccase, synthesized by *Trichoderma harzianum*, is involved in the degradation of UV-treated PE [77]. On the other hand, *M. luteus* seems able to synthesize a biopolymer, the polyhydroxybutyrate (PHB), a substitute for petrochemical plastic [108], itself degraded by *Bacillus* genus thanks to PHB depolymerase [31]. *M. yunnanensis* and *M. aloeverae* species were also isolated from the gut of the greater wax moth larvae and produce alkaline protease [109].

This investigation gives a global view of cultivable microorganisms present in microbiota of the caterpillars of interest and its potential applications in terms of plastic and polymer degradation and bioremediation abilities. Indeed, according to literature, some of bacteria are able to degrade plastic or complex polymer such as lignocellulosic material, while others synthesize enzymes involve in biodegradation of plastic additives like flame retardant and azo dye. However, no assertion related to plastic biodegradation can be claimed because no bacteria from those microbiotas was cultivated on LDPE during this work. Definitively, the lack of replicates gives weak outcomes resulting in light interpretations. Moreover, the BLAST results is limited by the obtained sequence. Indeed, bordered nucleotides were arbitrary removed due to background noise, discriminating stains comparison. Moreover, several species have a 100% identity match when their sequences are compared to the database, preventing the assertion of the presence of one or the other species in the considered microbiota. Concerning sample number 10, two genera are possible of Paenibacillaceae family; *Brevibacillus* and *Paenibacillus*, while other samples exhibit one genus but several species and strains.

Cultivable microorganisms from microbiota impacted by PE diet were not cultivated and sequenced. Obviously, it could be interesting to compare cultivable microorganisms from both diets and to investigate the ability of polyethylene degradation in both mono- and co-culture systems. Furthermore, plastic digestibility could be possible thanks to a consortium of microorganisms living in precise conditions, involving perhaps non-cultivable microorganisms. On the other hand, concerning the composition of cultivated microorganisms, it depends on ratio; overrepresented species in microbiota could prevent the growth of other cultivable species. Moreover, the culture conditions selected themselves the cultivable bacteria, while a universal medium was used.

According to the results obtained from the Master thesis [78], the three main identified phyla present in intestinal microbiota of *G. mellonella* larvae are Firmicutes, Proteobacteria and Actinobacteria for both standard diet and PE diet (Appendices page 77, Figure 22). Minor and unclassified phyla represent maximum 20% of total phyla. The tree main represented families in these microbiotas are Enterococcaceae, Comamonadaceae and Oxalobacteraceae, increasing the relative abundance of minor and unclassified families (Appendices page 77, Figure 23). Comamonadaceae and Oxalobacteraceae are both included in the Burkholderiales order, representing 21.8 % of total order of these microbiotas (average on PE diet and standard diet). This order is known to assimilate plastic [110]. Finally, the most represented genus is *Enterococcus*. This genus is displayed in DGGE and represented by square A on Figure 8, according to the sequencing of sample 1. This comparison matches with the hypothesis of overrepresented specie. However, surprisingly, *Paenibacillus* and *Brevibacillus*, illustrated by square D and thus present in microbiota from standard diet, are underrepresented even nonexistent according to the other Master thesis results [78]. Moreover these two genus are obtained for the same sample (according to nucleotide alignment), decreasing the fidelity of this result. The relative abundance of the genus *Bacillus* is not obtained but the Bacillaceae family is not negligeable (Appendices page 78, Figure 24) [78].

Furthermore, according to the results obtained from the Master thesis [78], there is no significant difference between both diets in terms of species richness and diversity, while DGGE results exhibit a visual difference. Again, this difference of species richness could be distorted by a wrong DNA extraction and thus non-displayed DNA fragments, leading to a potential species diversity instead of a species richness. In order to assess if DNA extraction impacted by bacteria isolation from the gut was not well performed, a comparison between DNA from [78] samples and extracted DNA carried out during this experimentation could be done, by depositing them side by side on the same gel. Moreover, a direct link between the Master thesis [78] and the efficiency of DGGE (in terms of species richness and diversity interpretation) would be highlighted.

4.2 Design of synthetic community for degradation of LDPE: mono- and co-culture of *Bacillus amyloliquefaciens* and *Trichoderma harzianum*

Next to this natural community investigation, a synthetic community was set up. The aim is to understand the biofilm development and its action on low density polyethylene. *Bacillus amyloliquefaciens* GA1 seems to be a perfect candidate for this approach. Indeed, as previously demonstrated, *Bacillus* genus is present in intestinal microbiota of *Galleria mellonella*, known to degrade plastic [24], and its biofilm formation abilities are well known [33]. Assessing the fact that the first step of microbial biodegradation of plastic is the biofilm development, it is hence logical to bear interest to physicochemical relation between biological systems and a plastic surface. Moreover, a co-culture settlement with the fungus *Trichoderma harzianum* was studied because of its relationship with *Bacillus* spp. Furthermore, this fungus synthesized laccase, an enzyme implied in PE degradation [77].

Mono- and co-culture of *Bacillus amyloliquefaciens* and *Trichoderma harzianum* were performed in flasks including a LDPE film. The analyses were performed over time, resulting in 9 flasks from which biofilm and plastic samples were extracted (Figure 9). Controls, without microbial inoculation, were carried out (see Section 3.2, page 28). The samples "Day 1" correspond to analyses performed on *B. amyloliquefaciens* after 24h of culture, *T. harzianum* after 72h of culture and the co-culture after 24h of co-culture (*B. amyloliquefaciens* was inoculated 48h after inoculation of *T. harzianum*). Physicochemical investigations of biotic and abiotic surfaces were achieved due to Zeta potential (ZP), while contact angle measurement (CAM) was only performed on plastic surfaces. Concerning ZP measurement on biologic systems, 3 repetitions of measurement were carried out. After that, the water included in the *Flat surface cell* was replaced with fresh one and a measurement was performed. This procedure of washing was repeated 4 times on each biofilm sample, followed by a measurement. Biological systems were then removed from plastic and ZP and CAM were performed on these abiotic surfaces. Finally, SEM imaging was achieved on the 9 plastic surfaces. Furthermore, on day 1, the three biological systems fixed on plastic surfaces were observed by SEM.

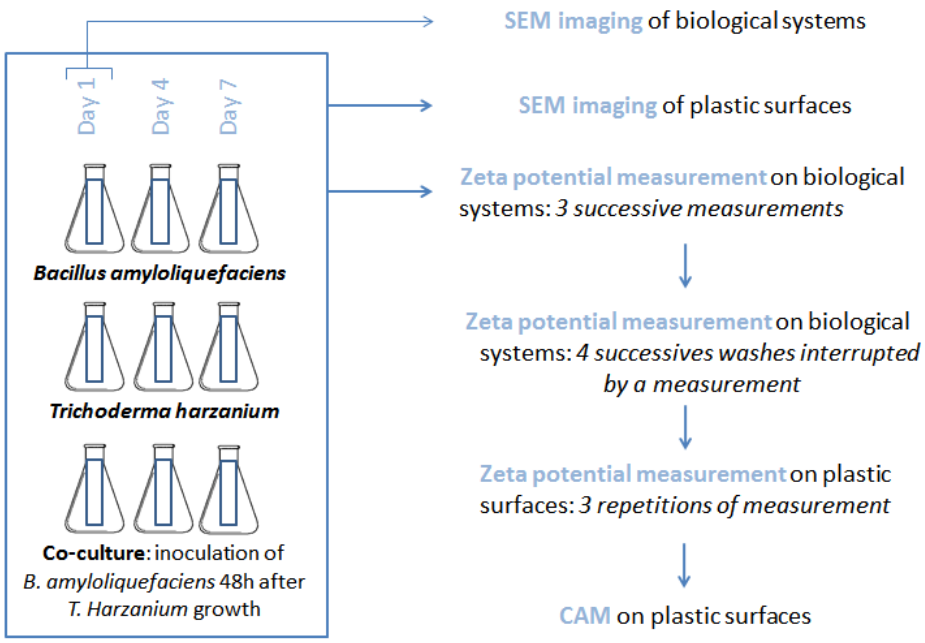

FIGURE 9: Experimental design applied on biofilms and plastics, including physicochemical analyses and SEM imaging

4.2.1 Properties of biofilm surfaces and plastic surfaces colonized by microbial systems

In order to understand interactions between biological systems and substrates, electrostatic aspect and the hydrophobicity of surfaces, both dictated by the XDLVO theory, enable the highlight of the physicochemical approach of these interactions. Indeed, short-range and long-range contributions (Lewis acid-base and Lifshitz-van der Waals respectively) are expressed with surface tensions calculated from CAM, while electrostatic aspect is related to Zeta potential of surfaces.

4.2.1.1 Zeta potential of biofilm

First of all, for each biofilm sample formed on PE, 3 repetitions of the Zeta potential analyses were performed for the same culture times (day 1, day 4 and day 7). For one analysis, the instrument considers 7 measurements according to 7 positions (x and y axes) on the surface. The averages were then calculated (named M1, M2 and M3) and compared in function of culture time and the considered biofilm (*B. amyloliquefaciens*, *T. harzianum* and the co-culture of both of them) (Figures 10, 11 and 12). Moreover, instrument performed one measurement of ZP on pure water where biofilms were immersed.

Biofilm formed by *B. amyloliquefaciens* discloses an expected negative value of ZP after 24 hours of growth (Figure 10) [53], in previously determined conditions. This Zeta potential increases until 4 days of growth (96h), reaching its maximum value of approximately zero, and then decreases slightly reaching a minimum mean value of -2.31 mV (Appendices page 79, Table 10). This evolution could be associated to the accommodation of the biological system to its environment and substrate, secreting various EPS dictating the ZP of the biofilm. It must be emphasizes that the ZP measurement was achieved on the biofilm part which is not directly in contact with polyethylene but at the opposite side. Thus, this measurement could reflect distorted values of ZP really involved in biofilm-substrate interaction.

The 3 successive measurements follow the same trend in function of time, although standard deviations (SD) are high for all the measurements, especially on day 1 and day 7 (24h and 168 respectively). This broad spectrum of ZP values for one analysis makes us believe a heterogeneity in terms of charges (positive and negative) as well as in terms of absolute values. Indeed, for the first day (24 h), the minimum value is equal to -15.6 mV and the maximum is close to 1 mV whereas for the seventh day (168h) the values goes from -14.89mV to 3.84 mV (Appendices page 79, Table 10). Moreover, small variations between successive measurements could traduce a possible molecular exchange from biofilm to pure water in which microbial system is immersed, reaching osmosis. This hypothesis is supported by the measurement of ZP of pure water carried out simultaneously. Indeed, the instrument performed one ZP measurement of water contained in the *Flat surface cell* where the biofilm was immersed. These values are not negligible in this case, supporting the loss of charged molecules from biofilm surfaces (Appendices page 79, Table 11). The other hypothesis is that the light variation between the three measurements may still display an heterogeneity of charged surface.

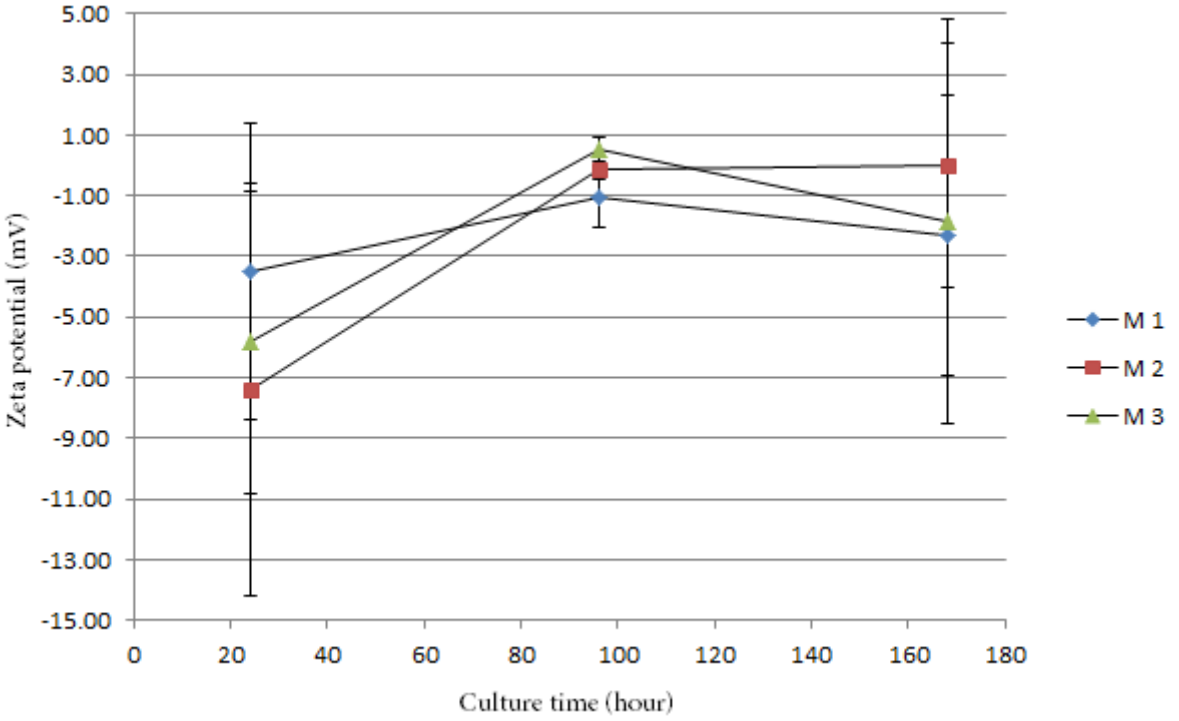

FIGURE 10: Evolution of Zeta potential of *B. amyloliquefaciens* biofilm surface in function of culture time and succesive measurements (M1, M2 and M3)

On the other hand, mycelium formed by *T. harzianum* gives more constant ZP values for successive measurements (Figure 11). Indeed, the three curves have the same behavior - excepted for the first measurement at 72h after fungal inoculation, meaning that interaction between fungal surface and aqueous environment is negligible in terms of charged molecules or that the surface is much more homogeneous in terms of charge distribution. Surprisingly, global drift is similar to ZP of *B. amyloliquefaciens*, however the ZP flatten out and becomes closed to zero between 144 and 192 hours of fungal growth. This last observation is unexpected. As filamentous fungus, *Trichoderma* spp. secretes hydrophobins, a surface-active proteins found at the interface of hyphae and the surrounding environment, as well as spore surfaces [111]. According to Singh *et al.*, the ZP values of different strains of *T. harzianum* ranged from -39 to -11 mV. Moreover, ZP values decrease with culture age, becoming more negative [112]. Nevertheless, the maximum value and the minimum one reach 37.9 mV and -33.29 mv respectively, and thus the standard deviations of measurements for the first day (72 hours) are really broad (Appendices 79, Table 10). In other words, surface heterogeneity of the fungus is demonstrated for the first day, while an homogeneous surface is display at a longer culture time. The ZP measurements concerning pure water associated to biofilm exhibits remarkable positive values for the three first measurements on the first day (Ap-

pendices page 79, Table 11) while the ZP of water of the last day (day 7 i.e. 192 hours) are insignificant which correlates with SD obtained for the ZP biofilm. Again, it may mean that molecular exchanges could lead to a variable ZP value of the mycelium surface such as previously expose in the case of *Bacillus amyloliquefaciens*.

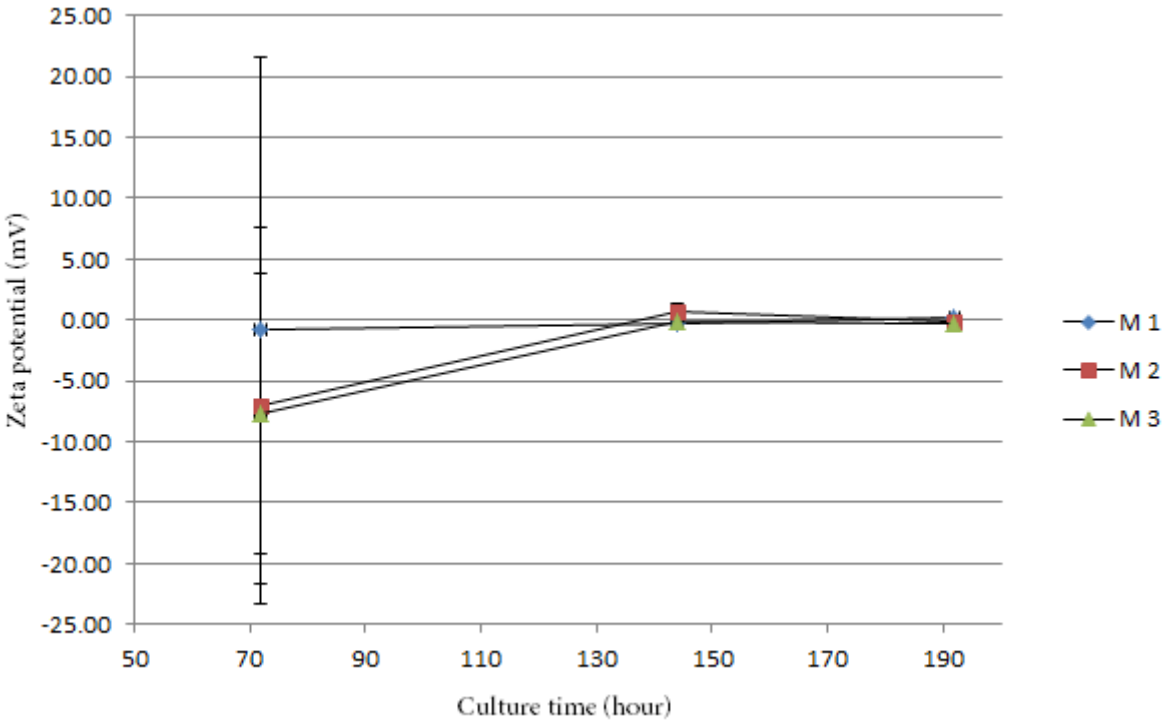

FIGURE 11: Evolution of Zeta potential of *T. harzianum* mycelium surface in function of culture time and successive measurements (M1, M2 and M3)

Concerning the co-culture, the ZP seems to reach an equilibrium from 24h to 168h (Figure 12). Indeed, the three measurements remain close to each other while its time evolution maintains the same level of ZP values (around zero) (Figure 12). Moreover the standard deviations are low compared to ZP scale and negligeable compared to the SD values obtained for *T. harzianum* after 72h of culture. This means that the charged surface of the co-culture is more homogeneous than mono-culture and stable over time. This ZP measurement is particular due to the fact that 3 surface interactions, immersed in an initial inert aqueous medium, are considered. Indeed, *T. harzianum* and *B. amyloliquefaciens* are in co-culture and adhere on the plastic surface. Plastic-fungus, plastic-bacteria and bacteria-fungus surfaces are thus taken into account. These low ZP values possibly highlight an equilibrium in terms of electrostatic interactions between all these surfaces. Or, on the contrary, that electrostatic interactions are negligible compared to other involved forces, such as hydropho-

bicity, hydrogen bonding and Lifshitz-van der Waals interaction. Finally, it should not be forgotten that the ZP measurement is directly linked to the charge concentration and pH. Even if methodology was identically replicated from one sample to another concerning the culture conditions and the ZP measurement, these two factors have to be taken into account.

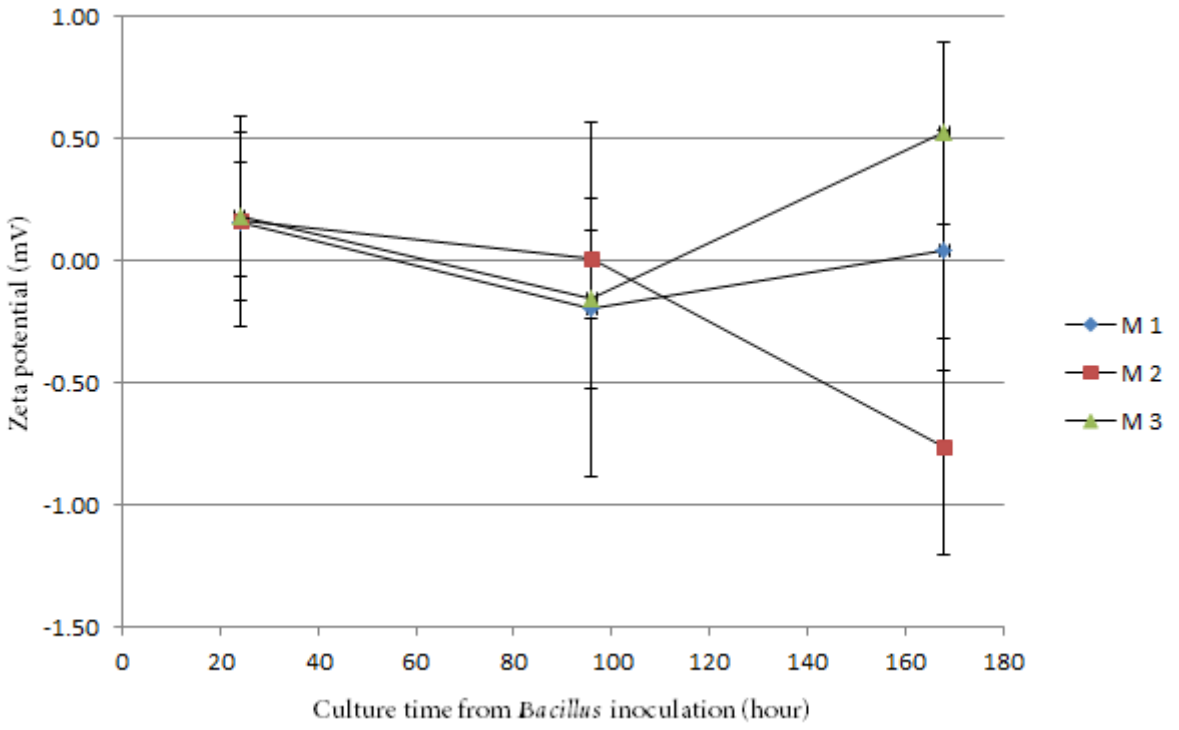

FIGURE 12: Evolution of Zeta potential of co-culture in function of culture time and successive measurements (M1, M2 and M3)

In order to understand impact of water on the Zeta potential measurement performed on biological systems, 4 washes with pure water were applied on these biofilms included in the *Flat surface cell*.

Concerning the *Bacillus* sample, the first and last wash do not express a variation and this for both ZP measurement (biological system and water) (Appendices page 80, Figures 25a and 25b respectively). Moreover, wash 2 on day 7 and wash 3 on day 4 express the same values of ZP for both systems (biofilm and water) and thus seem to reach a perfect charge equilibrium between both environments. At the reverse, the second wash of day 4 displays an opposite value (positive and negative) for both environment studied, as if the positive charges of the biofilm went through water.

However, the ZP of water for the third wash on day 1 is not insignificant but is not

correlated to a similar ZP value for the biological system. Globally, the ZP behavior varies over time.

The ZP of water associated to *Trichoderma* is widely effected on day 1 (Appendices page 80, Figure 26b). This observation is in line with these displayed previously (Figure 11), even though washes 1 and 2 do not cause a ZP modification on mycelium. On the contrary, washes 3 and 4 display negative ZP values on day 1 (Figure 26a, correlated to those obtained for water data (Figure 26b).

At last, ZP measurements on co-culture after wash stay constant between -1 and 1 mV (Appendices page 81, Figure 27a), as the values obtained in previous experiment (repetition on measurement, Figure 12). Whereas ZP values of associated water (Appendices page 81, Figure 27b) are much higher and globally included between -50 and 50 mV. Furthermore, the extreme values such as 250 mV or above are considered as artefacts.

No global trend can be highlighted between both investigated environment (solid and liquid) and this over time, while ZP of water shows an interesting behavior of the associated biofilms. Indeed, it emphasizes that a loss of charges (ions or hydrophilic and amphiphilic molecules, such as lipopetides) from the biological systems to water is not minor and thus has consequences on the ZP measurement of biofilms interacting with its surrounding environment. With more replicates, this method of ZP measurement could give interesting data concerning electrostatic aspect of biofilm and its behavior in aqueous environment.

4.2.1.2 Zeta potential of plastic

A two way ANOVA was performed on the ZP values of plastic that underwent a biofilm growth (Appendices page 81, Table 12). The p-value of the interaction between both factors (biological systems and time) is higher than 0.05 meaning that there is no significant interaction. The p-values of independent factors exceed 0.05. The null hypotheses are then accepted, meaning that the averages of each factor are equal. In other words, the Zeta potential of plastic is not impacted in a significant way by the interaction nor by the individual factors (Appendices page 82, Table 13).

Nevertheless, light variabilities of the ZP values are displayed on Figure 13, although it remains low compared to the global ZP scale. These light variations could be a sign of a chemical modification of the plastic surface attacked by micro-organisms, compared to the control. Indeed, biodegradation results in functional groups on the plastic surface which may

be dissociated for a given pH and ionic strength. This statement raises questions because the surface is supposed to be immersed in pure water. It is not excluded that ionic residues remain or that functional groups react with oxygen or carbon dioxide dissolved in water (although a prior degassing was performed).

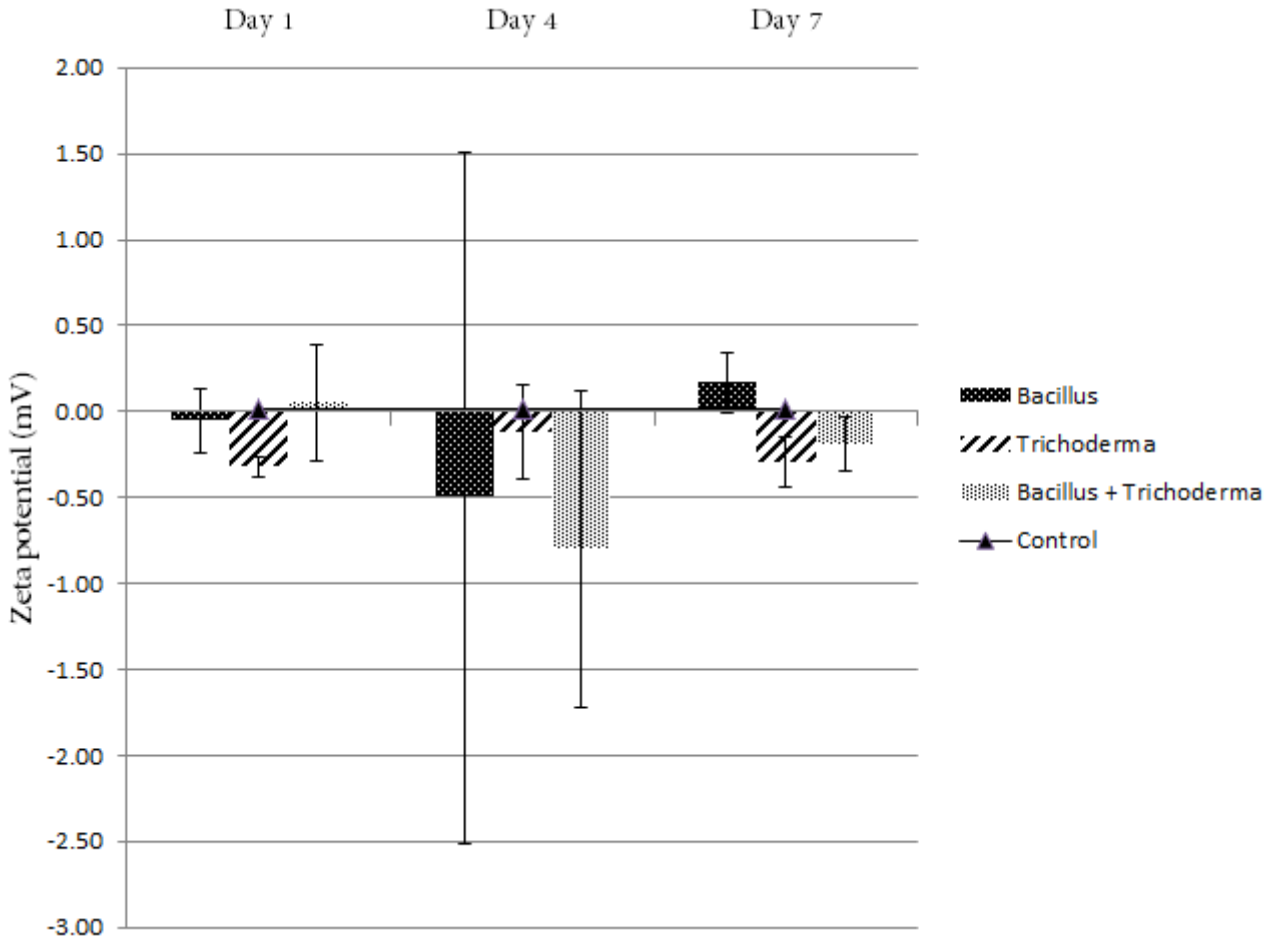

FIGURE 13: Zeta potential values of plastic in function of time and biofilm

Obviously, more replicates have to be carried out and this at longer culture time to assert a real modification of the LDPE surfaces. Anyhow, the obtained ZP values remain low meaning that other forces are involved in adhesion like that including hydrophobicity. Moreover, some ZP values are positive while most of them are negative such as ZP of biological systems (see Section 4.2.1.1). At this state of investigation, it is difficult to link the ZP of biofilms with ZP of plastics due to the lack of replicates.

4.2.1.3 Contact angle measurement and surface tension calculation

Surface tensions of solid material can not be directly measured but it is evaluated thanks to the contact angle measurement (Appendices page 82, Table 14) and Young's relation (Equation 25, page 31).

Unsurprisingly, the polar contribution remains low (Appendices page 82, Table 14, γ^{AB}) and close to the control plastic and this for all surfaces. Nevertheless, slight evolution could be observed on Figure 14, illustrating total surface tension (the sum of the polar and apolar components). Indeed, surface tension of plastic having supported the *Bacillus* biofilm decreases by 7% between the first and the seventh day. Concerning that supporting *Trichoderma* mycelium, a decreasing evolution is visible but far less important in terms of percentage of variation. On the other hand, evolution of surfaces tensions of plastic related to co-culture does not show an absolute reduction of the surface tension like both mono-cultures.

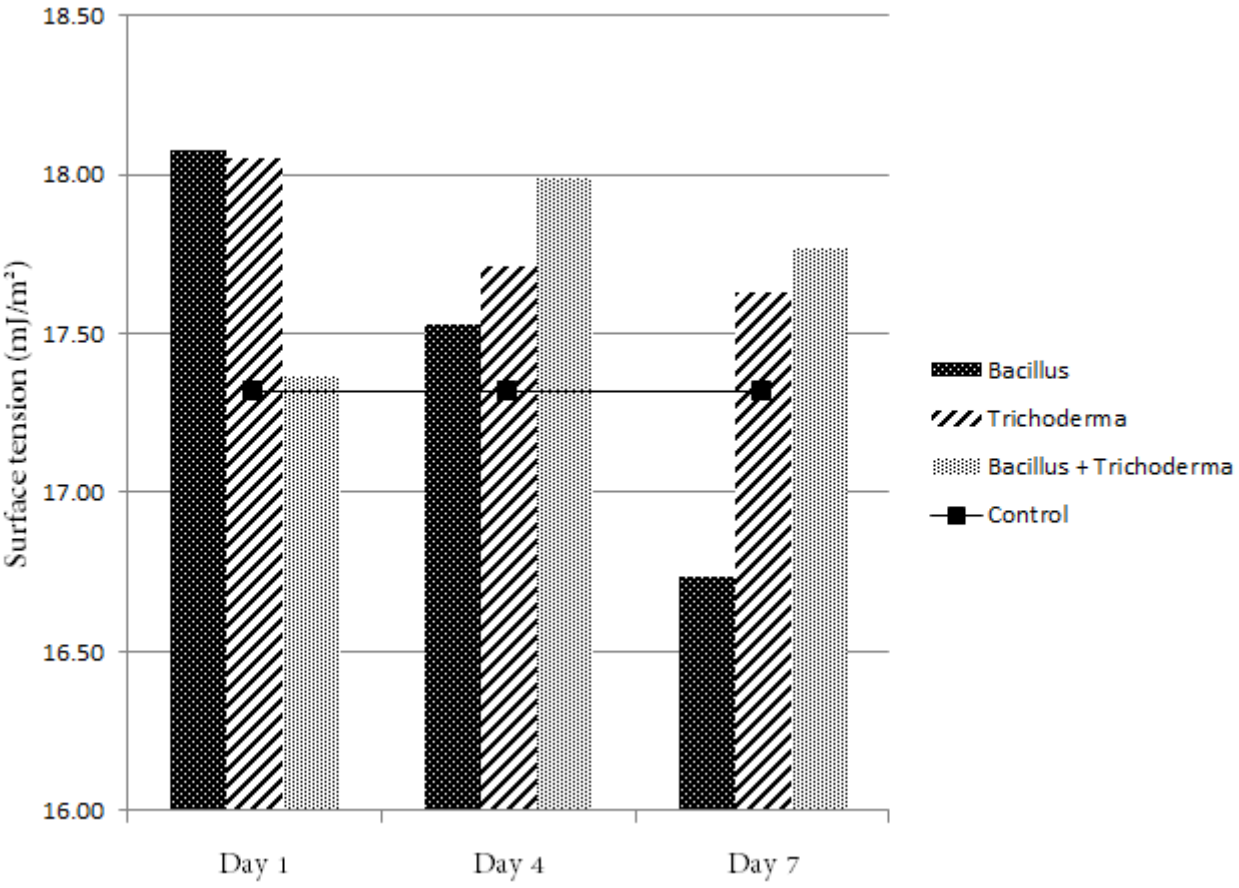

FIGURE 14: Surface tension of plastic having supported biofilms

Surface tension of polymers are dictated by molecular weight and crystallinity [113, 114]. Indeed, according to Wei *et al.* (2010), surface tension goes down with increasing

percentage of crystallinity [114]. On the other hand, an amorphous polymer is more accessible to enzymes biosynthesized by microorganisms, increasing thus the percentage of crystallinity [115]. These observations could explain the decline of surface tension of plastic surface associated to mono-cultures, suggesting a polyethylene biodegradation. This remains only a supposition and must be confirmed by various measurements, such as differential scanning calorimetry (DSC), and more replicates. Moreover, lower surface tension increases the bioavailibilty of polymer for microorganisms and hence is a compatible way to explain surface tension reduction over time due to the addition of functional groups coming from biodegradation. Furthermore those groups are polar and hence increase hydrophilicity of plastic. It needs to be added that the roughness of surface was not be taken into account in this case while it impacts contact angle measurement.

4.2.2 SEM imaging

SEM imaging was performed in order to observe biofilm formation on polyethylene substrate and plastic degradation at the micrometer scale. Biofilm imaging was carried out after a growth of 24 hours for mono-culture of *Bacillus amyloliquefaciens*, a growth of 72h for mono-culture of *Trichoderma harzianum*, while the co-culture imaging was achieved after 72h of fungal growth and 24h of bacterial growth (inoculated on 48h old fungal culture).

4.2.2.1 Biological systems

Biofilm formation is achieved by 6 main steps (see Section 2.2.3.1, page 13), while four of them are perfectly illustrated on Figure 15, the planktonic phase and the released cells are not seen. The first step is the adhesion of planktonic cells to plastic substrate (1). These isolated cells on plastic proceed then to interact with each other, producing EPS (2) and leading to irreversible adhesion. Micro-colonies are then formed (3) and grow to reach a mature biofilms (4). It is not excluded that short-range EPS seen on Figure 15 are actually fimbriae, macromolecular extracellular complexes formed by proteins and involved in the biofilm formation and the bacterial motility [116, 117].

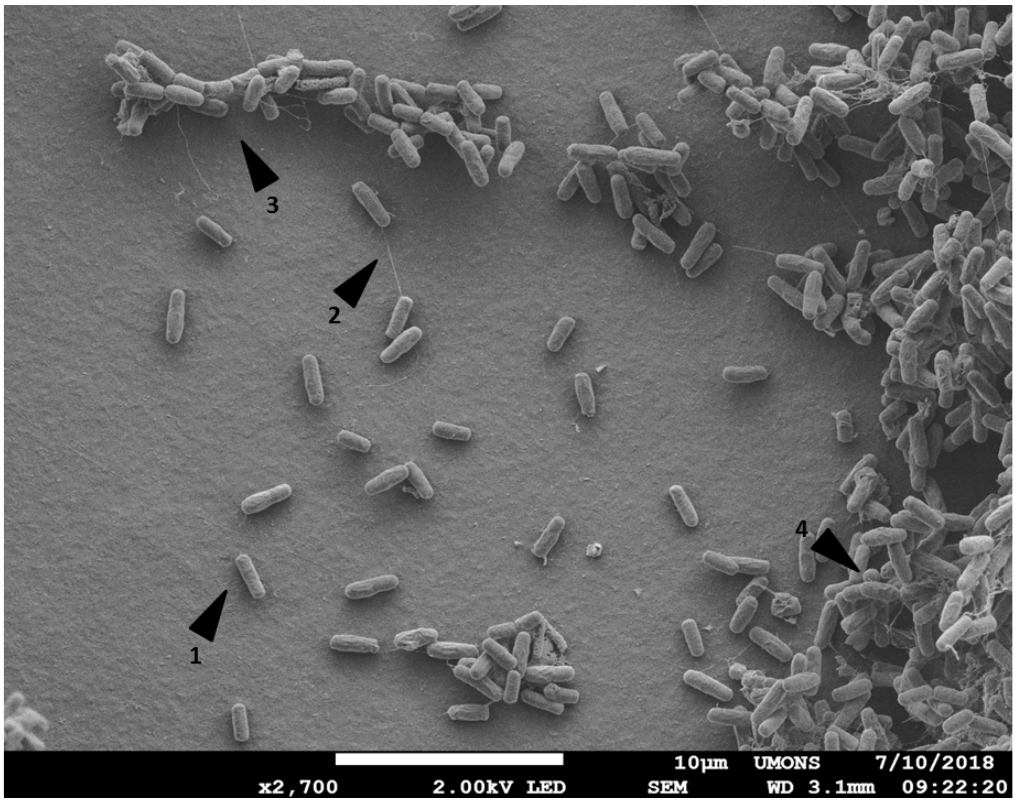

FIGURE 15: Biofilm formation of *B. amyloliquefaciens* after 24h of growth on polyethylene substrate

1: Initial attachment of planktonic cell on plastic; **2**: EPS production and cells interaction; **3**: Micro-colonies formation; **4**: Biofilm maturation

After 24 hours of bacterial growth, the biofilm reaches a mature state involving strong relations of cells to cells (Figure 16a). This link is physically visualized thanks to EPS structure looking like a fiber network. This arrangement of EPS is unexpected because EPS is usually present as a matrix overlaying and confining bacteria. In fact, herein, the EPS morphology is impacted by the dehydration step during the sample preparation [118]. Indeed, EPS is characterized by a highly hydrated structure while the aim of SEM is to dehydrate biological substrate and to preserve native shape. Bacterial structure are not impacted by dehydration. Hence, SEM exhibits an inaccurate morphology of the initial biofilm. Long-distance interaction without substrate adhesion is shown on Figure 16b. Indeed, the development was formed above the plastic without adhering to it in the forefront, while a micro-colony is displayed in the background on the plastic surface. However, the EPS matrix between cells and plastic surface may been removed or contracted during drying.

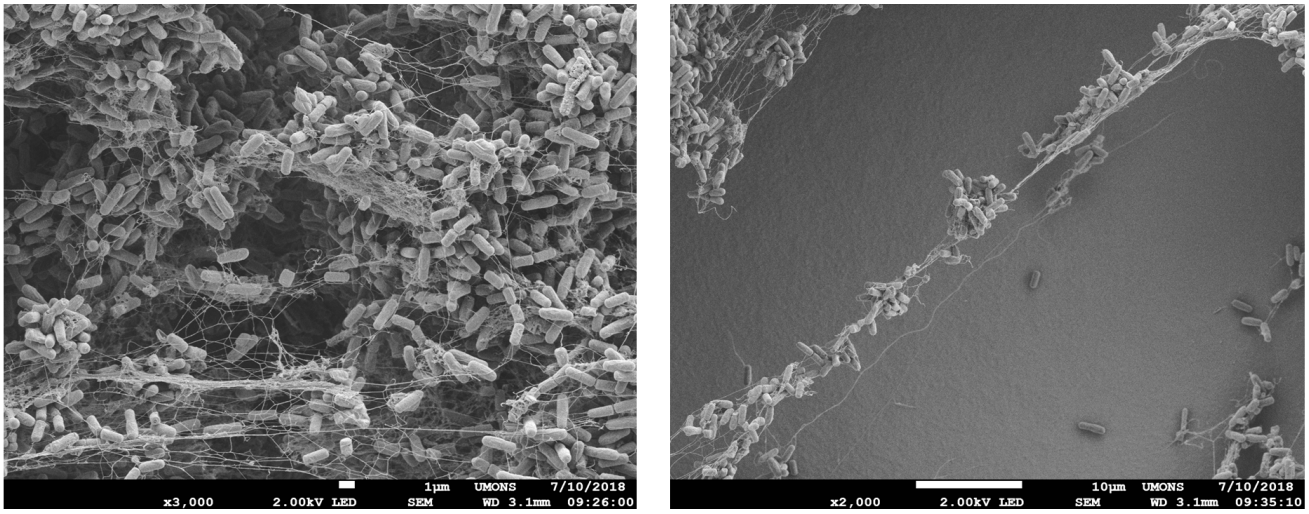

(A) Mature biofilm (B) Long distance interaction

FIGURE 16: Biofilm formation of *B. amyloliquefaciens* after 24h of growth on polyethylene substrate

SEM imaging is a way to consider the physical interaction between *T. harzianum* and *B. amyloliquefaciens* (Figures 17 and 18). At the peripheral part of mycelium, the relation between *Bacillus amyloliquefacines* and *Trichoderma harzianum* is visible (Figure 17). Indeed, bacteria are attached to fungus thanks to EPS, even if this attachment remains light (Figure 17b). In fact, bacterial concentration is low but a lot of EPS residues are present. Longer distance interactions, from a hypha to another one, and stronger interaction arise (Figure 17d and 17c respectively), still at the external part of the mycelium. Moreover, EPS residues on hyphae indicates the spreading of these excreted molecules and thus the biofilm development. The cell division in the picture can also correlate this statement (Figure 17d). These EPS residues are probably due to *B. amyloliquefaciens*, according to the fact that an experiment showed that *T. harzianum* alone does not form a biofilm (Appendices page 83, Figure 28). However, the physiology of mono-culture is supposed to be different than in a co-culture context.

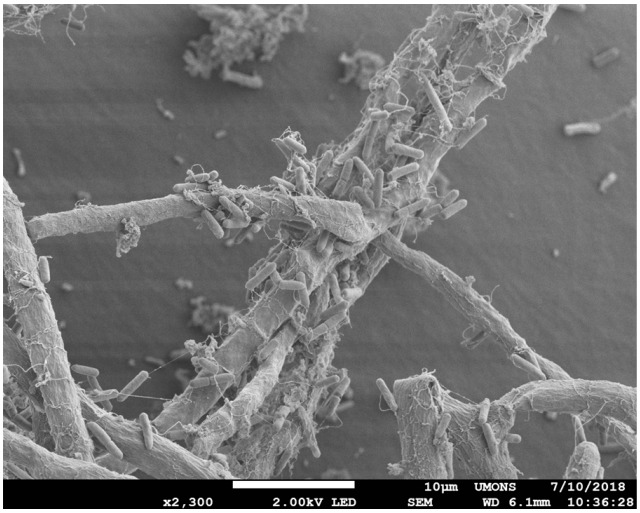

(A) General overview

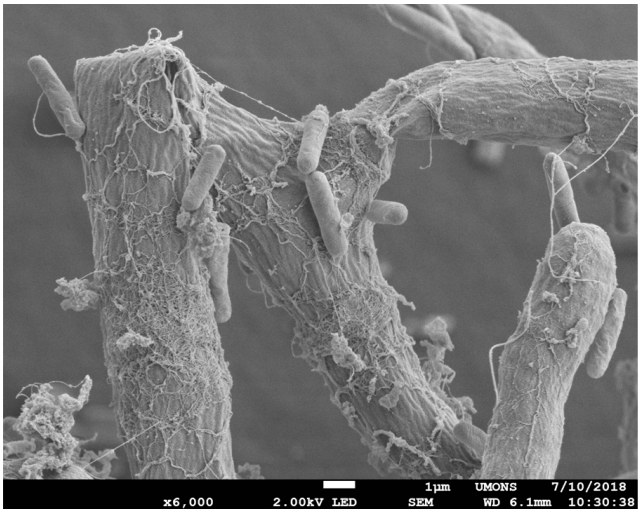

(B) Light interaction bacteria/fungus with high EPS residues

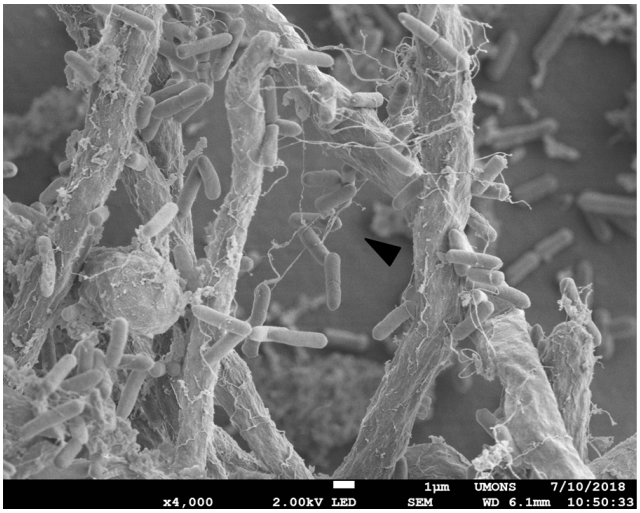

(C) *Bacillus* colonization from a hypha to another one

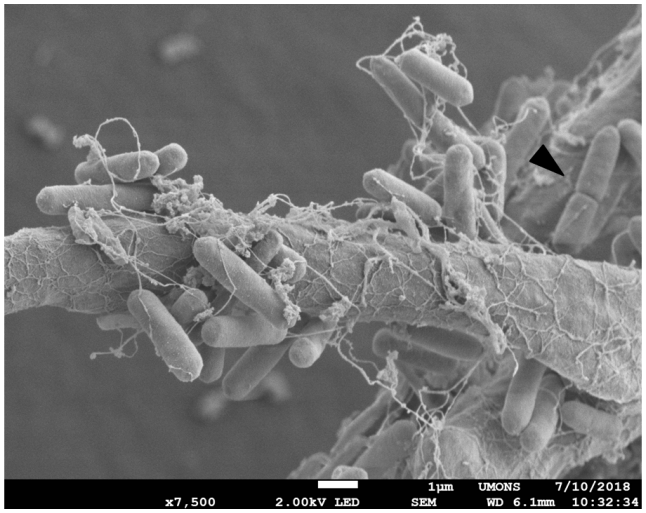

(D) Bacterial growth and adhesion on hypha

FIGURE 17: *B. amyloliquefaciens* and *T. harzianum* interaction at the peripheral part of mycelium formation on polyethylene substrate

On the other hand, inside the mycelium, relation and bacterial settlement seem to be different (Figure 18). Indeed, bacteria concentration is higher than at the external part (Figure 18a). Excretion of EPS is still visible on hyphae and below the bacterial cells (Figure 18b). However it does not form a global network between bacterial cells, contrary to the mono-culture. Indeed, bacterial cells are accumulated inside the mycelium, without displaying a biofilm state neither a close and physical interaction with the fungus. Either the EPS were lixiviated during sample preparation or mature biofilm state is not reached and bacteria are just confined inside hyphae, preparing a development of the biofilm and thus stronger interactions with the mycelium. It is also possible that the molecular composition of EPS

matrix may be influenced by the presence of *Trichoderma*, exhibiting a different behavior and thus a different appearance on SEM imaging. According to the results of a PhD thesis in progress, led on co-cultures of *Bacillus amyloliquefaciens* and *Trichoderma harzianum* on structured packing metals, *B. amyloliquefaciens* does not express surfactin in a 24h old co-culture with *T. harzianum*, while it does it at 48h. However, the structure of this lipopeptide is different to that the one expressed in a mono-culture condition [119] (see Appendices page 84, Figure 30). These results suggest a modification in the biofilm formation and in the behavior in terms of molecular composition released in surrounding environment which, in return, influences this bacterial behavior.

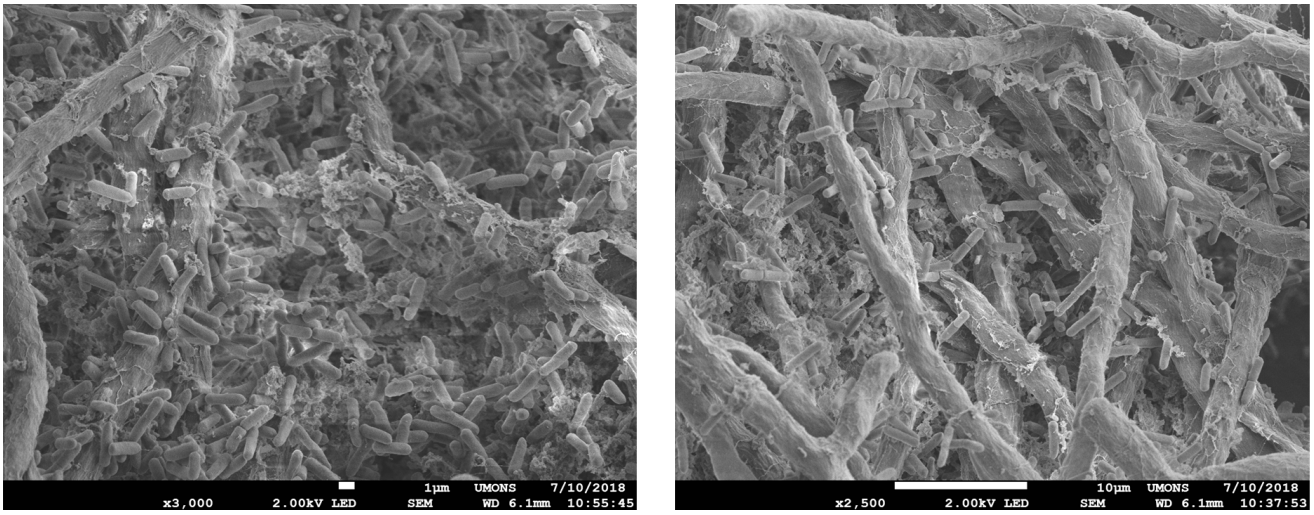

(A) (B)

FIGURE 18: *B. amyloliquefaciens* and *T. harzianum* interaction in the bulk of biomass formation on polyethylene substrate

4.2.2.2 Plastic surfaces

Polyethylene surfaces scanned by SEM allow to observe the presence or absence of visible plastic degradation. Indeed, according to Figure 19, holes are displayed on plastic substrate having supported a 24h old biofilm of *B. amyloliquefaciens* (Figure 19a) and on a plastic surface having supported the co-culture *B. amyloliquefaciens* (24h old) and *T. harzianum* (72h old) (Figure 19b). However, plastic controls display holes too (Appendices page 83, Figure 29a), compared to smooth plastic surface (Appendices page 83, Figure 29b).

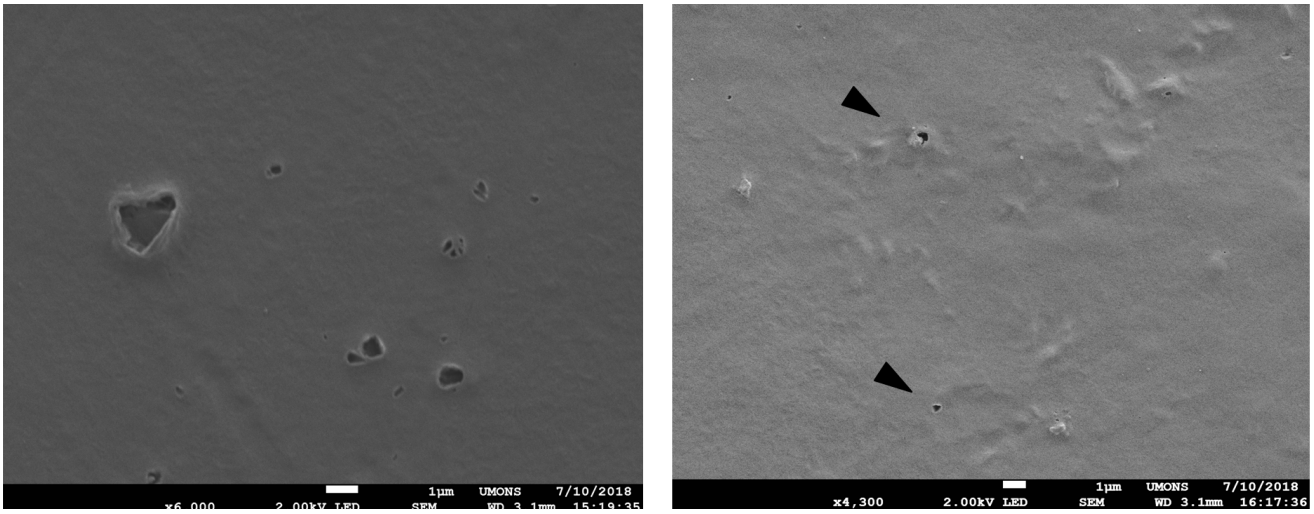

(A) Plastic surface having supported a 24h old biofilm of *B. amyloliquefaciens* (B) Plastic surface having supported the co-culture *B. amyloliquefaciens* (24h old) and *T. harzianum* (72h old)

FIGURE 19: SEM of polyethylene surfaces having supported a microbial growth

In any case, this kind of observation itself is not reliable enough to prove a synthetic polymer degradation. Combination of several tests such as, among other, FTIR, molecular weight, weight loss and thermo gravimetric analysis (TGA) can determine a biodegradation achievement. Indeed, biodegraded plastic is affected by the addition of functional groups [16] visible thanks to FTIR (where the wavelength corresponds to a particular chemical bond associated to a particular functional group). Molecular weight measurement also determines chemical variation of plastic and can be performed by a gel permeation chromatography (GPC), currently used for polymer examination. Another analytical tool is TGA, including DSC. Indeed, amorphous regions of polymer are consumed instead of the crystalline one, increasing thus the crystalline part of the polymer.

In addition, CO_2 evolution measurement in a close culture is a method to assume that plastic degradation results from microbial consumption of polyethylene as the sole carbon source. Indeed, variation in FTIR and/or DCS spectra could be the consequence of abiotic factors impacting chemical composition of plastic, such as UV-light and heating, affecting conclusion about PE biodegraded from a microbial attack.

5 Conclusion and outlook

Plastic degradation is a developing field of study including lot of scientific approaches such as polymer degradation itself and its chemical structure variation leading to thermal and physical modifications of the degraded plastic. Microbial involvement constitutes an important field of research, especially marine bacteria, whereas some microorganisms from soil are able to degrade plastics. Nevertheless, it remains a complex field of study because of the wide plastic family and its associated additives impacting positively or negatively biodegradation. Moreover, this natural degradation takes into account abiotic factors such as UV-light and heating. In the case of the plastic biodegradation, these abiotic factors are considered as an essential pretreatment leading firstly to the biofilm adhesion on polyethylene and secondly to the speeding up of the plastic degradation processes. Thus, impact of abiotic factors and a longer culture times are both missing in this present work and constitute therefore fundamental outlooks.

This work was focused on a natural community and a synthetic community both supposed to be able to degrade plastic. The natural one was extracted from the gut of the caterpillar of *Galleria mellonella*, a larvae known to assimilate polyethylene. The impact of diets of larvae on the specie richness and diversity of the intestinal microbiotas was investigated due to several denaturing gradient gel electrophoreses (DGGE). Unfortunately, despite several enhancements, this aim was not reached whereas DGGE is a current method to analyze specie richness and diversity. Indeed, double bands occur on DGGE fingerprints, resulting to a distorted interpretation of specie richness and diversity. The first step of extraction of intestinal microbiotas may have been deficient, while performed DNA amplification and its improvement were based on literature. Moreover, low abundant species can be underestimated and may not be displayed on DGGE fingerprint. Thus, the diet seems to impact species diversity, while the species richness can remain stable. Furthermore, according to literature, the sequenced cultivable bacteria, extracted from the intestinal microbiota of *G. mellonella* larvae exhibit interesting behavior in terms of polymer degradation abilities. In the future, these cultivable bacteria should be cultivated on polyethylene surface to study its degradation. Mono- and co-culture of these bacteria should be performed. Indeed, physiology of species can depend on the behavior of the other species of the community. It also means that the degradation ability of cultivable bacteria can depend on non-cultivable species.

Currently, a combinaison of the metagenomic and bioinformatic analyses lead to a powerful understanding of the specie richness and diversity of the microbiota, as well as a phylogenic view of the community composition. At this end, high-throughput sequencing is a technology widely used. Finally, in order to understand enzymatic activities involve into the polymer degradation, functional proteomic should be analyzed on this microbiota coming from *Galleria mellonella*.

As a reminder, the biofilm adhesion to the plastic surface is the first step of the plastic degradation. The understanding of biofilm attachment is thus the main point for the investigation of plastic degradation. To this end, the XDLVO theory was investigated on polyethylene and on the synthetic community constituted by *Bacillus amyloliquefaciens* and *Trichoderma harzanium*.

The Zeta potential measurements led on biofilm, thus including the extracellular polymeric substances (EPS) matrix, is totally exploratory. Indeed, nowadays, ZP analyses on biological systems are carried out on planktonic cells or resuspended cells from biofilm, not on a biofilm state. In this work, the Zeta measurement were performed due to a *Flat surface cell* and an electrophoretic light scattering analyzer under an applied electric field. Due to the cell configuration, it has been observed that the Zeta potential of both biological systems and external water varies in function of the measurement. It is thus difficult to attribute a fixed ZP value of biological systems in given conditions of growth, because ZP water support loss of charge from the biological surfaces. This ZP variation exhibits the complexity and heterogeneity of biofilms through time and space. Moreover, the ZP potential measurements were carried out simultaneously on bacterial surfaces and EPS matrix, both involved in a given surrounding environment. As a perspective, ZP investigations should be led separately on resuspended bacteria and recovered EPS and then compared. Moreover, more replicates and longer culture time can give a global view of ZP evolution. The quantification of biological systems due to real-time qrRT-PCR as well as the quantification of synthesized lipopetides due to a chromatographic method leads to a better relation between the bacterial growth, biofilm formation and the Zeta potential evolution. Concerning the hydrophobic aspect, contact angle measurement should be carried out on biofilm surface. To conclude this point, the surface free energy, the thermodynamic approach of the XDLVO theory, is the best way to express the interaction between a biological surface and a substrate.

Finally, small variation of ZP of plastic surface, as well as contact angle measurement, can assume a chemical modification of plastic surface leading to a better adhesion of biofilm and suggesting a biodegradation. As a perspective, differential scanning calorimetry (DSC) and Fourier transform infrared spectroscopy (FTIR) are two methods expressing a chemical variation of the polymer surface. Indeed, DSC gives the percentage of crystallinity of the substrate, which is supposed to increase with microbial degradation. On the other hand, FTIR carries out information about chemical composition in terms of functional groups absorbing or reflecting at precise wavelengths, leading to spectral fingerprints associated to chemical structures. Indeed, presence of functional groups on plastic surface is a sign of degradation. Ultimately, culture conditions should be free of carbon source in the culture medium, where polyethylene is both the substrate and the carbon source for biofilms.

Together, these suggested improvements will better understand the interactions between biofilms and polyethylene and the biodegradation of the latter.

References

[1] American Society of Chemistry National Historic Chemical Landmarks. Bakelite: The world's first synthetic plastic, 1993. https://www.acs.org/content/acs/en/education/whatischemistry/landmarks/bakelite.html, (2018-03-19).

[2] Kirk M. Cantor and Patrick Watts. Plastics Materials. In *Applied Plastics Engineering Handbook*, pages 3–5. Elsevier, 2011.

[3] Plastics Europe. The facts 2017. http://www.plasticseurope.org/en/resources/publications/plastics-facts-2017, (2018-02-19).

[4] Telmo Ojeda. Polymers and the Environment. In *Polymer Science*, chapter 1, pages 1–34. InTech, 2013.

[5] Alka Grover, Akanksha Gupta, Shivani Chandra, Abha Kumari, and SM Paul Khurana. Polythene and Environment. *International journal of environmental sciences*, 5(6):1091–1105, 2015.

[6] Sara Ronca. Polyethylene. In *Brydson's Plastics Materials*, pages 247–278. Elsevier, 2017.

[7] Eric R. Larson. An Overview of Thermoplastic Materials. In *Thermoplastic Material Selection*, pages 97–143. Elsevier, 2015.

[8] Plastics Europe. The facts 2015. $https://www.plasticseurope.org/fr/resources/publications/93-plastics-facts-2015, (2018-02-21)$.

[9] Li Shen and Ernst Worrell. Plastic Recycling. In *Handbook of Recycling*, pages 179–190. Elsevier, 2014.

[10] Ernst Worrell and Markus A. Reuter. Definitions and Terminology. In *Handbook of Recycling*, chapter 2, pages 9–16. Elsevier, 2014.

[11] Ernest A. Coleman. Plastics Additives. In Myer Kutz, editor, *Applied Plastics Engineering Handbook*, Plastics Design Library, chapter 23, pages 419–428. William Andrew Publishing, 2011.

[12] David K A Barnes, Francois Galgani, Richard C Thompson, and Morton Barlaz. Accumulation and fragmentation of plastic debris in global environments. *Philosophical Transactions of the Royal Society B: Biological Sciences*, 364:1985–1998, 2009.

[13] E. L. Teuten, J. M. Saquing, D. R. U. Knappe, M. A. Barlaz, S. Jonsson, A. Bjorn, S. J. Rowland, R. C. Thompson, T. S. Galloway, R. Yamashita, D. Ochi, Y. Watanuki, C. Moore, P. H. Viet, T. S. Tana, M. Prudente, R. Boonyatumanond, M. P. Zakaria, K. Akkhavong, Y. Ogata, H. Hirai, S. Iwasa, K. Mizukawa, Y. Hagino, A. Imamura, M. Saha, and H. Takada. Transport and release of chemicals from plastics to the environment and to wildlife. *Philosophical Transactions of the Royal Society B: Biological Sciences*, 364(1526):2027–2045, 2009.

[14] Ee-Ling Ng, Esperanza Huerta Lwanga, Simon M. Eldridge, Priscilla Johnston, Hang-Wei Hu, Violette Geissen, and Deli Chen. An overview of microplastic and nanoplastic pollution in agroecosystems. *Science of The Total Environment*, 627:1377–1388, 2018.

[15] Gwen O Sullivan and David Megson. Brief Overview : Discovery, Regulation, Properties, and Fate of POPs. In *Environmental Forensics for Persistent Organic Pollutants*, chapter 1, pages 1–20. Elsevier B.V., 2014.

[16] J Arutchelvi, M Sudhakar, Ambika Arkatkar, Mukesh Doble, Sumit Bhaduri, and Parasu Veera Uppara. Biodegradation of polyethylene and polypropylene. *Indian Journal of Biotechnology*, 7:9–22, 2008.

[17] Ambika Arkatkar, J Arutchelvi, M Sudhakar, Sumit Bhaduri, Parasu Veera Uppara, and Mukesh Doble. Approaches to Enhance the Biodegradation of Polyolefins. *The Open Environmental Engineering Journal*, 2:68–80, 2009.

[18] S Bonhomme, A Cuer, A-m Delort, J Lemaire, M Sancelme, and G Scott. Environmental biodegradation of polyethylene. *Polymer Degradation and Stability*, 81:441–452, 2003.

[19] Katarzyna Leja and Grażyna Lewandowicz. Polymer Biodegradation and Biodegradable Polymers – a Review. *Polish Journal of Environmental Studies*, 19(2):255–266, 2010.

[20] Mélanie Gardette, Anthony Perthue, Jean Luc Gardette, Tünde Janecska, Eniko Földes, Béla Pukánszky, and Sandrine Therias. Photo- and thermal-oxidation of

polyethylene: Comparison of mechanisms and influence of unsaturation content. *Polymer Degradation and Stability*, 98(11):2383–2390, 2013.

[21] Telmo F M Ojeda, Emilene Dalmolin, Maria M C Forte, Rodrigo J S Jacques, Fátima M. Bento, and Flávio A O Camargo. Abiotic and biotic degradation of oxo-biodegradable polyethylenes. *Polymer Degradation and Stability*, 94:965–970, 2009.

[22] Raymond B. Seymour Cornelia Vasile. Degradation and decomposition. In New York Marcel Dekker Inc, editor, *Handbook of polyolefins synthesis and properties*, pages 479–506. 1993.

[23] Jun Yang, Yu Yang, Wei-min Wu, Jiao Zhao, and Lei Jiang. Evidence of Polyethylene Biodegradation by Bacterial Strains from the Guts of Plastic-Eating Waxworms. *Environmental Science and Technology*, 48(23):13776–13784, 2014.

[24] Paolo Bombelli, Christopher J. Howe, and Federica Bertocchini. Polyethylene biodegradation by caterpillars of the wax moth Galleria mellonella. *Current Biology*, 27(8):292–293, 2017.

[25] Charles A. Kwadha, George O. Ong'Amo, Paul N. Ndegwa, Suresh K. Raina, and Ayuka T. Fombong. The biology and control of the greater wax moth, Galleria mellonella. *Insects*, 8(2):1–17, 2017.

[26] Catherine Jia-Yun Tsai, Jacelyn Mei San Loh, and Thomas Proft. Galleria mellonella infection models for the study of bacterial diseases and for antimicrobial drug testing. *Virulence*, 7(3):214–229, 2016.

[27] Merina Paul Das and Santosh Kumar. An approach to low-density polyethylene biodegradation by Bacillus amyloliquefaciens. *3 Biotech*, 5(1):81–86, 2015.

[28] Merina Paul Das and Santosh Kumar. Influence of cell surface hydrophobicity in colonization and biofilm formation on LDPE biodegradation. *International Journal of Pharmacy and Pharmaceutical Sciences*, 5(4):690–694, 2013.

[29] M Rosenberg and Rosenberg E Gutnick D. Adherence of bacteria to hydrocarbons: a simple method for measuring cell-surface hydrophobicity. *FEMS Microbiology Letters*, 9, 1980.

[30] P.K. Roy, S Titus, P Surekha, E Tulsi, C Deshmukh, and C Rajagopal. Degradation of abiotically aged LDPE films containing pro-oxidant by bacterial consortium. *Polymer Degradation and Stability*, 93(10):1917–1922, 2008.

[31] Bozena Nowak, Jolanta Pajak, Magdalena Drozd-Bratkowicz, and Grazyna Rymarz. Microorganisms participating in the biodegradation of modified polyethylene films in different soils under laboratory conditions. *International Biodeterioration and Biodegradation*, 65(6):757–767, 2011.

[32] G. Y. Yu, J. B. Sinclair, G. L. Hartman, and B. L. Bertagnolli. Production of iturin A by Bacillus amyloliquefaciens suppressing Rhizoctonia solani. *Soil Biology and Biochemistry*, 34(7):955–963, 2002.

[33] Anthony Arguelles-Arias, Marc Ongena, Badre Halimi, Yannick Lara, Alain Brans, Bernard Joris, and Patrick Fickers. Bacillus amyloliquefaciens GA1 as a source of potent antibiotics and other secondary metabolites for biocontrol of plant pathogens. *Microbial Cell Factories*, 8(1):63, 2009.

[34] J M Raaijmakers, M Vlami, and J T de Souza. Antibiotic production by bacterial biocontrol agents. *Antonie Van Leeuwenhoek International Journal of General and Molecular Microbiology*, 81(1-4):537–547, 2002.

[35] Zaki A. Siddiqui. *PGPR: Biocontrol and Biofertilization*. Springer, 2006.

[36] Peter L. Graumann. In *Bacillus: Cellular and Molecular Biology (Third edition)*. Caister Academic Press, 2017.

[37] Michel Vert, Yoshiharu Doi, Karl-heinz Hellwich, Michael Hess, Philip Hodge, Przemyslaw Kubisa, Marguerite Rinaudo, and François Schué. Terminology for biorelated polymers and applications (IUPAC Recommendations 2012). 84(2):377–410, 2012.

[38] Marry Ellen Davey and George A. O'toole. Microbial Biofilms: from Ecology to Molecular Genetics. *Microbiology and Molecular Biology Reviews*, 64(4):847–867, 2000.

[39] Hans-curt Flemming, Jost Wingender, Ulrich Szewzyk, Peter Steinberg, and Scott A Rice. Biofilms : an emergent form of bacterial life. *Nature Publishing Group*, 14(9):563–575, 2016.

[40] Rolf Bos, H C van der Mei, and Henk J. Busscher. Physico-chemistry of initial microbial adhesive interactions -its mechanisms and methods for study. *FEMS microbiology reviews*, 23(2):179–230, 1999.

[41] P Stoodley, K Sauer, D G Davies, and J W Costerton. Biofilm as complex differentiated communities. *Annual review of Microbiology*, 56:187–209, 2002.

[42] Huan Gu and Dacheng Ren. Materials and surface engineering to control bacterial adhesion and biofilm formation: A review of recent advances. *Frontiers of Chemical Science and Engineering*, 8(1):20–33, 2014.

[43] Björn Dahlbäck, Malte Hermansson, Staffan Kjelleberg, and Birgitta Norkrans. The hydrophobicity of bacteria - An important factor in their initial adhesion at the air-water inteface. *Archives of Microbiology*, 128(3):267–270, 1981.

[44] Malte Hermansson. The DLVO theory in microbial adhesion. *Colloids and Surfaces B: Biointerfaces*, 14(1-4):105–119, 1999.

[45] K. C. Marshall, R. Stout, and R Mitchell. Mechanism of the Initial Events in the Sorption of Marine Bacteria to Surfaces. *Journal of General Microbiology*, 68(3):337–348, 1971.

[46] E. J W. Verwey and J. TH. G. Overbeek. *Theory of stability of lyophobic colloids.* Esevier Publishing Compagny, INC., 1948.

[47] C.J Van Oss, R.J Good, and M.K Chaudhury. The role of van der Waals forces and hydrogen bonds in "hydrophobic interactions" between biopolymers and low energy surfaces. *Journal of Colloid and Interface Science*, 111(2):378–390, 1985.

[48] Sonia Bayoudh, Ali Othmane, Laurence Mora, and Hafedh Ben Ouada. Assessing bacterial adhesion using DLVO and XDLVO theories and the jet impingement technique. *Colloids and Surfaces B: Biointerfaces*, 73(1):1–9, 2009.

[49] David Fairhurst. An overview of the zeta potential (particle sciences, technical brief, vol. 2). $https://www.americanpharmaceuticalreview.com/Featured-Articles/133232-An-Overview-of-the-Zeta-Potential-Part-1-The-Concept/$, (2018−03−21).

[50] Carel Jan Van Oss. Long-range and short-range mechanisms of hydrophobic attraction and hydrophilic repulsion in specific and aspecific interactions. *Journal of Molecular Recognition*, 16(4):177–190, 2003.

[51] C.J. Van Oss. Hydrophobic, hydrophilic and other interactions in epitope-paratope binding. *Molecular Immunology*, 32(3):199–211, 1995.

[52] T. Young. An essay on the cohesion of fluids. *Philosophical Transactions of the Royal Society London*, 95:65–87, 1805.

[53] Albert T Poortinga, Rolf Bos, Willem Norde, and Henk J Busscher. Electric double layer interactions in bacterial adhesion to surfaces. *Surface Science Reports*, 47(1):1–32, 2002.

[54] Albert van der Wal, Willem Norde, Alexander J.B. Zehnder, and Johannes Lyklema. Determination of the total charge in the cell walls of Gram-positive bacteria. *Colloids and Surfaces B: Biointerfaces*, 9:81–100, 1997.

[55] Yea-ling Ong, Anneta Razatos, George Georgiou, and Mukul M Sharma. Adhesion Forces between E . coli Bacteria and Biomaterial Surfaces. *Langmuir*, 15:2719–2725, 1999.

[56] Terri A. Camesano and Bruce E. Logan. Probing Bacterial Electrosteric Interactions Using Atomic Force Microscopy. *Environmental Science and Technology*, 34(16):3354–3362, 2000.

[57] Subir Bhattacharjee and Menachem Elimelech. Surface Element Integration : A Novel Technique for Evaluation of DLVO Interaction between a Particle and a Flat Plate. *Journal of Colloid and Interface Science*, 285(193):273–285, 1997.

[58] Eric M V Hoek and Gaurav K Agarwal. Extended DLVO interactions between spherical particles and rough surfaces. *Journal of Colloid and Interface Science*, 298:50–58, 2006.

[59] C. J. van Oss and R. F. Giese. Role of the properties and structures of liquid water in colloidal and interfacial systems. *Journal of Dispersion Science and Technology*, 25(5):631–655, 2004.

[60] J. Andrew Jones and Xin Wang. Use of bacterial co-cultures for the efficient production of chemicals. *Current Opinion in Biotechnology*, 53:33–38, 2018.

[61] Lisa Goers, Paul Freemont, and Karen M Polizzi. Co-culture systems and technologies : taking synthetic biology to the next level. *Jornal of the Royal Society Interface*, 11(96), 2014.

[62] Jan Dolinšek, Felix Goldschmidt, and David R. Johnson. Synthetic microbial ecology and the dynamic interplay between microbial genotypes. *FEMS Microbiology Reviews*, 40(6):961–979, 2016.

[63] Stephanie G. Hays, William G. Patrick, Marika Ziesack, Neri Oxman, and Pamela A. Silver. Better together: Engineering and application of microbial symbioses. *Current Opinion in Biotechnology*, 36:40–49, 2015.

[64] Niels Klitgord and Daniel Segrè. Environments that induce synthetic microbial ecosystems. *PLOS Computational Biology*, 6(11):1–17, 11 2010.

[65] Jasmine Shong, Manuel Rafael Jimenez Diaz, and Cynthia H. Collins. Towards synthetic microbial consortia for bioprocessing. *Current Opinion in Biotechnology*, 23(5):798–802, 2012.

[66] Sonia R Vartoukian, Richard M Palmer, and William G Wade. Strategies for culture of ‘ unculturable ’ bacteria. *FEMS Microbiol Lett*, 309:1–7, 2010.

[67] Katie Brenner, Lingchong You, and Frances H. Arnold. Engineering microbial consortia: a new frontier in synthetic biology. *Trends in Biotechnology*, 26(9):483–489, 2008.

[68] Michael T. Mee and Harris H. Wang. Engineering ecosystems and synthetic ecologies. *Molecular BioSystems*, 8(10):2470, 2012.

[69] Sodimalla Triveni, Radha Prasanna, Livleen Shukla, and Anil Kumar Saxena. Evaluating the biochemical traits of novel Trichoderma-based biofilms for use as plant growth-promoting inoculants. *Annals of Microbiology*, 63(3):1147–1156, 2013.

[70] Aurélie Deveau, Gregory Bonito, Jessie Uehling, Mathieu Paoletti, Matthias Becker, Saskia Bindschedler, Stéphane Hacquard, Vincent Hervé, Jessy Labbé, Olga A Lastovetsky, Sophie Mieszkin, Larry J Millet, Balázs Vajna, Pilar Junier, Paola Bonfante, Bastiaan P Krom, Stefan Olsson, Jan Dirk van Elsas, and Lukas Y Wick. Bacterial–fungal interactions: ecology, mechanisms and challenges. *FEMS Microbiology Reviews*, (April):1–18, 2018.

[71] Yuanchen Zhang, Erik K. Kastman, Jeffrey S. Guasto, and Benjamin E. Wolfe. Fungal networks shape dynamics of bacterial dispersal and community assembly in cheese rind microbiomes. *Nature Communications*, 9(1):1–12, 2018.

[72] Monika Jangir, Ritika Pathak, and Satyawati Sharma. Trichoderma and its potential applications. In Dhananjaya Pratap Singh, Harikesh Bahadur Singh, and Ratna Prabha, editors, *Plant-Microbe Interactions in Agro-Ecological Perspectives: Volume 2: Microbial Interactions and Agro-Ecological Impacts*. Springer Singapore, 2017.

[73] Ricardo Feliciano dos Santos, Leise Inês Heckler, Marilia Lazarotto, Lucas da Ressureiçao Garrido, Cecilia Rego, and Elena Blume. Trichoderma spp . and Bacillus subtilis for control of Dactylonectria macrodidyma in grapevine. *Phytopathologia Mediterranea*, 55(2):293–300, 2016.

[74] Mansour T Abdullah, Nida Y Ali, and Patrice Suleman Ã. Biological control of Sclerotinia sclerotiorum (Lib .) de Bary with Trichoderma harzianum and Bacillus amyloliquefaciens. *Crop Protection*, 27:1354–1359, 2008.

[75] Peter Kipngeno, Turoop Losenge, Naomi Maina, Esther Kahangi, and Patrick Juma. Efficacy of Bacillus subtilis and Trichoderma asperellum against Pythium aphanidermatum in tomatoes. *Biological Control*, 90:92–95, 2015.

[76] Dhananjaya Pratap Singh, Harikesh Bahadur Singh, and Ratna Prabha. *Plant-microbe interactions in agro-ecological perspectives*, volume 1. 2017.

[77] H. V. Sowmya, Ramalingappa, M. Krishnappa, and B. Thippeswamy. Degradation of polyethylene by Trichoderma harzianum—SEM, FTIR, and NMR analyses. *Environmental Monitoring and Assessment*, 186(10), 2014.

[78] Samuel Latour. *Etude du microbiome du tube digestif de Galleria mellonella et rôle dans la dégradation du polyéthylène*. Master thesis, Gembloux Agro bio tech (ULiège, Belgium), 2018.

[79] G. Muyzer, E. C. De Waal, and A. G. Uitterlinden. Profiling of complex microbial populations by denaturing gradient gel electrophoresis analysis of polymerase chain reaction-amplified genes coding for 16S rRNA. *Applied and Environmental Microbiology*, 59(3):695–700, 1993.

[80] R. H. Don, P. T. Cox, B. J. Wainwright, K. Baker, and J. S. Mattick. 'Touchdown' PCR to circumvent spurious priming during gene amplification. *Nucleic Acids Research*, 19(14):4008, 1991.

[81] Ingmar Janse, Jasper Bok, and Gabriel Zwart. A simple remedy against artifactual double bands in denaturing gradient gel electrophoresis. *Journal of Microbiological Methods*, 57(2):279–281, 2004.

[82] Sourav Bhattacharjee. Review article DLS and zeta potential – What they are and what they are not ? *Journal of Controlled Release*, 235:337–351, 2016.

[83] Olga Sánchez, Josep M. Gasol, Ramon Massana, Jordi Mas, and Carlos Pedrós-Alió. Comparison of different denaturing gradient gel electrophoresis primer sets for the study of marine bacterioplankton communities. *Applied and Environmental Microbiology*, 73(18):5962–5967, 2007.

[84] Weibing Shi, Ugur Uzuner, Lingxia Huang, Palmy R. Jesudhasan, Suresh D. Pillai, and Joshua S. Yuan. Comparative analysis of insect gut symbionts for composition-function relationships and biofuel application potential. *Biofuels*, 2(5):529–544, 2011.

[85] Shin-Ichi Aizawa. Enterococcus casseliflavus — Edible Flagella. *The Flagellar World*, pages 34–35, 2014.

[86] Shaoyu Tang, Hua Yin, Shuona Chen, Hui Peng, Jingjing Chang, Zehua Liu, and Zhi Dang. Aerobic degradation of BDE-209 by Enterococcus casseliflavus: Isolation, identification and cell changes during degradation process. *Journal of Hazardous Materials*, 308:335–342, 2016.

[87] M. Carina Audisio, Horacio R. Terzolo, and María C. Apella. Bacteriocin from Honeybee Beebread Enterococcusavium, Active against Listeriamonocytogenes. *Applied and environmental microbiology*, 71(6):3373–3375, 2005.

[88] a Wahyudi, M N Cahyanto, M Soejono, and Z Bachruddin. Potency of lignocellulose degrading bacteria isolated from buffalo and horse gastrointestinal tract and elephant dung for feed fiber degradation. *J.Indonesian Trop.Anim.Agric.*, 35(1):34–41, 2010.

[89] Shangling Fang, Li Wang, Wei Guo, Xia Zhang, Donghai Peng, Chunping Luo, Ziniu Yu, and Ming Sun. Bacillus thuringiensis bel protein enhances the toxicity of Cry1Ac protein to Helicoverpa armigera larvae by degrading insect intestinal mucin. *Applied and Environmental Microbiology*, 75(16):5237–5243, 2009.

[90] Leslie S. Lepore, Peter R. Roelvink, and Robert R. Granados. Enhancin, the granulosis virus protein that facilitates nucleopolyhedrovirus (NPV) infections, is a metalloprotease. *Journal of Invertebrate Pathology*, 68(2):131–140, 1996.

[91] Karen E Nelson, Derrick E Fouts, Steven R Gill, Erik K Holtzapple, Jennifer Rilstone, Martin Wu, James F Kolonay, Maureen J Beanan, Robert J Dodson, Lauren M Brinkac, Michelle Gwinn, Robert T Deboy, Ramana Madpu, Sean C Daugherty, A Scott Durkin, Daniel H Haft, William C Nelson, Jeremy D Peterson, Mihai Pop, Hoda M Khouri, Diana Radune, Jonathan L Benton, Yasmin Mahamoud, Lingxia Jiang, Ioana R Hance, Janice F Weidman, Kristi J Berry, Roger D Plaut, Alex M Wolf, Kisha L Watkins, William C Nierman, Alyson Hazen, Robin Cline, Owen White, Brendan Thomasonq, Arthur M Friedlander, and Philip C Hannaq. The genome sequence of Bacillus anthracis Ames and comparison to closely related bacteria. *Nature*, pages 81–86, 2003.

[92] Natalia Ivanova, Alexei Sorokin, Iain Anderson, Nathalie Galleron, Benjamin Candelon, Vinayak Kapatral, Anamitra Bhattacharyya, Gary Reznik, Natalia Mikhailova, Alla Lapidus, Lien Chu, Michael Mazur, Eugene Goltsman, Niels Larsen, Mark D'Souza, Theresa Walunas, Yuri Grechkin, Gordon Pusch, Robert Haselkorn, Michael Fonstein, S. Dusko Ehrlich, Ross Overbeek, and Nikos Kyrpides. Genome sequence of Bacillus cereus and comparative analysis with Bacillus anthracis. *Nature*, 423(6935):87–91, 2003.

[93] Rachel A. Miller, Sarah M. Beno, David J. Kent, Laura M. Carroll, Nicole H. Martin, Kathryn J. Boor, and Jasna Kovac. Bacillus wiedmannii sp. nov., a psychrotolerant and cytotoxic bacillus cereus group species isolated from dairy foods and dairy environments. *International Journal of Systematic and Evolutionary Microbiology*, 66(11):4744–4753, 2016.

[94] P.P. Vimala and Lea Mathew. Biodegradation of Polyethylene Using Bacillus Subtilis. *Procedia Technology*, 24:232–239, 2016.

[95] Asma Ait Kaki, Noreddine Kacem Chaouche, Laid Dehimat, Asma Milet, Mounia Youcef-Ali, Marc Ongena, and Philippe Thonart. Biocontrol and Plant Growth Promotion Characterization of Bacillus Species Isolated from Calendula officinalis Rhizosphere. *Indian Journal of Microbiology*, 53(4):447–452, 2013.

[96] Jyoti Kumar Thakur, Sangeeta Paul, Prem Dureja, K. Annapurna, Jasdeep C. Padaria, and Madhuban Gopal. Degradation of sulphonated azo dye red HE7B by Bacillus sp. and elucidation of degradative pathways. *Current Microbiology*, 69(2):183–191, 2014.

[97] Amit Bafana, Tapan Chakrabarti, and Sivanesan Saravana Devi. Azoreductase and dye detoxification activities of Bacillus velezensis strain AB. *Applied Microbiology and Biotechnology*, 77(5):1139–1144, 2008.

[98] E. Hosseini Koupaie, M. R. Alavi Moghaddam, and S. H. Hashemi. Evaluation of integrated anaerobic/aerobic fixed-bed sequencing batch biofilm reactor for decolorization and biodegradation of azo dye Acid Red 18: Comparison of using two types of packing media. *Bioresource Technology*, 127:415–421, 2013.

[99] Julia Ebeling, Henriette Knispel, Gillian Hertlein, Anne Fünfhaus, and Elke Genersch. Biology of Paenibacillus larvae, a deadly pathogen of honey bee larvae. *Applied Microbiology and Biotechnology*, 100(17):7387–7395, 2016.

[100] Eva Garcia-Gonzalez, Lena Poppinga, Anne Fünfhaus, Gillian Hertlein, Kati Hedtke, Agata Jakubowska, and Elke Genersch. Paenibacillus larvae Chitin-Degrading Protein PlCBP49 Is a Key Virulence Factor in American Foulbrood of Honey Bees. *PLoS Pathogens*, 10(7), 2014.

[101] Lakshmi Prasanna, Vincent G.H. Eijsink, Richard Meadow, and Sigrid Gåseidnes. A novel strain of Brevibacillus laterosporus produces chitinases that contribute to its biocontrol potential. *Applied Microbiology and Biotechnology*, 97(4):1601–1611, 2013.

[102] Mayur B. Kurade, Tatoba R. Waghmode, and Sanjay P. Govindwar. Preferential biodegradation of structurally dissimilar dyes from a mixture by Brevibacillus laterosporus. *Journal of Hazardous Materials*, 192(3):1746–1755, 2011.

[103] Jinlong Song, Yanwei Wang, Yi Song, Bingqiang Zhao, Huimin Wang, Shan Zhou, Delong Kong, Xiang Guo, Yanting Li, Mingxiong He, Kedong Ma, Zhiyong Ruan, and Yanchun Yan. Brevibacillus halotolerans sp. nov., isolated from saline soil of a paddy field. *International Journal of Systematic and Evolutionary Microbiology*, 67(4):772–777, 2017.

[104] S. Singh, S. Chatterji, P. T. Nandini, A. S.A. Prasad, and K. V.B. Rao. Biodegradation of azo dye Direct Orange 16 by Micrococcus luteus strain SSN2. *International Journal of Environmental Science and Technology*, 12(7):2161–2168, 2015.

[105] J. Kanagaraj, T. Senthilvelan, and R. C. Panda. Biodegradation of azo dyes in industrial effluent: An eco-friendly way toward green technology. *Clean Technologies and Environmental Policy*, 17(2):331–341, 2015.

[106] Tirupati Sumathi, Buddolla Viswanath, Akula Sri Lakshmi, and D V R Saigopal. Production of Laccase by Cochliobolus sp . Isolated Low Molecular Weight PVC. *Biochemistry Research International*, 2016:1–10, 2016.

[107] Sana Sheik, K. R. Chandrashekar, K. Swaroop, and H. M. Somashekarappa. Biodegradation of gamma irradiated low density polyethylene and polypropylene by endophytic fungi. *International Biodeterioration and Biodegradation*, 105:21–29, 2015.

[108] K. Mohanrasu, N. Premnath, G. Siva Prakash, Muniyasamy Sudhakar, T. Boobalan, and A. Arun. Exploring multi potential uses of marine bacteria; an integrated approach for PHB production, PAHs and polyethylene biodegradation. *Journal of Photochemistry and Photobiology B: Biology*, 185:55–65, 2018.

[109] Om Prakash, Yogesh Nimonkar, Mahesh S. Chavadar, Nidhi Bharti, Shrikant Pawar, Ashutosh Sharma, and Yogesh S. Shouche. Optimization of Nutrients and Culture Conditions for Alkaline Protease Production Using Two Endophytic Micrococci: Micrococcus aloeverae and Micrococcus yunnanensis. *Indian Journal of Microbiology*, 57(2):218–225, 2017.

[110] Martin Ogonowski, Asa Motiei, Karolina Ininbergs, Eva Hell, Zandra Gerdes, Klas I. Udekwu, Zoltan Bacsik, and Elena Gorokhova. Evidence for selective bacterial community structuring on microplastics. *Environmental Microbiology*, 00(00):00–00, 2018.

[111] Markus Linder, Geza R. Szilvay, Tiina Nakari-Setälä, Hans Söderlund, and Merja Penttilä. Surface adhesion of fusion proteins containing the hydrophobins HFBI and HFBII from Trichoderma reesei. *Protein Science*, 11(9):2257–2266, 2009.

[112] Tanuja Singh, Ratul Saikia, Tarakanta Jana, and Dilip K. Arora. Hydrophobicity and surface electrostatic charge of conidia of the mycoparasitic Trichoderma species. *Mycological Progress*, 3(3):219–228, 2004.

[113] José Carlos Moreira and Nicole Raymonde Demarquette. Influence of temperature, molecular weight, and molecular weight dispersity on the surface tension of PS, PP, and PE. I. Experimental. *Journal of Applied Polymer Science*, 82(8):1907–1920, 2001.

[114] H. Wei, R. B. Thompson, C. B. Park, and P. Chen. Surface tension of high density polyethylene (HDPE) in supercritical nitrogen: Effect of polymer crystallization. *Colloids and Surfaces A: Physicochemical and Engineering Aspects*, 354(1-3):347–352, 2010.

[115] T. Volke-Seplveda, G. Saucedo-Castaeda, M. Gutirrez-Rojas, A. Manzur, and E. Favela-Torres. Thermally treated low density polyethylene biodegradation by Penicillium

pinophilum and Aspergillus niger. *Journal of Applied Polymer Science*, 83(2):305–314, 2002.

[116] Xia Zhao, Yun Wang, Qianhan Shang, Yuyao Li, Haiting Hao, Yubao Zhang, Zhihong Guo, Guo Yang, Zhongkui Xie, and Ruoyu Wang. Collagen-like proteins (ClpA, ClpB, ClpC, and ClpD) are required for biofilm formation and adhesion to plant roots by Bacillus amyloliquefaciens FZB42. *PLoS ONE*, 10(2):1–16, 2015.

[117] Xia Zhao, Ruoyu Wang, Qianhan Shang, Haiting Hao, Yuyao Li, Yubao Zhang, Zhihong Guo, Yun Wang, and Zhongkui Xie. The new flagella-associated collagen-like proteins ClpB and ClpC of Bacillus amyloliquefaciens FZB42 are involved in bacterial motility. *Microbiological Research*, 184:25–31, 2016.

[118] Alice C. Dohnalkova, Matthew J. Marshall, Bruce W. Arey, Kenneth H. Williams, Edgar C. Buck, and James K. Fredrickson. Imaging hydrated microbial extracellular polymers: Comparative analysis by electron microscopy. *Applied and Environmental Microbiology*, 77(4):1254–1262, 2011.

[119] Barbara Fifani. *Exploitation du dialogue moléculaire bactérie/champignon pour le dimensionnement de nouveaux procédés pour la production de métabolites secondaires.* PhD thesis, University of Lille (France) and University of Liège (Gembloux Agro bio tech, Belgium), 2 October 2017.

A Appendices

T_m adjustment of PCR: results

Four annealing temperatures were tested and compared to the addition of an enhancer (GC clamp), E letter on Figure 20.

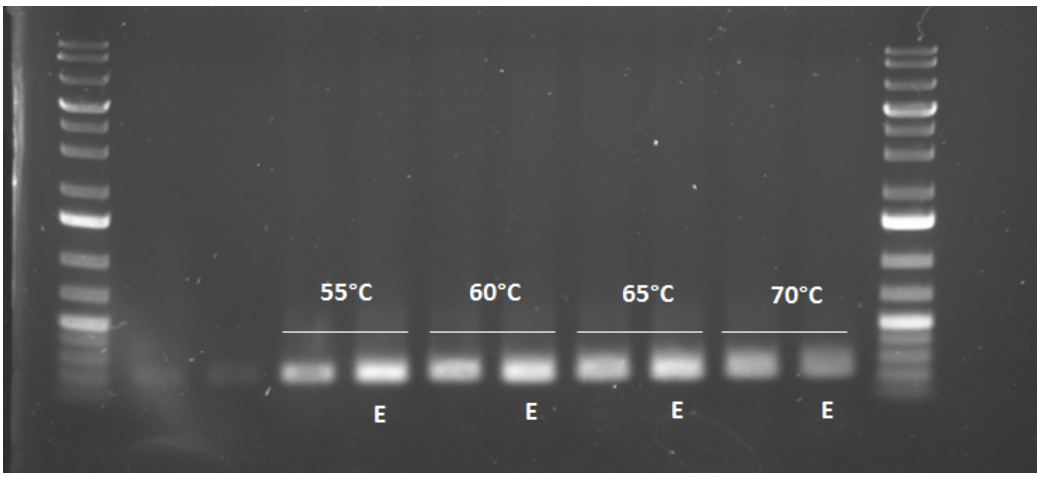

FIGURE 20: PCR adjustment carried out on a mix of *Bacillus* spp.

DGGE results

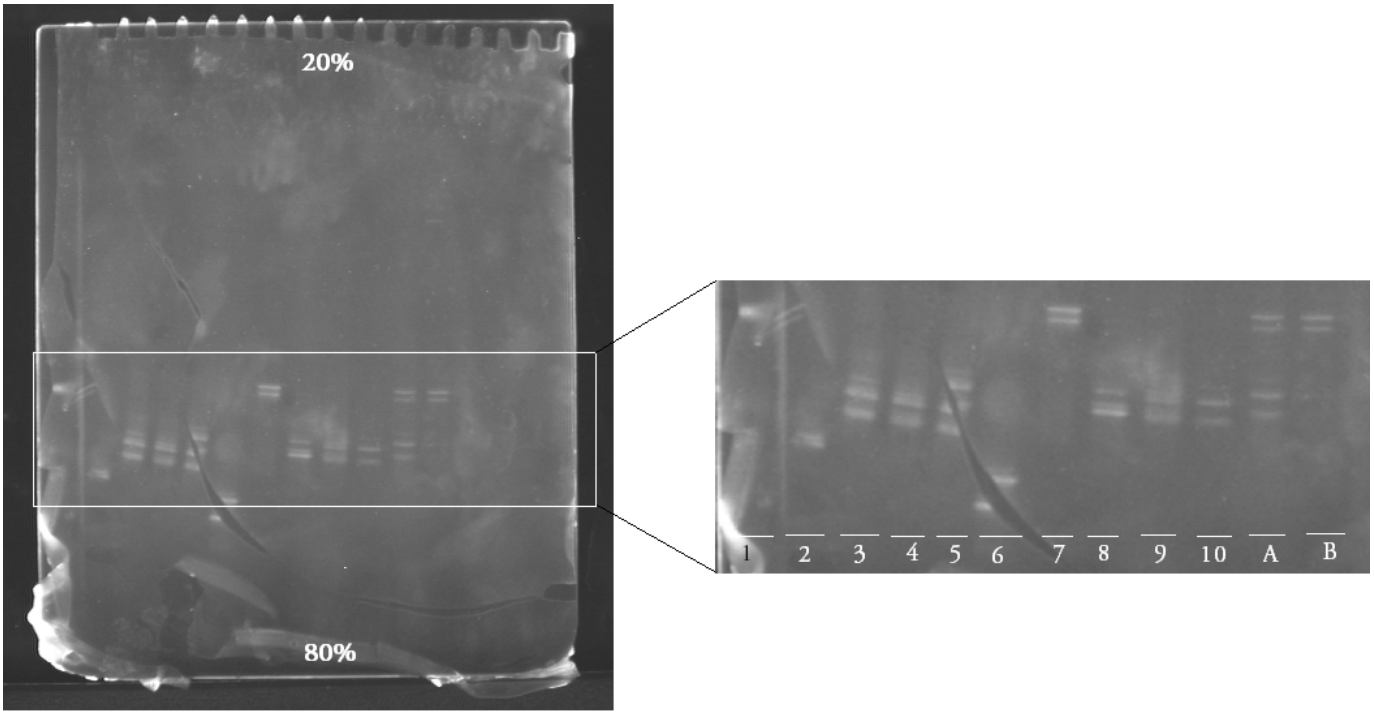

FIGURE 21: DGGE result from microbial mix of standard diet and classical PCR applied
Numbered sample: Isolated colonies from the standard diet; **A and B**: Microbial mix from phase A and B (see section 3.1.2.2, page 22)

Species identification

TABLE 7: Species identification from forward primer based on 16S rDNA sequencing

	Specie	**Max score**	**Total score**	**Query cover**	**E value**	**Identity**
Sample 1	*Enterococcus casseliflavus*	603	603	100%	1E-168	100%
Sample 2	*Bacillus amyloliquefaciens*	880	880	100%	0.0	100%
	Bacillus velezensis	880	880	100%	0.0	100%
Sample 4	*Paenibacillus larvae*	942	942	100%	0.0	99%
	Brevibacillus laterosporus	942	942	100%	0.0	99%
Sample 6	*Micrococcus yunnanensis*	294	294	100%	4E-76	100%
	Micrococcus aloeverae	294	294	100%	4E-76	100%
	Micrococcus luteus	294	294	100%	4E-76	100%
Sample 8	*Bacillus cereus*	1149	1149	100%	0.0	100%
	Bacillus thuringiensis	1149	1149	100%	0.0	100%
Sample 10	*Paenibacillus larvae*	1074	1074	100%	0.0	100%
	Brevibacillus laterosporus	1074	1074	100%	0.0	100%

TABLE 8: Species identification from reverse primer based on 16S rDNA sequencing

	Specie	**Max score**	**Total score**	**Query cover**	**E value**	**Identity**
Sample 1	*Enterococcus casseliflavus*	1000	1000	100%	0.0	100%
	Enterococcus avium	1000	1000	100%	0.0	100%
	Enterococcus gallinarium	1000	1000	100%	0.0	100%
Sample 2	*Bacillus velezensis*	909	8126	100%	0.0	100%
	Bacillus subtilis	909	9096	100%	0.0	100%
	Bacillus amyloliquefaciens	909	909	100%	0.0	100%
Sample 4	*Brevibacillus laterosporus*	907	907	100%	0.0	100%
	Brevibacillus halotolerans	907	907	100%	0.0	100%
Sample 6	*Micrococcus yunnanensis*	944	944	100%	0.0	100%
	Micrococcus luteus	944	944	100%	0.0	100%
	Micrococcus aloeverae	944	944	100%	0.0	100%
Sample 8	*Bacillus cereus*	1055	1055	100%	0.0	100%
	Bacillus subtilis	1055	1055	100%	0.0	100%
	Bacillus thuringiensis	1055	1055	100%	0.0	100%
	Bacillus wiedmannii	1055	1055	100%	0.0	100%
Sample 10	*Brevibacillus laterosporus*	1013	1013	100%	0.0	100%
	Brevibacillus halotolerans	1013	1013	100%	0.0	100%

Metagenomic approach: relative abundance of taxa

Figures 22, 23 and 24 are based on Samuel's results. Horizontal axes are samples, one sample represent one larvae (8 Standard diets (**STD**) and 8 polyethylene diet (**PE**)). Vertical axes are relative abundance of considered taxa. The top three of most abundant taxa are illustrated, while Figure 24 takes into account Bacillaceae.

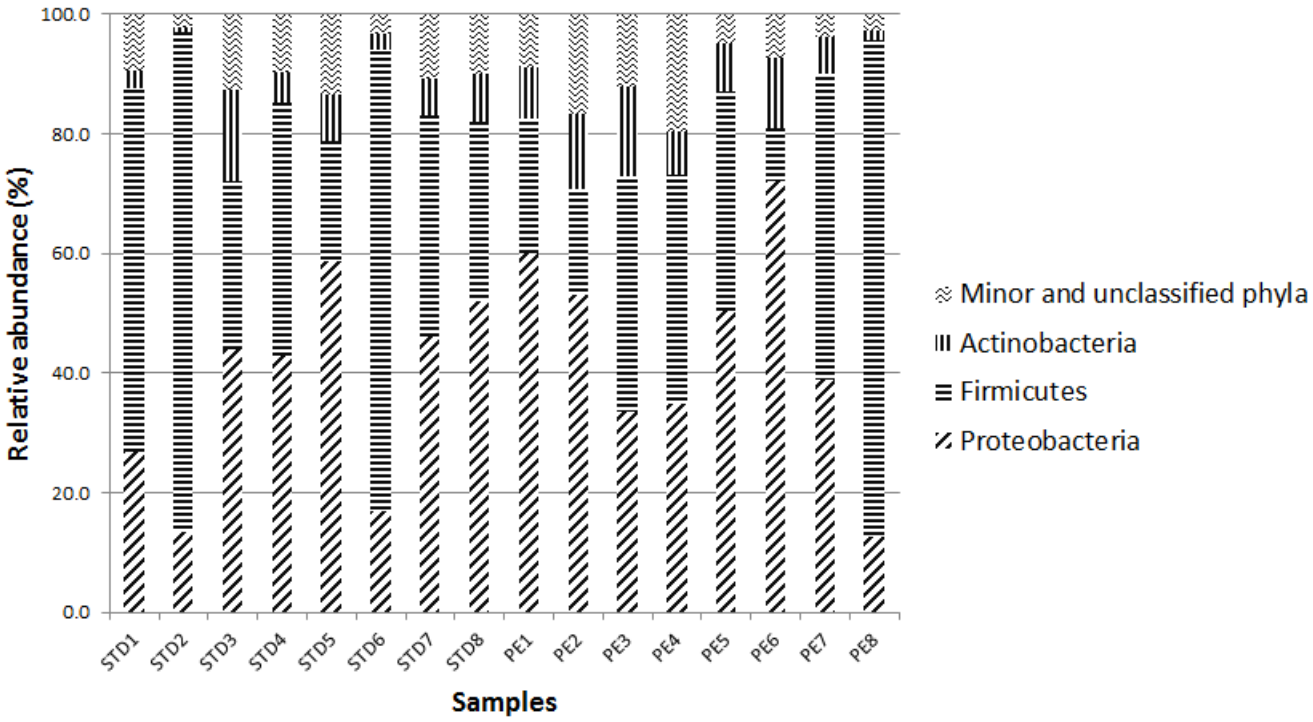

FIGURE 22: Relative abundance of phyla in function of samples and diets

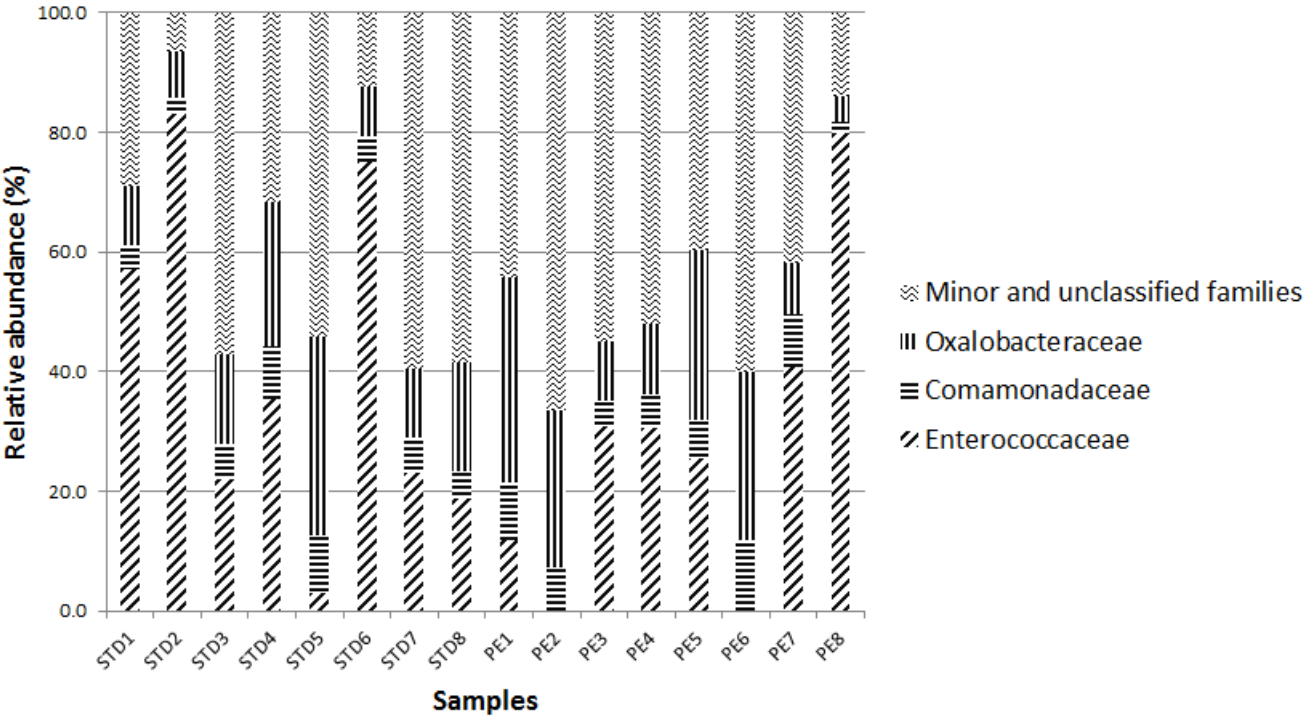

FIGURE 23: Relative abundance of families in function of samples and diets

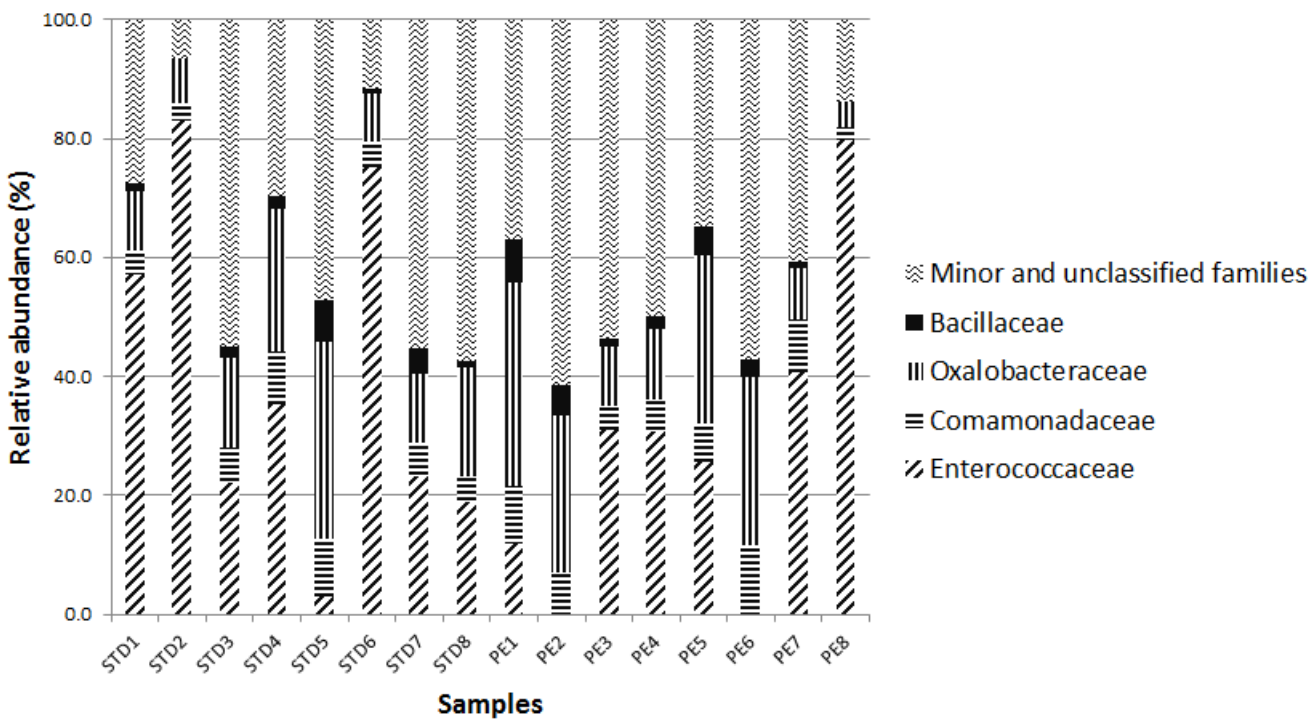

FIGURE 24: Relative abundance of families in function of samples and diets

Zeta potential measurement: instrument parameters

TABLE 9: Implemented parameters for Zeta potential measurement

Parameters	**Flat surface cell**
Temperature	20°C
Measurement type	Type 1
Cell constant	66
Accumulation time	10
Cell position	0.8/0.6/0.3/0/-0.3/-0.6/-0.8
Applied voltage	60
Conversion equation	Smoluchowski
Solvent properties	**Flat surface cell**
Refractive index	1.3328
Dielectric constant	78.3

Zeta potential measurement

TABLE 10: Mean values of Zeta potential of biofilms (mV)

	Day 1			Day 4			Day 7		
Sample	**Average**	**Minimum Value**	**Maximum Value**	**Average**	**Minimum Value**	**Maximum Value**	**Average**	**Minimum Value**	**Maximum Value**
B	-3,50	-12,22	1,25	-1,09	-3,24	-0,36	-2,31	-11,66	1,59
B	-7,39	-15,60	0,27	-0,10	-0,35	0,54	0,02	-8,92	2,80
B	-5,82	-14,16	0,63	0,53	-0,03	1,04	-1,84	-14,89	3,84
T	-0,83	-27,19	37,19	-0,21	-0,62	0,54	0,14	-0,47	1,65
T	-7,07	-33,29	9,66	0,65	0,17	2,56	-0,18	-0,53	0,36
T	-7,69	-26,35	5,89	-0,17	-0,65	0,18	-0,30	-0,94	0,86
BT	0,16	-0,48	0,79	-0,20	-0,61	0,19	0,04	-0,74	0,65
BT	0,17	-0,17	0,43	0,01	-0,47	0,25	-0,76	-1,32	-0,12
BT	0,19	-0,11	0,74	-0,16	-1,00	1,27	0,52	0,05	1,14

Repetition of measurement on each sample (**T**: *Trichoderma harzianum*; **B**: *Bacillus amyloliquefaciens*; **BT**: co-culture of *Trichoderma harzianum* and *Bacillus amyloliquefaciens*)

TABLE 11: Zeta potential values of water associated to biofilms (mV)

Sample	**Day 1**	**Day 4**	**Day 7**
B	17.08	-0.22	-6.5
B	-58.92	11.94	-15.25
B	14.63	100.65	9.1
T	57.11	0.3	-0.81
T	24.03	0.08	0.5
T	38.72	-10.36	-0.86
BT	-25.33	-0.47	0.02
BT	11.96	-0.48	0.53
BT	7.3	0.6	-0.16

Repetition of measurement on each sample (**T**: *Trichoderma harzianum*; **B**: *Bacillus amyloliquefaciens*; **BT**: co-culture of *Trichoderma harzianum* and *Bacillus amyloliquefaciens*)

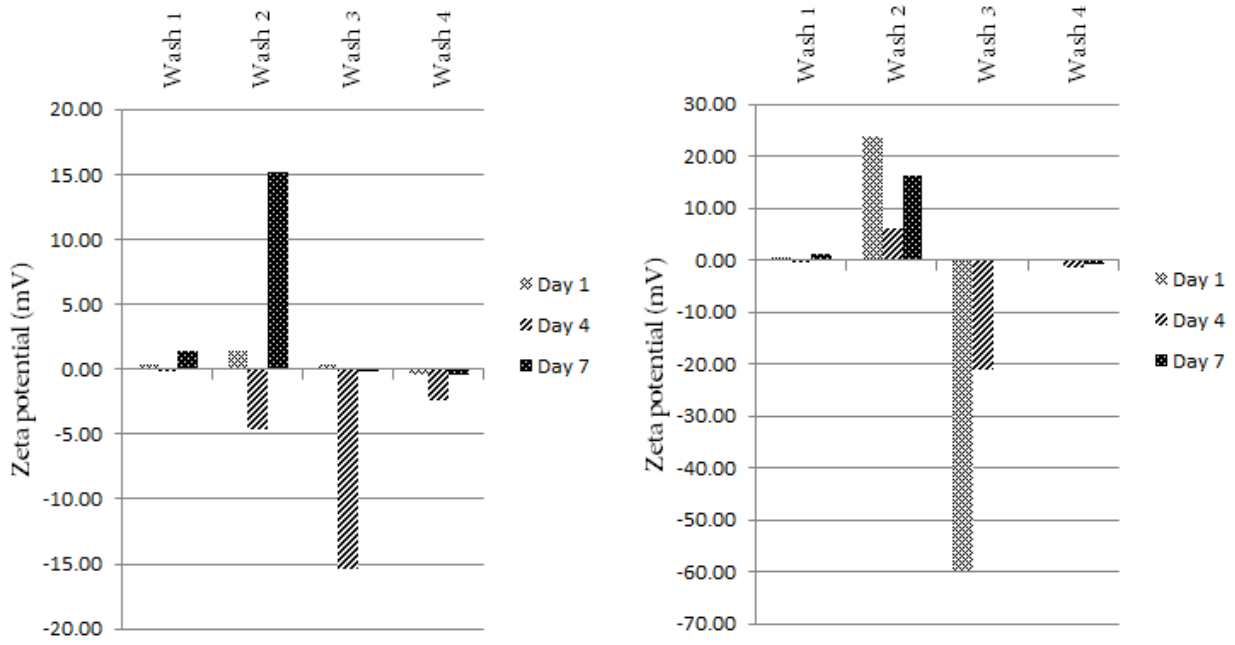

(A) ZP of biological system

(B) ZP of associated water

FIGURE 25: Zeta potential evolution of water and biofilm formed by *B. amyloliquefaciens*, impacted by washes in function of culture time

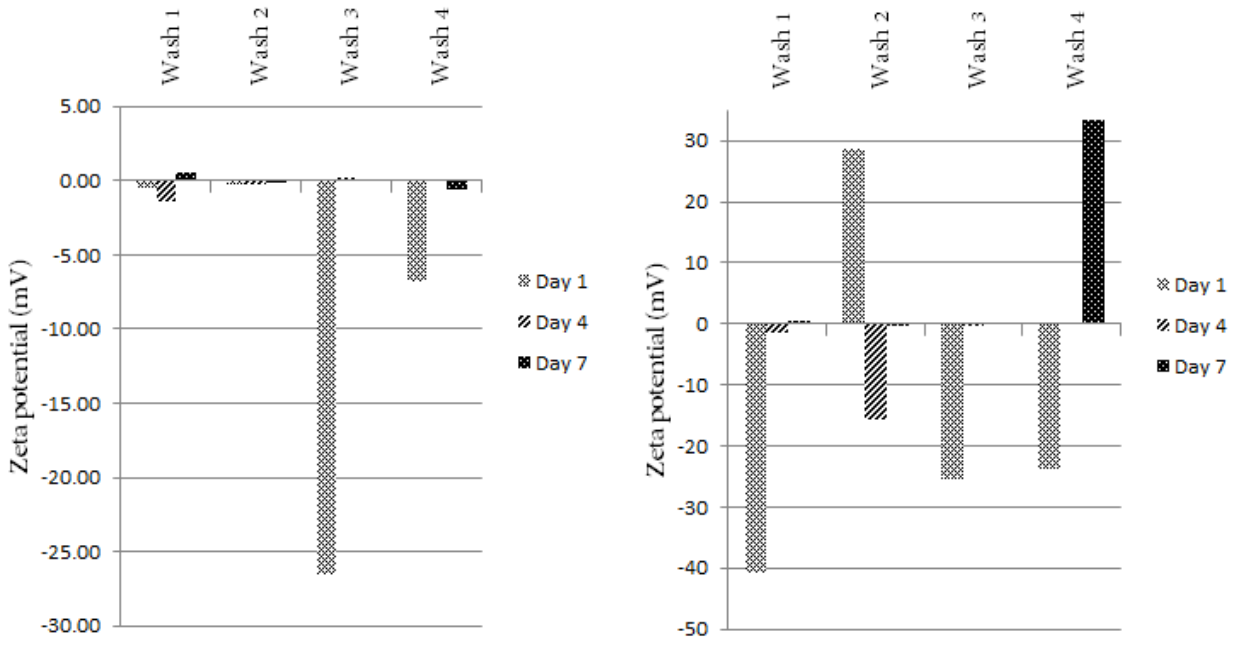

(A) ZP of biological system

(B) ZP of associated water

FIGURE 26: Zeta potential evolution of water and mycelium of *T. harzianum*, impacted by washes in function of culture time

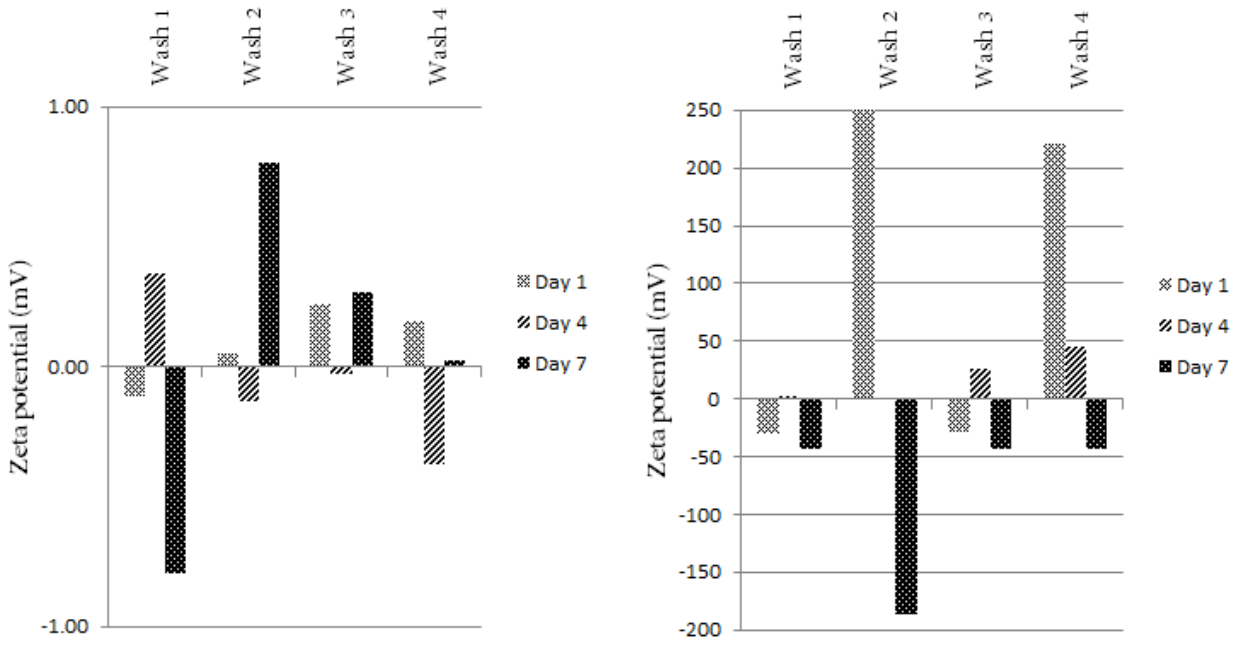

(A) ZP of biological system

(B) ZP of associated water

FIGURE 27: Zeta potential evolution of water and biofilm co-culture, impacted by washes in function of culture time

TABLE 12: Zeta potential values of plastics after adhesion of biofilms (mV)

	Day 1		**Day 4**		**Day 7**	
Sample	**Average**	**SD**	**Average**	**SD**	**Average**	**SD**
B	0.01	0.21	-3.34	7.06	0.39	0.1
B	-0.31	0.72	0.87	2.5	-0.05	0.21
B	0.13	0.21	0.98	0.74	0.17	0.1
T	-0.38	0.21	0.06	0.30	-0.41	0.55
T	-23.26	1.75	-0.51	1.41	-0.08	0.23
T	-0.26	0.99	0.1	0.73	-0.39	0.62
BT	-0.27	0.25	-0.43	1.22	-0.14	0.5
BT	-0.10	0.27	0.10	1.17	-0.02	0.59
BT	0.53	0.41	-2.06	2.73	-0.40	0.51

Repetition of measurement on each sample (**T**: *Trichoderma harzianum*; **B**: *Bacillus amyloliquefaciens*; **BT**: co-culture of *Trichoderma harzianum* and *Bacillus amyloliquefaciens*)

TABLE 13: Results of the ANOVA model tested on ZP values of PE surface

Factor	**p-value**
Day	0.4430
Biofilm	0.3900
Day*Biofilm	0.4160

TABLE 14: Contact angle measurement of plastic surfaces after adhesion of biofilm and surface tension calculation

Samples	θ_W	θ_{EtOH}	θ_{Hexane}	γ^{AB}	γ^+	γ^-	γ^{LW}	γ^{Tot}
LDPE Control	92.9	14.5	20.25	0.01	0.005	0.011	17.31	17.32
B D1	78.8	25.5	11.6	0.02	0.004	0.023	18.06	18.08
B D4	98.8	24.15	18.2	0.01	0.004	0.008	17.52	17.53
B D7	69.25	25.3	25.25	0.03	0.004	0.0036	16.71	16.74
T D1	79.85	10.8	11.9	0.02	0.005	0.021	18.04	18.06
T D4	96.4	29.85	16.25	0.01	0.004	0.01	17.7	17.71
T D7	82.55	25.55	17.2	0.02	0.004	0.02	17.61	17.63
BT D1	78.6	11.8	11.9	0.02	0.005	0.024	17.35	17.37
BT D4	95.5	14.1	12.75	0.01	0.005	0.009	17.98	17.99
BT D7	100.95	27.75	15.55	0.01	0.004	0.007	17.76	17.77

T: *Trichoderma harzianum*; **B**: *Bacillus amyloliquefaciens*; **BT**: co-culture of *Trichoderma harzianum* and *Bacillus amyloliquefaciens;* ***D1, D4 and D7****: first, fourth and seventh day after the inoculation of Bacillus amyloliquefaciens*

SEM imaging

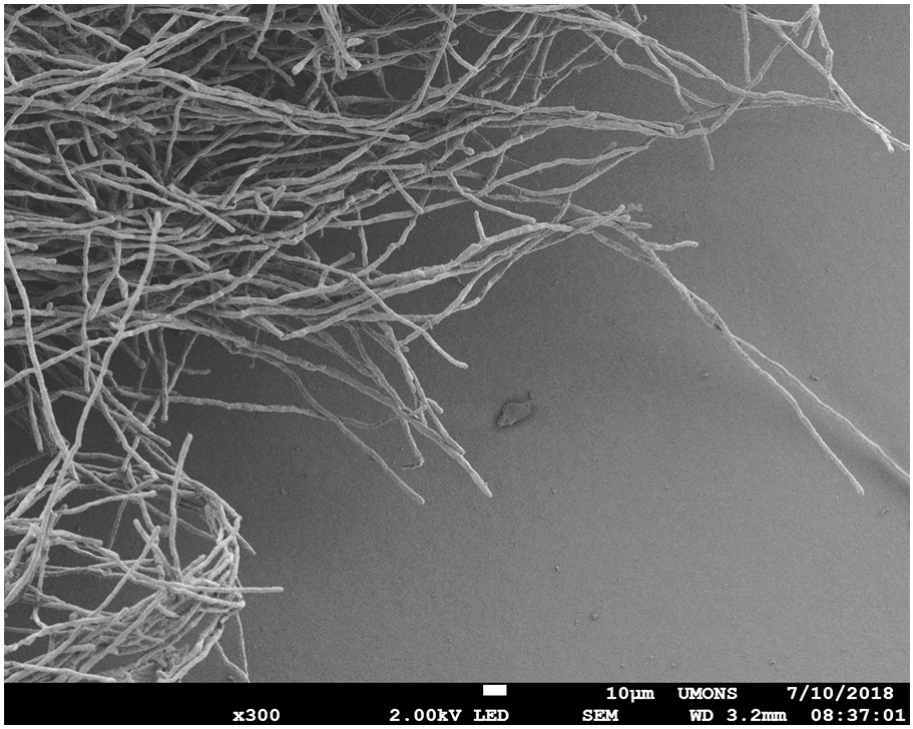

FIGURE 28: SEM of a 72h old mycelium formation of *T. harzianum* on plastic surface

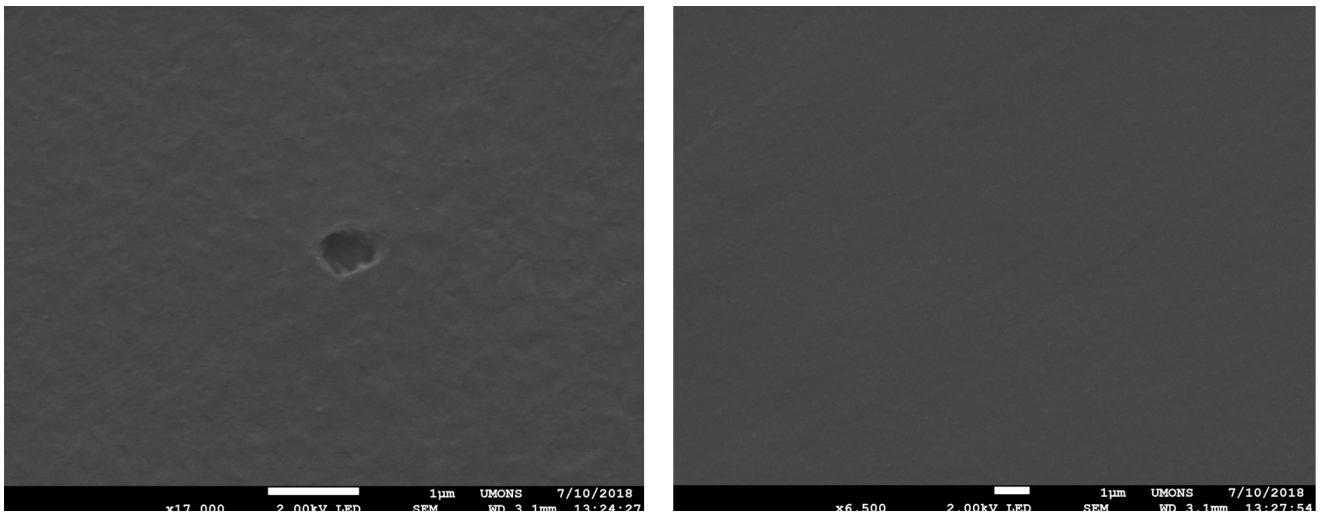

(A) Polyethylene manufacturing defect

(B) Smooth surface

FIGURE 29: SEM of polyethylene surface controls

Lipopeptides: UPLC results from [119]

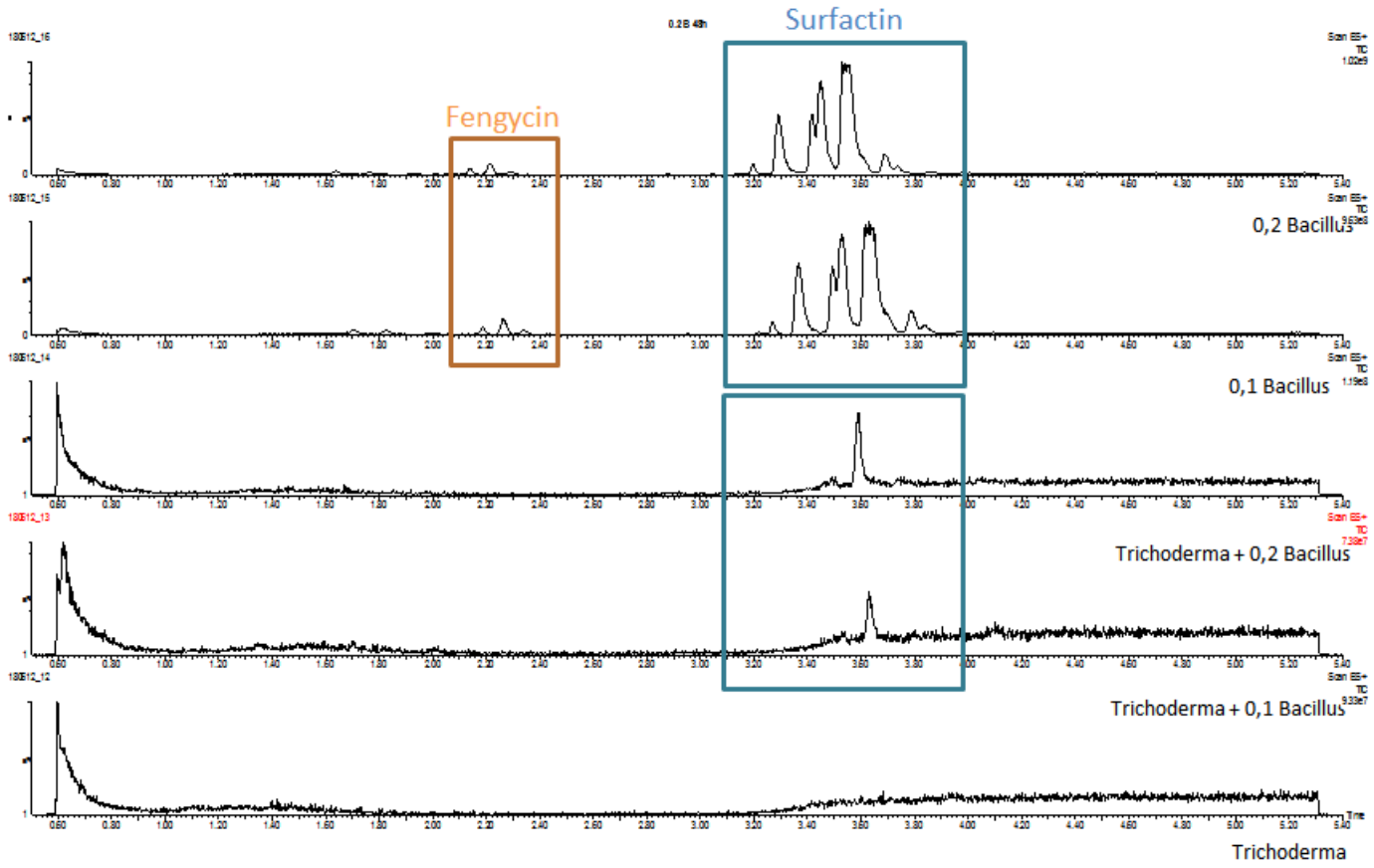

FIGURE 30: Differences of lipopeptide production between monoculture (*B. amyloliquefaciens*) and co-culture (*B. amyloliquefaciens* and *T. harzanium*)